State Space Model for New-Generation Network Alternative to Transformers: A Survey

Xiao Wang, *Member, IEEE*, Shiao Wang, Yuhe Ding, Yuehang Li, Wentao Wu, Yao Rong, Weizhe Kong, Ju Huang, Shihao Li, Haoxiang Yang, Ziwen Wang, Bo Jiang, Chenglong Li, Yaowei Wang, *Member, IEEE*, Yonghong Tian, *Fellow, IEEE*, Jin Tang

Abstract—In the post-deep learning era, the Transformer architecture has demonstrated its powerful performance across pre-trained big models and various downstream tasks. However, the enormous computational demands of this architecture have deterred many researchers. To further reduce the complexity of attention models, numerous efforts have been made to design more efficient methods. Among them, the State Space Model (SSM), as a possible replacement for the self-attention based Transformer model, has drawn more and more attention in recent years. In this paper, we give the first comprehensive review of these works and also provide experimental comparisons and analysis to better demonstrate the features and advantages of SSM. Specifically, we first give a detailed description of principles to help the readers quickly capture the key ideas of SSM. After that, we dive into the reviews of existing SSMs and their various applications, including natural language processing, computer vision, graph, multi-modal and multi-media, point cloud/event stream, time series data, and other domains. In addition, we give statistical comparisons and analysis of these models and hope it helps the readers to understand the effectiveness of different structures on various tasks. Then, we propose possible research points in this direction to better promote the development of the theoretical model and application of SSM. More related works will be continuously updated on the following GitHub https://github.com/Event-AHU/Mamba_State_Space_Model_Paper_List.

Index Terms—State Space Model, Mamba, Transformer, Linear Attention, Computer Vision, Natural Language Processing

✦

1 INTRODUCTION

ARTIFICIAL intelligence develops rapidly in the third wave which starts from the year 2010, among them, connectionism-based deep learning technology plays an extremely important role. The singular point of deep learning can be traced back to the proposal of AlexNet [1] which achieves the best performance (a far better result than second place) in the ImageNet [2] competition. After that, various Convolutional Neural Networks (CNN) are proposed one after another, such as VGG [3], ResNet [4], GoogleNet [5], etc. The ideas of blocks, residual connection, and inception inspire the design of many follow-up deep neural networks [6], [7]. On the other hand, the family of Recurrent Neural Networks (RNN), such as Long Short-Term Memory (LSTM) [8] and Gated Recurrent Unit (GRU) [9], dominates the sequence-based learning community, including natural language processing, and audio processing. Graph Neural Networks (GNNs) [10], [11] are proposed to further extend the applications of deep neural networks on graph data. However, these mainstream models still encounter bottlenecks when the datasets and computing power support are at their maximum.

To handle the issues of only local relations captured by CNN/RNN/GNN models, the Transformer [13] proposed in the year 2017 learns the long-range feature representations well. The core operation is the self-attention mechanism which transforms the input tokens into query, key, and value features, and outputs the long-range features by multiplying the similarity matrix (obtained via product between the query and key features) with the value features. The Transformer architecture first swept the NLP community with the help of *pre-training and fine-tuning* paradigm [14], such as BERT [15], ERNIE [16], BART [17], GPT [18]. Then, other communities are also boosted with such networks, for example, the ViT [19] and Swin-Transformer [20] released in computer vision. Many researchers also exploit the hybrid network architectures by combining Transformer and other networks, or adapting the Transformer for multi-modal research problems [21], [22]. In the current stage, large foundation models are emerging, and Parameter-Efficient Fine-Tuning (PEFT) strategies [23] also have been greatly developed. However, the current Transformer-based models still require high-end graphics cards with larger memory for training and testing/deployment, which greatly limits their wider application.

- *Xiao Wang, Shiao Wang, Yuhe Ding, Yuehang Li, Yao Rong, Ju Huang, Haoxiang Yang, Ziwen Wang, Bo Jiang, and Jin Tang are with the School of Computer Science and Technology, Anhui University, Hefei 230601, China. (email: xiaowang@ahu.edu.cn)*
- *Weizhe Kong, Wentao Wu, Shihao Li, and Chenglong Li are with the School of Artificial Intelligence, Anhui University, Hefei 230601, China. (email: lcl1314@foxmail.com)*
- *Yaowei Wang is with Peng Cheng Laboratory, Shenzhen, China; Harbin Institute of Technology (HITSZ), Shenzhen, China. (email: wangyw@pcl.ac.cn)*
- *Yonghong Tian is with Peng Cheng Laboratory, Shenzhen, China; National Key Laboratory for Multimedia Information Processing, School of Computer Science, Peking University, China; School of Electronic and Computer Engineering, Shenzhen Graduate School, Peking University, China (email: yhtian@pku.edu.cn)*
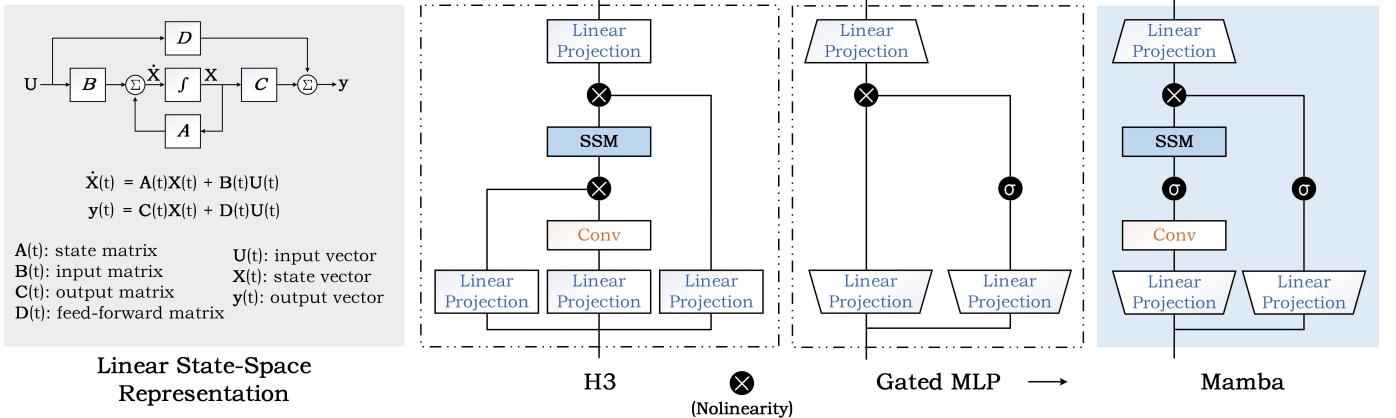- *Corresponding author: Bo Jiang (jiangbo@ahu.edu.cn)*

Fig. 1. [left gray sub-figure] Block diagram representation of the linear state-space equations (re-draw based on state-space representation); [right sub-figure] The formulation of widely used Mamba architecture (re-draw from [12]).

To further decrease the computing cost, while capturing long-range dependency and maintaining high performance, many new sparse attention based models or new neural network paradigms are proposed [24]–[28]. Among them, State Space Model (e.g., Mamba [12], S4 [29], S4nd [30]), as shown in Fig. 1, becomes the center of attention. As shown in the left part of Fig. 2, the amount of SSM-related papers released shows the trend of explosive growth. The State Space Model (SSM) is a framework initially proposed to model a dynamic system using state variables in the field of control theory, computational neuroscience, etc [1]. When adapting this concept for deep learning, we usually refer to linear invariant (or stationary) systems. The original SSM is a continuous-dynamic system that can be discretized for *recurrent* and *convolutional* views for the computer to handle. SSMs can be adopted for various data processing and feature learning, including image/video data, text data, structured graph data, event streams/point cloud data, multi-modal/multi-media data, audio and speech, time series data, tabular data, etc. It can also be utilized to build efficient generative models, such as SSMs-based diffusion generative models [31]–[33]. In order to help readers better understand the SSM and keep track of the latest research progress and various applications, this paper conducts a systematic review of the field and verifies the performance of the SSM model in downstream tasks experimentally. It is hoped that this review can better lead and promote the development of the field of SSM.

Organization of this review. In this paper, we first give a preliminary preview of the working principle of the State Space Model in Section 2. Then, in Section 3, we focus on reviewing the related works of SSMs from multiple aspects, including origin and variation of SSMs, natural language processing, computer vision, graph, multi-modal and multi-media, point cloud/event stream, time series data, and other domains. An overview of the structure and key State Space Model related papers reviewed in this survey is illustrated in Fig. 3. More importantly, we conduct extensive experiments on multiple downstream tasks to validate the effectiveness of SSMs in Section 4. The downstream tasks

involve single-/multi-label classification, visual object tracking, pixel-level segmentation, image-to-text generation, and person/vehicle re-identification. We also propose several possible research directions to the theory and applications of SSMs in Section 5. Finally, we give a conclusion about this paper in Section 6.

2 FORMULATION OF SSM

State Space Model (SSM) originates from the classic Kalman filter [35], as illustrated in Fig. 1, it takes the 1-D input signal $\mathbf{U}(t)$ and maps it into N-D latent state $\mathbf{X}(t)$, then, it projects into a 1-D output signal $\mathbf{y}(t)$. The general computing procedure can be defined in Eq. 1:

$$\dot{\mathbf{X}}(t) = \mathbf{A}(t)\mathbf{X}(t) + \mathbf{B}(t)\mathbf{U}(t)$$
$$\mathbf{y}(t) = \mathbf{C}(t)\mathbf{X}(t) + \mathbf{D}(t)\mathbf{U}(t) \quad (1)$$

where $\mathbf{X}(t) \in \mathbb{R}^n$, $\mathbf{y}(t) \in \mathbb{R}^q$, $\mathbf{U}(t) \in \mathbb{R}^p$ denotes the *state vector*, *output vector*, and *input (or control) vector*. $\dot{\mathbf{X}}(t) = \frac{d}{dt}\mathbf{X}(t)$. $\mathbf{A}(t) \in \mathbb{R}^{n \times n}$, $\mathbf{B}(t) \in \mathbb{R}^{n \times p}$, $\mathbf{C}(t) \in \mathbb{R}^{q \times n}$, and $\mathbf{D}(t) \in \mathbb{R}^{q \times p}$ represents state matrix, input matrix, output matrix, and feed-forward matrix. When there is no direct feedthrough in the system model, $\mathbf{D}(t)$ is a zero matrix, thus, we get the following simplified equations:

$$\dot{\mathbf{X}}(t) = \mathbf{A}(t)\mathbf{X}(t) + \mathbf{B}(t)\mathbf{U}(t)$$
$$\mathbf{y}(t) = \mathbf{C}(t)\mathbf{X}(t). \quad (2)$$

As the raw system is continuous, we need to first discretize them before feeding the computer, as shown in Fig. 2. For the Mamba architecture, the zero-order hold (ZOH) [2] is adopted for the discretization and we have:

$$\mathbf{X}_t = \overline{\mathbf{A}}\mathbf{X}_{t-1} + \overline{\mathbf{B}}\mathbf{U}_t$$
$$\mathbf{y}_t = \mathbf{C}\mathbf{X}_t \quad (3)$$

where $\overline{\mathbf{A}} = exp(\Delta\mathbf{A})$, $\overline{\mathbf{B}} = (\Delta\mathbf{A})^{-1}(exp(\Delta\mathbf{A}) - \mathbf{I}) \cdot \Delta\mathbf{B}$, Δ denotes the step size. If we denote the *state vector* and *input vector* using $\mathbf{h}$ and $\mathbf{x}$, we obtain the following functions
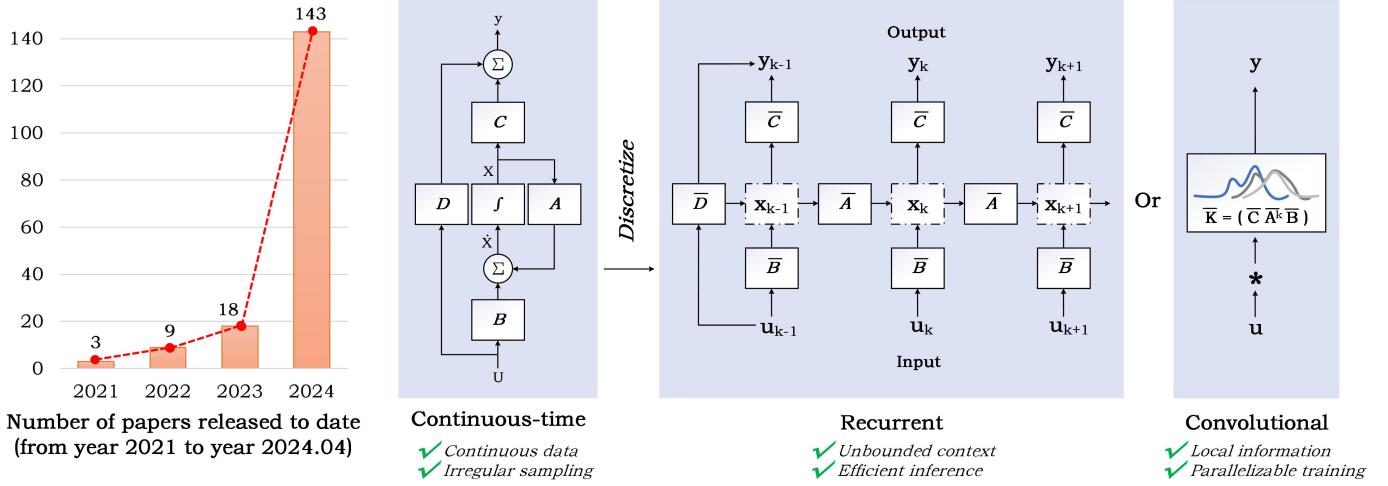

Fig. 2. [left sub-figure] Number of papers released to date (from year 2021 to year 2024.04); [right sub-figure] Three different representations of SSM can be viewed and computed, i.e., continuous-time, recurrent, or convolutional model. This figure is re-draw based on [34].
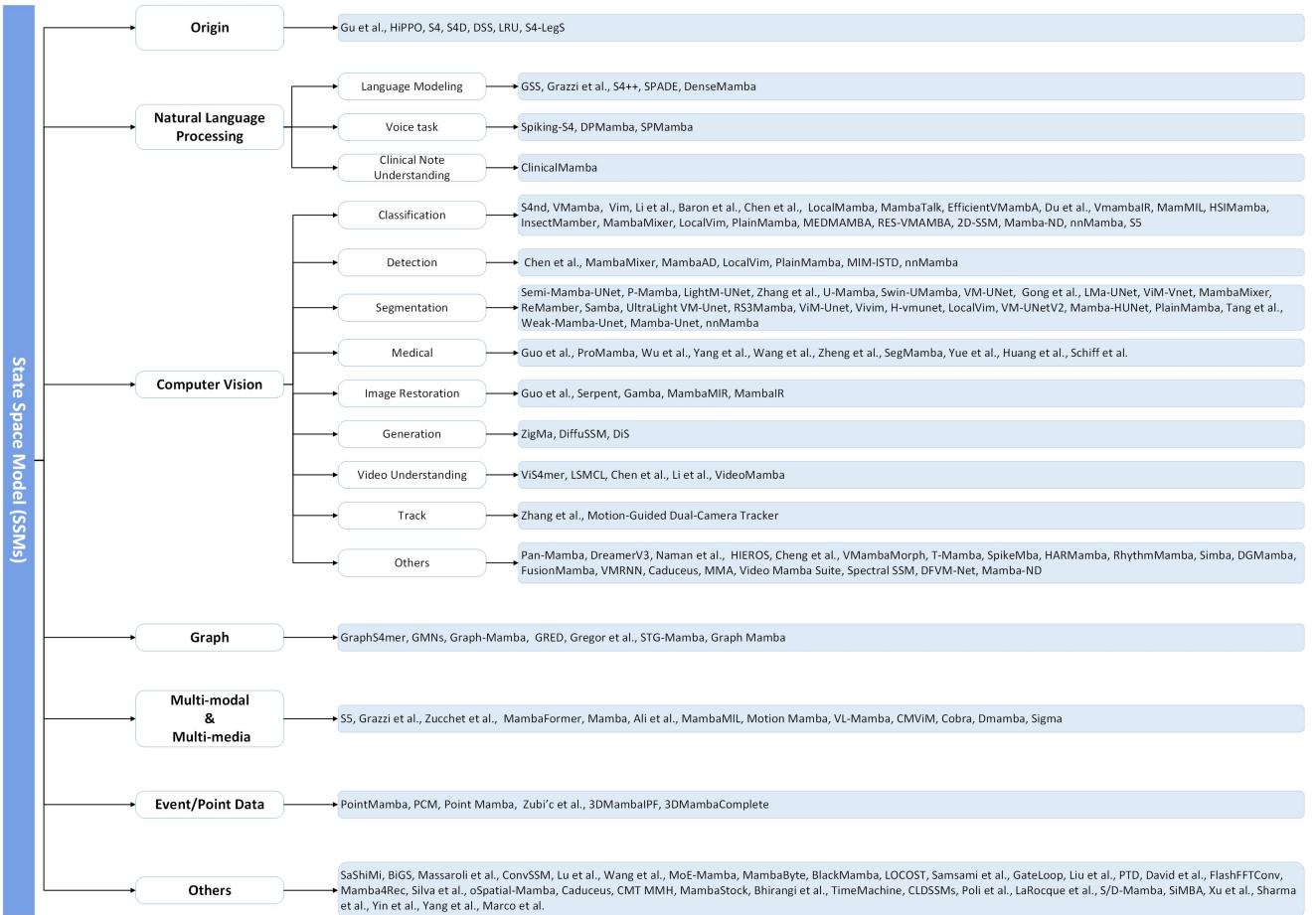

Fig. 3. Structure and key State Space Model papers reviewed in this survey.

similar to the computing procedure of the Recurrent Neural Network (RNN) model, as shown in Fig. 5(b):

$$\mathbf{h}_t = \overline{\mathbf{A}}\mathbf{h}_{t-1} + \overline{\mathbf{B}}\mathbf{x}_t$$
$$\mathbf{y}_t = \mathbf{C}\mathbf{h}_t. \tag{4}$$

However, similar to the RNN model, we face the dilemma that the computation cannot be *parallelized*. By simply expanding the above formula, we have:

$$\mathbf{y}_0 = \mathbf{C}\overline{\mathbf{A}}^0\overline{\mathbf{B}}\mathbf{x}_0$$
$$\mathbf{y}_1 = \mathbf{C}\overline{\mathbf{A}}^1\overline{\mathbf{B}}\mathbf{x}_0 + \mathbf{C}\overline{\mathbf{A}}^0\overline{\mathbf{B}}\mathbf{x}_1 \tag{5}$$
$$\mathbf{y}_2 = \mathbf{C}\overline{\mathbf{A}}^2\overline{\mathbf{B}}\mathbf{x}_0 + \mathbf{C}\overline{\mathbf{A}}^1\overline{\mathbf{B}}\mathbf{x}_1 + \mathbf{C}\overline{\mathbf{A}}^0\overline{\mathbf{B}}\mathbf{x}_2.$$

It is easy to find that the multiplier of the last and penultimate term is always $\mathbf{C}\overline{\mathbf{A}}^0\overline{\mathbf{B}}$ and $\mathbf{C}\overline{\mathbf{A}}^1\overline{\mathbf{B}}$. Therefore, we can treat these multipliers as the convolutional kernel $\overline{\mathbf{K}} = \mathbf{C}\overline{\mathbf{B}} \cdot (\overline{\mathbf{A}}^0, \overline{\mathbf{A}}^1, \overline{\mathbf{A}}^2, ..., \overline{\mathbf{A}}^L)$, here, L is the length of the given input sequence. We can rewrite the Equ. (4) as the following convolutional formulations:

$$\overline{\mathbf{K}} = (\mathbf{C}\overline{\mathbf{B}}, \mathbf{C}\overline{\mathbf{A}}\overline{\mathbf{B}}, ..., \mathbf{C}\overline{\mathbf{A}}^k\overline{\mathbf{B}}, ...)$$
$$\mathbf{y} = \mathbf{x} * \overline{\mathbf{K}}. \tag{6}$$

At this moment, we get the complete SSM model that can realize the parallelism of training and is suitable for the recurrent form of linear complexity of inference. In the Transformer architecture, the context information is stored in the similarity matrix, however, the SSM doesn't have a similar module which makes it perform poorly in contextual learning.

To address this issue, Gu et al. propose the Mamba [12] architecture which improves the SSM from the following two aspects: *1). Selective Scan Operator* allows the model to filter relevant information out. In practical implementation, the Δ, $\mathbf{B}$, and $\mathbf{C}$ become the functions of the input, meanwhile, the matrix $\mathbf{A}$ keeps unchanged. *2). Hardware-aware Algorithm* that allows efficient storage of (intermediate) results through parallel scanning, kernel fusion, and recalculation. An illustration of the architecture of the Mamba block is provided in the right part of Fig. 1. Due to the key features, many researchers attempt to design their model using SSM or Mamba architectures.

3 STATE SPACE MODEL

In this section, we focus on reviewing the related works on the SSM architectures and applications. We divide the related works into the following domains, i.e., the origin and variation of SSM, natural language processing, computer vision, graph, multi-modal and multi-media, point cloud/event stream, time series data, and others. In the following subsections, we will introduce these algorithms one after another.

3.1 Origin and Variation of SSM

The State Space Model originates from Kalman filtering [35] which mainly introduces a linear filtering and prediction method. Kalman filtering can be divided into two steps, i.e., the prediction and correction step. The prediction is to estimate the current state based on the state of the previous time, and the correction is to estimate the
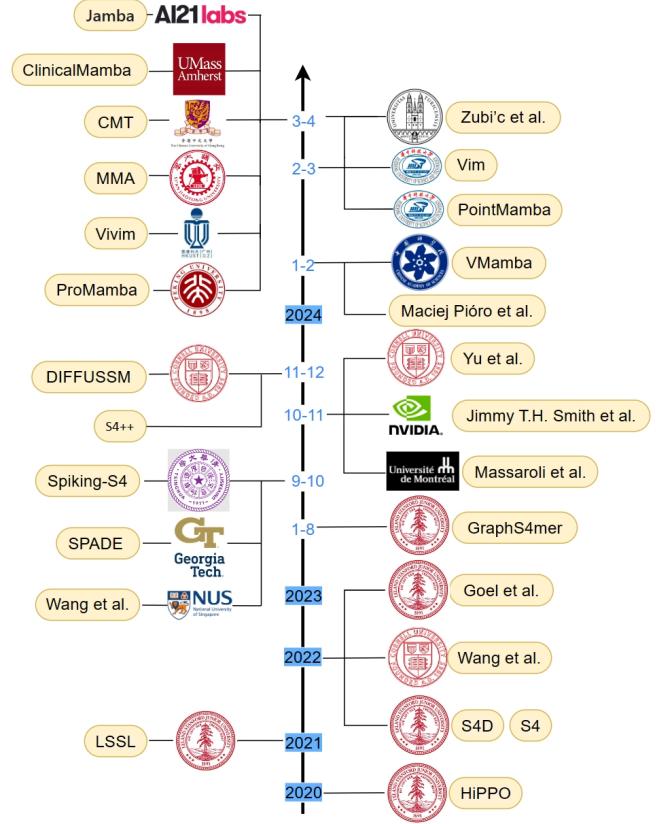

Fig. 4. The timeline of representative SSMs-based algorithms (from year 2020 to 2024.04.)

optimal state by integrating the estimated state and the observed state of the current time. The State Space Model is a mathematical model that describes the behavior of a dynamic system using a set of first-order differential equations (continuous-time systems) or difference equations (discrete-time systems) to represent the evolution of the internal state of the system, and another set of equations to describe the relationship between the state and the output of the system. These equations can be expressed in matrix and vector form to deal with multivariable systems. Subsequently, Gu et al. [34] introduces a Linear State Space Layer (LSSL) that combines the advantages of recurrent neural networks (RNNs), temporal convolutional networks, and neural differential equations (NDEs) while addressing their shortcomings in model power and computational efficiency. This new sequence model is inspired by control systems and implemented through the linear state space layer (LSSL).

Similar to RNNs, SSM also suffers from the vanishing/exploding gradients problem when modeling longer sequences. To tackle this issue, HiPPO [36] model combines the concepts of Recurrent Memory and Optimal Polynomial Projections, which can significantly improve the performance of recursive memory, This mechanism is very helpful for SSM to handle long sequences and long-term dependencies. The formula can be expressed as follows:

$$A_{nk} = \begin{cases} (2n+1)^{1/2}(2k+1)1/2 & \text{if } n > k \\ n+1 & \text{if } n = k \\ 0 & \text{if } n < k \end{cases} \tag{7}$$

TABLE 1
Summary of existing SSM-based models (Part-I).

#ID	Algorithm	Publish	Domain	Parameters	Architecture	Downstream Tasks	Accuracy	Efficiency	Code
1	Gu et al. [34]	NeurIPS21	Origin	-	LSSL	Classification	(sMNIST)acc: 99.50 (pMNIST)acc: 98.60 (sCIFAR)acc: 81.97	-	-
2	HiPPO [36]	NeurIPS20	Origin	-	-	Classification	(pMNIST)acc: 98.34	Speed: 470,000 (elements/sec)	URL
3	S4 [29]	ICLR22	Origin	249M	DPLR	Classification	(sMNIST)acc: 99.63 (pMNIST)acc: 98.70 (sCIFAR)acc: 91.13	Length1024: $1.58 \times$ Tranformer Length4096: $5.19 \times$ Tranformer MemoryAlloc: 33.5MB TrainingStep: 4.75MS	URL
4	S4D [37]	arXiv22	Origin	-	Diagonal	-	(LRA)avg: 86.09	-	-
5	DSS [38]	NeurIPS22	Origin	-	SSM	Classification Commands	(LRA)avg:81.88, Speech Commands acc:98.2	-	URL
6	LRU [39]	ICML23	Origin	-	RNNs, SSM	Classification CIFAR	(PATH-X)acc:94.2	Speed 15.9(steps/sec)	-
7	S4-LegS [40]	ICLR23	Origin	150K	S4, Math	Classification Commands, CIFAR	(LRA)avg:86.09 (CIFAR)avg:86.49 Speech Commands avg:90.67	-	-
8	GSS [41]	arXiv22	NLP	GSS-192M GSS-L-352M GSS-Hybrid-L-373M	SSM-former	Language modeling	Perplexity 10.52(arXiv)(↓)	5.6(steps/sec)	URL
9	Spiking-S4 [42]	arXiv23	NLP	0.53M	S4	Deep Noise Suppression	SISNR 14.58(DNS 2023)(↑) WB-PESQ 3.39 (Voice-Bank+Demand)(↑)	FLOPs:$1.5 * 10^9$	-
10	DPMamba [43]	arXiv24	NLP	DPMamba-XS 2.3M DPMamba-S 8.1M DPMamba-M 15.9M DPMamba-L 59.8M	Mamba	Speech Separation	SISNR 24.4(WSJ0-2mix)(↑)	-	-
11	SPMamba [44]	arXiv24	NLP	6.14M	Mamba	Speech Separation	SISNR 15.20 (SPMamba self-built)	Macs 78.69	URL
12	Grazzi et al. [45]	arXiv24	NLP	–	Mamba	Algorithmic Knowledge Linguistic Translation	Acc 0.93(Next letter) Acc 0.82(Location continent) Acc 0.90(Plural singular) Acc 0.78(En es)	–	-
13	S4++ [46]	-	NLP	ALM S4++: 49.85M BLM S4++: 134.11M	S4	Language Modeling Long-Range Dependency Modeling	PPL 25.31(WikiText-103)(↓) Avg 76.61(CLUE)(↑) Avg 78.31(LRA)(↑)	–	-
14	SPADE [47]	-	NLP	SPADEbase++: 290M	S4+Transformer	Language Modeling Long-Range Dependency Modeling Language Generation	PPL 18.5(WikiText-103)(↓) Avg 87.40(LRA)(↑) Avg 86.8(CLUE)(↑) ROUGE-2 21.65(arXiv)(↑)	sequence length 6k Memory: 27G	URL
15	DenseMamba [48]	arXiv24	NLP	DenseMamba-360M DenseMamba-1.3B	Mamba	Common-Sense Reasoning Question-Answering	Zero-shot Avg 54.51 (ARC_E,ARC_C) four-shot Avg 55.05 (ARC_E,ARC_C)	-	URL
16	ClinicalMamba [49]	arXiv24	NLP	ClinicalMamba-130M ClinicalMamba-2.8B	Mamba	Cohort Selection ICD Coding	Prec 88.6(n2c2 challenge in 2018) Prec 75.28(Code-rare) Prec 75.53(Code-common)	-	URL
17	MDLT [50]	arXiv24	NLP	-	Mamba	Translation	PhantomDance MDLT-T AJE:0.87 ± 0.02 FID: 0.39 ± 0.02 MDLT-M AJE:0.73 ± 0.01 FID:0.82 ± 0.01	-	URL
18	Graph-Mamba [51]	arXiv24	Graph	MalNet-Tiny 1400node FLOPs: $1.5 * 10^9$	GNN+Mamba	Graph-based prediction	MALNET-TINY: 93.4	MalNet-Tiny 1400node GPU Memory:150MB	URL
19	GraphS4mer [52]	CHIL23	Graph	TUSZ 32.768K	GNN+S4	ECG classification	TUSZ AUPRC 0.723±0.023 AUROC 0.906±0.012 F1-Score 0.680±0.012	-	URL
20	GRED [53]	arXiv23	Graph	-	GNN	Classification	MNIST: 98.223 ± 0.095	Average training time per epoch GPU: 3.7s memory: 1.5GB	URL
21	Graph Mamba [53]	arXiv24	Graph	-	GNN+Mamba	Classification	MNIST: 0.9839±0.0018	MalNet-Tiny 1200node GPU Memory:250MB	URL
22	Gregor et al. [54]	arXiv24	Graph	-	SSM	Prediction	graph Autoregressive accuracies: 48.5	-	URL
23	STG-Mamba [55]	arXiv24	Graph	-	SSSMs	Prediction	-	Inference Time on PeMS04: 3.08s	-

where n and k indicate the row and column indices of A.

Based on the above theoretical foundation, Gu et al. [29] propose the Structured State Space Sequence model (S4), which is a new parameterization method based on the vanilla State Space Model (SSM). Furthermore, Gu et al. [40] introduce a new approach to training State Space Model for capturing long-range dependencies in sequences, particularly showcased through the Structured State Space sequence model. By devising a generalized interpretation of the HiPPO framework and employing various basis functions like Legendre polynomials and Fourier transforms, the study significantly enhances S4's performance, shedding light on its theoretical underpinnings and practical applications in machine learning tasks. Gu et al. [122] also

explore how to parameterize and initialize Diagonal State Space Models (DSSM) and systematically investigate how to parameterize and initialize these diagonal State Space Models, demonstrating the importance of initialization for performance. Further, Gupta et al. [38] presents a compelling alternative to the Structured State Space (S4) model which further demonstrates that diagonal state spaces can achieve comparable performance even without the low-rank corrections. The Diagonal State Space (DSS) model offers simplicity in formulation and implementation while maintaining effectiveness in capturing long-range dependencies across various modalities, making it a promising avenue for practical applications in machine learning tasks. Orvieto et al. [39] investigates the resurgence of Recurrent Neural Net-

TABLE 2
Summary of existing SSM-based models (Part-II).

#ID	Algorithm	Publish	Domain	Parameters	Architecture	Downstream Tasks	Accuracy	Efficiency	Code
24	**S4nd** [30]	NeurIPS22	CV	S4ND-ViT-B (88.8M) S4ND-ConvNeXt-T (30.0M)	SSM+Former SSM+CNN	Classification	80.4(ImageNet) 82.2(ImageNet)	-	URL
25	**ViS4mer** [56]	ECCV22	CV	-	S4+Former	Understanding	Relation: 57.14(LVU) Speak: 40.79(LVU) Scene: 67.44(LVU)	-	URL
26	**S5(Smith et al.)** [57]	ICLR23	CV	280K	S4	Classification	16kHz: 96.52 8kHz: 94.53	-	-
27	**DiffuSSM** [31]	CVPR24	CV	673M	SSM	Generation	ImageNet 256 × 256 FID: 9.07	FLOPs 1.85×10^{11}	-
28	**LSMCL** [58]	CVPR23	CV	-	S4	Understanding	90.81(Kinetics-600) 90.70(COIN)	-	-
29	**DreamerV3** [59]	arXiv23	CV	XS: 8M S: 18M M: 37M L: 77M XL: 200M	RSSM	BSuite	Category mean: 0.627	-	URL
30	**VMamba** [60]	arXiv24	CV	Tiny: 22M Small: 44M Base: 75M	Mamba	Classification	ImageNet-1K top1 VMamba-T: 82.2 VMamba-S: 83.5 VMamba-B: 83.2	FLOPs Tiny: 4.5×10^9 Small: 9.1×10^9 Base: 15.2×10^9	URL
31	**Vim** [61]	arXiv23	CV	Vim-Ti:7M Vim-S:26M	Mamba	Classification	ImageNet-1K top1 Vim-Ti: 76.1 Vim-S: 80.5	-	URL
32	**SegMamba** [62]	arXiv24	CV	-	Mamba+CNN	Segmentation	BraTS2023 Dice-Avg: 91.32 HD95-Avg: 3.56 AIIB2023 IoU: 88.59	-	URL
33	**U-Mamba** [63]	arXiv24	CV	-	SSM+CNN	Segmentation	Abdomen CT organ 3D DSC:0.8683 MRI organ 3D DSC:0.8501 segmentation 2D F1:0.5607	-	URL
34	**Swin-UMamba** [64]	arXiv24	CV	28M	SSM+CNN	Segmentation	AbdomenMRI DSC:0.7760 NSD:0.8421 Endoscopy DSC:0.6783 NSD:0.6933	-	URL
35	**VM-UNet** [65]	arXiv24	CV	30M	SSM+CNN	Segmentation	ISIC17 mIoU:0.8023 Acc:0.9629 ISIC18 mIoU:0.8135 Acc:0.9491 Synapse DSC:0.8108 HD95:0.1921	-	URL
36	**nnMamba** [66]	arXiv24	CV	15.55M	SSM+CNN	Segmentation Classification Detection	BraTS2023GIL Dice:89.97 HD95:6.53 sMCIVSpMCI ACC:75.79±1.79 F156.55±2.37 AUC:76.84±0.84 landmark detection Error Rate:2.11	FLOPs 141.14G	URL
37	**Mamba-UNet** [67]	arXiv24	CV	-	SSM+CNN	Segmentation	MRI Cardiac Test Set Dice:0.9281 IoU:0.8698 Acc:0.9972 HD:2.4645 ASD:0.7677	-	URL
38	**Mamba-ND** [68]	arXiv24	CV	Mamba-2D-S:24M Mamba-2D-B:92M Mamba-3D:36M	Mamba	Classification Recognition Forecasting	ImageNet-1K Mamba-2D-S:81.7 Mamba-2D-B:83.0 HMDB-51 Mamba-2D:51.2 Mamba-3D:60.9 ERA5 Mamba-3D:90.1	-	URL
39	**DiS** [33]	arXiv24	CV	DiS-S/2:28M DiS-H/2:900M	Mamba	Generation	CIFAR10 DiS-S/2: 3.25 CelebA 64×64 DiS-S/2: 2.05 ImageNet 256×256 DiS-H/2: 2.10 ImageNet 512×512 DiS-H/2: 2.88	GFLOPs Small:0.43 Base:1.86 Medium:3.70 Large:6.57 Huge:14.79	URL
40	**DFVM-Net** [69]	arXiv24	CV	-	Mamba	Enhancement	33.99(E-kvasri)	-	URL
41	**Semi-Mamba-UNet** [70]	arXiv24	CV	-	SSM+CNN	Segmentation	0.9964(MRI)	-	URL
42	**P-Mamba** [71]	arXiv24	CV	-	Mamba	Segmentation	0.9316(PSAX) 0.9025(A4C)	-	-
43	**Weak-Mamba-Unet** [72]	arXiv24	CV	-	CNN ViT Mamba	Segmentation	MRI Cardiac Test Set Dice:0.9171 IoU:0.9963 Acc:0.9095	-	URL

TABLE 3
Summary of existing SSM-based models (Part-III).

#ID	Algorithm	Publish	Domain	Parameters	Architecture	Downstream Tasks	Accuracy	Efficiency	Code
44	**Pan-Mamba** [73]	arXiv24	CV	0.1827M	Mamba	pan-sharpening	42.2354(WorldView-II) 47.6453(Gaofen-2) 31.1551(WorldView-III)	FLOPs:3.0088G	URL
45	**Spectral SSM** [74]	arXiv24	CV	-	SSM	Prediction	91.3(CIFAR) 60.33(ListOps) 89.6(Text) 90.0(Retrieval) 95.6(Pathfinder) 90.1(PathX)	-	URL
46	**HIEROS** [75]	arXiv24	CV	37.1 M	SSM	Learning	Mean:120(Atari100k) Median:56(Atari100k) IQM:53(Atari100k) OptimalityGap:49(Atari100k)	-	URL
47	**2D-SSM** [76]	ICLR24	CV	ViT+SSM 2.73M Mega+2D-SSM 2.84M Swin+SSM 7.26M DeiT-T+SSM 5.541M DeiT-S+SSM 21.691M DeiT-B+SSM 85.845M Swin-T+SSM 27.558M	SSM	Classification	ImageNet-100 DeiT-T+2D-SSM 81.16 DeiT-S+2D-SSM 84.82 Swin-T+2D-SSM 82.29 CIFAR-10 MEGA+2D-SSM 91.31	-	URL
48	**MambaIR** [77]	arXiv24	CV	-	SSM	Restoration	image denoising: SIDD:(SSIM)0.960 DND:(SSIM)0.956	-	URL
49	**MambaMIR** [78]	arXiv24	CV	-	SSM+GAN	Reconstruction	0.600(fastMRI) Low-Dose CT Image 0.868	-	URL
50	**RES-VMAMBA** [79]	arXiv24	CV	-	SSM	Classification	top-1(val).ACC:79.54 top-5(val).ACC:95.72 top-1(test).ACC:78.26 top-5(test).ACC:95.31	-	URL
51	**MIM-ISTD** [80]	arXiv24	CV	1.16M	SSM	Detection	NUAA-SIRST IOU(80.80) nIoU(80.20) IRSTD-1k IOU(70.33) nIoU(67.82)	FLOPs: 1.01G GPU Memory: 1774M inference time: 0.03s	URL
52	**MEDMAMBA** [81]	arXiv24	CV	-	CNN+SSM	Classification	PathMNIST: AUC(0.997) ACC(0.951) DermaMNIST: AUC(0.907) ACC(0.758) BreastMNIST: AUC(0.879) ACC(0.872) OrganCMNIST: AUC(0.995) ACC(0.924)	-	URL
53	**Tang et al.** [82]	arXiv24	CV	18.41M	SSM+CNN	Segmentation	ISIC 2017 mIoU:80.51 Acc:96.46 ISIC 2018 mIoU:81.55 Acc:95.08	FLOPs:3.42G	-
54	**MamMIL** [83]	arXiv24	CV	-	SSM	Classification	Acc: 81.78(Camelyon16) 65.23(BRCAS) F1: 80.15(Camelyon16) 59.34(BRCAS) AUC: 82.92(Camelyon16) 84.23(BRCAS)	-	-
55	**VideoMamba** [84]	arXiv24	CV	Tiny:7M Small:26M Middle:74M Base:98M	SSM	Understanding	IN-1K(Top-1) Tiny:79.6 Small:83.5 Middle:84.0	FLOPs Tiny:7.1G Small:28.0G Middle:83.1G	URL
56	**LMa-UNet** [85]	arXiv24	CV	-	Mamba	Segmentation	90.02(3D Abdomen CT) 83.80(2D Abdomen MR)	-	URL
57	**MMA** [86]	arXiv24	CV	Scale ×2:796K Scale ×3:899K Scale ×4:879K	Vim	Super-Resolution	Manga109(Scale ×2) PSNR/SSIM:40.43/0.9814 Urban100(Scale ×2) PSNR/SSIM:34.13 / 0.9446	-	URL
58	**Caduceus** [87]	arXiv24	CV	Caduceus-PS:470K Caduceus-PH:470K	Mamba	Modeling	0.973(BMC Genomic Data)	-	URL
59	**Motion-Guided Dual-Camera Tracker** [88]	arXiv24	CV	-	Mamba+CMT	2D tracking 3D tracking	SUC 79.6(GIF-FQ260Z) PRE 79.8(GIF-FQ260Z)	-	-
60	**LightM-UNet** [89]	arXiv24	CV	1.87M	SSM+CNN	Segmentation	DSC 84.58 (LiTS) mIoU 77.48(LiTS)	-	URL
61	**Video Mamba Suite** [90]	arXiv24	CV	ViViM-T:7M ViViM-S:26M	SSM+ViT	Modeling	Acc:38.7(EgoSchema)	-	URL
62	**VM-UNetV2** [91]	arXiv24	CV	17.91M	SSM+CNN	Segmentation	mIoU 82.34(ISIC17) Acc 96.70(ISIC17) DSC 90.31(ISIC17)	-	URL
63	**LocalVim** [92]	arXiv24	CV	LocalVim-S:28M LocalVMamba-T:26M LocalVMamba-S:50M LocalVim-T:8M	SSM+former SSM	Classification Detection Segmentation	acc top-1 imagenet-1k 83.7 mIoU(ss) mIoU(ms) COCO 50.0 51.0	-	URL

TABLE 4
Summary of existing SSM-based models (Part-IV).

#ID	Algorithm	Publish	Domain	Parameters	Architecture	Downstream Tasks	Accuracy	Efficiency	Code
64	**MambaTalk** [93]	arXiv24	CV	-	SSM	Synthesis	FGD BC diversity 5.951 8.010 12.401 MSE LVD 0.760 7.531	-	-
65	**EfficientVMamba** [94]	arXiv24	CV	Tiny:6M Small:11M Base:33M	SSM	Classification Detection Segmentation	acc imagenet-1k Tiny:76.5 Small:78.7 Base:81.8	-	URL
66	**Du et al.** [95]	arXiv24	CV	-	SSM	Classification	top1 83.7(ImageNet-1K) 54.1(ImageNet-1K+FGSM) 34.7(ImageNet-1K+PGD)	-	-
67	**VmambaIR** [96]	arXiv24	CV	10.5M	SSM	Restoration Deraining	LPIPS 0.3379(NTIRE2020) 0.3891(AIM2019) PSNR 27.06(NTIRE2020) 23.90(AIM2019) SSIM 0.7501(NTIRE2020) 0.6972(AIM2019)	-	-
68	**MambaMorph** [97]	arXiv24	CV	7.59M	Mamba	Registration	SR-Reg(MR-CT) Dice(%)↑:82.71±1.45 HD95(mm)↓:2.00±0.22 IXI(T1-T2) Dice(%)↑:87.52±1.51 HD95(mm) ↓:1.53±0.24	GPU Memory:7.60GB	URL
69	**Vivim** [98]	arXiv24	CV	-	Mamba	Segmentation	breast US Jaccard:73.92 Dice:82.81 Precision:84.16 Recall:86.18	FPS: 37.04	URL
70	**ZigMa** [32]	arXiv24	CV	ZigMa-S:31.3M ZigMa-B:133.8M ZigMa-L:472.5M ZigMa-XL:1058.7M	Mamba	Generation	MS-COCO FID5k:33.8 FacesHQ-1024 FID5k:26.6 FDD5k:31.2 UCF101dataset Frame-FID5k:121.2 FVD5k:140.1	-	URL
71	**ProMamba** [99]	arXiv24	CV	102M	Mamba	Segmentation	Mean Dice:0.8528 IOU:0.7628	-	-
72	**H-vmunet** [100]	arXiv24	CV	-	VM-UNet	Segmentation	ISIC2017:0.9680 Spleen:0.9987 CVC-ClinicDB:0.9833	-	URL
73	**PlainMamba** [101]	arXiv24	CV	PlainMamba-L1:7.3M PlainMamba-L2:25.7M PlainMamba-L3:50.5M	Mamba	Classification Detection Segmentation	ImageNet-1K PlainMamba-L1: acc/top1:77.9 PlainMamba-L2: acc/top1:81.6 PlainMamba-L3: acc/top1:82.3	FLOPs:3.0G FLOPs:8.1G FLOPs:14.4G	URL
74	**Mamba-HUNet** [102]	arXiv24	CV	-	Mamba+UNet	Segmentation	U-Net：IOU(0.8170) Swin-Unet:IOU(0.7947) Mamba-UNet :IOU(0.8322) Mamba-HUNet:IOU(0.8536)	-	-
75	**VMRNN** [103]	arXiv24	CV	2.6M	VMamba+LSTM	Forecasting	MSE:16.5(Moving MNIST) SSIM:0.965(Moving MNIST)	FLOPs:0.9G	URL
76	**Gamba** [104]	arXiv24	CV	-	Mamba	Reconstruction	OmniObject3D PSNR↑:19.20 LPIPS↓:0.15 CLIP-D ↓:0.39	-	-
77	**VMambaMorph** [105]	arXiv24	CV	9.64MB	Mamba	Registration	SR-Reg Dice:82.49±1.99	GPU Memory:3.25GB	URL
78	**T-Mamba** [106]	arXiv24	CV	-	Mamba	Segmentation	IoU:88.31 SO:97.53	-	URL
79	**SpikeMba** [107]	arXiv24	CV	-	Mamba	Grounding	R1:64.13 mAP:43.79	-	-
80	**RS3Mamba** [108]	arXiv24	CV	43.32M	Mamba+CNN	Segmentation	ISPRS VAIHINGEN mF1:90.34 mIoU:82.78 LOVEDA URBAN mF1:66.86 mIoU:50.93	-	URL
81	**HARMamba** [107]	arXiv24	CV	0.7966M (PAMAP2) 0.7880M (UCI) 0.7883M (UNIMIB HAR) 0.7877M(WISDM)	Mamba	HAR	Accuracy 99.91 (PAMAP2) 97.65(UCI) 88.08 (UNIMIB HAR) 98.25(WISDM)	FLOPs(M) 279.21 (PAMAP2) 237.83 (UCI) 238.36 (UNIMIB HAR) 256.52 (WISDM)	-
82	**HSIMamba** [108]	arXiv24	CV	-	HSIMamba+SpatialBlock	Classification	UH2013: (OA)0.9789 (AA)0.9813 (Kappa)0.9771	Training (s):161 Memory (MB):126	URL
83	**Chen et al.** [109]	arXiv24	CV	MambaBCD Tiny:17.13M Small:49.94M Base:84.70M MamabaSCD Tiny:19.44M Small:51.82M Base:87.47M	Mamba	Detection	ManbaBCD F1:83.11 (SYSU) IoU:71.10(SYSU) F1:88.39 (LEVIR-CD+) IoU:79.20 (LEVIR-CD+) MambaSCD F1:64.10(SECOND) IoU:73.61(SECOND)	-	URL

TABLE 5
Summary of existing SSM-based models (Part-V).

#ID	Algorithm	Publish	Domain	Parameters	Architecture	Downstream Tasks	Accuracy	Efficiency	Code
84	**Serpent** [110]	arXiv24	CV	-	SSM	Restoration	Gaussian deblurring(×512) PSNR:28.51 SSIM:0.7799 LPIPS:0.4124	-	-
85	**ReMamber** [111]	arXiv24	CV	-	Mamba	Segmentation	RefCOCO testA:76.74 testB:70.89 RefCOCO+ testA:70.78 testB:57.53 G-Ref test:64.0	-	-
86	**InsectMamber** [112]	arXiv24	CV	-	Mamba	Classification	Farm Insects F1: 76.74 Agricultural Pests F1: 0.91 Insect Recognition F1: 0.86 Forestry Pest Identification F1: 0.94	-	-
87	**Samba** [113]	arXiv24	CV	Samba: 51.9M ResNet50 64.0M Swin-T 58.9M	Mamba	Segmentation	LoveDA dataset: Samba mIoU:43.32 ResNet50 mIoU:32.86 Swin-T mIoU:41.08	-	URL
88	**MambaMixer** [114]	arXiv24	CV	ViM2-MLP: 40M ViM2-T: 20M ViM2-S: 43M ViM2-B: 74M	SSM+CNN	Classification, Detection, Segmentation, Forecasting	ImageNet-1K ViM2-B acc: 83.9 ADE20K ViM2-S: mIoU (ss): 50.2 mIoU (ms): 51.4 COCO ViM2-S 69.9 66.8		-
89	**UltraLight VM-UNet** [115]	arXiv24	CV	0.049M	VMamba+CNN	Segmentation	ISIC2017 DSC/top1: 0.9091 SE/top1: 0.9053 SP: 0.9790 ACC: 0.9646 ISIC2018 DSC/top1: 0.8940 SE: 0.8680 SP: 0.9781 ACC/top1: 0.9558 PH^2 DSC/top1: 0.9265 SE/top1: 0.9345 SP/top1: 0.9606 ACC/top1: 0.9521	GPU Memory: 32GB GFLOPs: 31.65	URL
90	**RhythmMamba** [116]	arXiv24	CV	1.065M	Mamba	Measurement	PURE MAE:0.23 RMSE:0.34	-	URL
91	**MambaAD** [117]	arXiv24	CV	25.7M	SSM	Detection	MVTec-AD (Image-level) AP:99.6 F1-max:97.8 (Pixel-level) AP:56.3 F1-max:59.2	FLOPs:8.3G	URL
92	**Simba** [118]	arXiv24	CV	-	SSM	Recognition	NTU RGB+D 60 X-Sub:89.03 X-View:94.38 NTU RGB+D 120 X-Sub:79.75 X-Set:86.28	-	-
93	**ViM-UNet** [119]	arXiv24	CV	ViM-UNet_T:18M ViM-UNet_S: 39M	Vim	Segmentation	(LIVECell) ViM-UNet_T:0.05 (2.7e-3) ViM-UNet_S:0.05 (4.6e-3) (CREMI) ViM-UNet_T:0.74 (3e-2) ViM-UNet_S:0.82 (2.4e-2)	ViM-UNet_T:⩽ 9GB ViM-UNet_S:⩽ 10GB	URL
94	**DGMamba** [120]	arXiv24	CV	22M	Mamba	Generalization	Art:91.3 Cartoon:87.0 Photo:99.0 Sketch:87.3 Avg:80.8	GFlOPs:5	URL
95	**FusionMamba** [121]	arXiv24	CV	0.77M	Mamba	Fusion	Reduced-Resolution PSNR:39.283±2.986 Q8:0.921±0.085 SAM:2.848±0.571 ERGAS:2.107±0.507	GFLOPs:30.4	-

works (RNNs) for handling long sequences by leveraging insights from deep SSMs. By refining RNN architectures through techniques such as linearization, diagonalization, and improved parameterization, the research unveils a new RNN block called the Linear Recurrent Unit (LRU) capable of achieving comparable performance to deep SSMs while maintaining computational efficiency. Mamba [12] was achieved by combining the design of the previous SSM architecture with the MLP block of Transformer to simplify the architecture. Mamba introduces a selection mechanism in the structured State Space Model to filter out irrele-vant information and retain useful information. Adding a Hardware-aware algorithm improves computing efficiency. Mamba achieves the most advanced results in different areas, especially in language, and is a strong candidate as the backbone of general sequences. Some works [123], [124] offer an accessible overview of SSMs, which have garnered attention for their effectiveness in handling long sequential data and laying a foundation for understanding future SSM variants.

In addition to these models, some works can also be seen as the SSM, such as RWKV [125], Vision-RWKV [126],
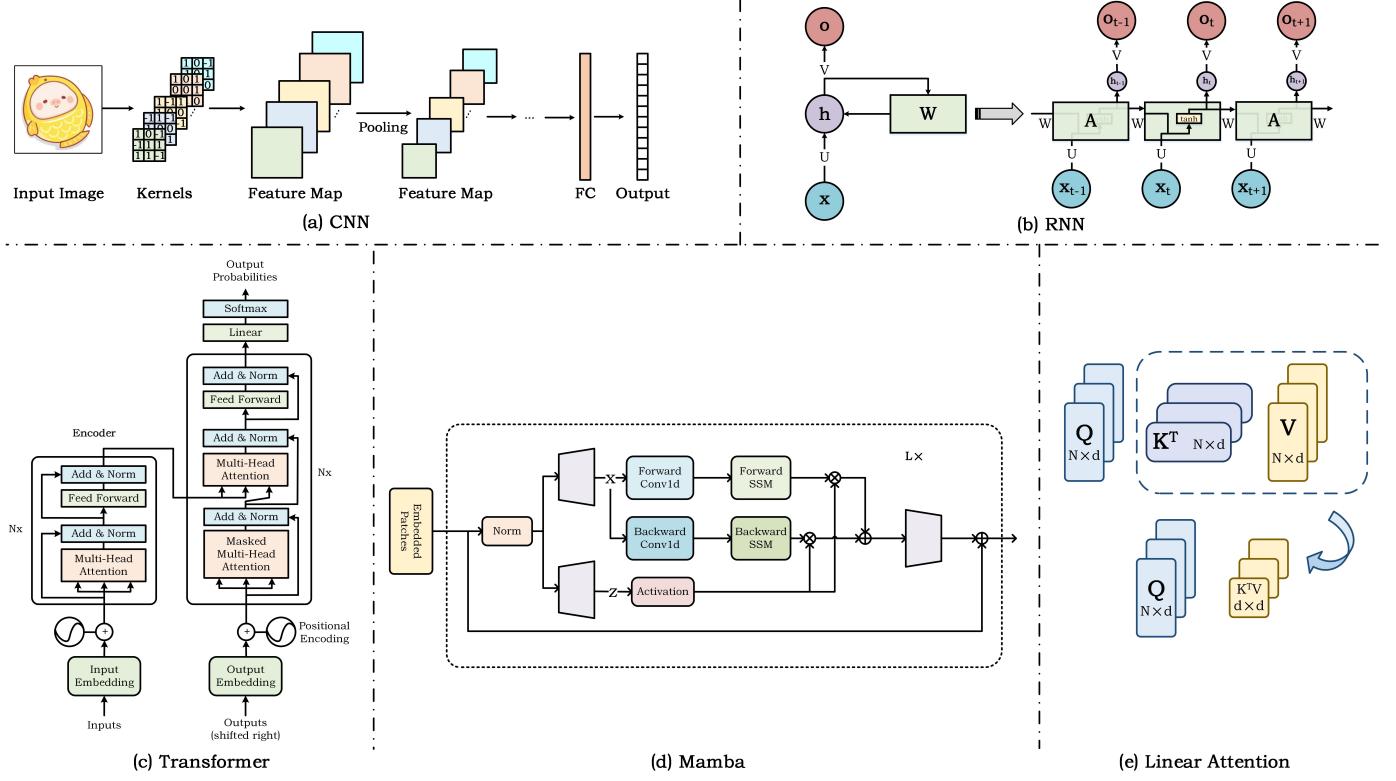
Fig. 5. A comparison between CNN, RNN, Transformer, Mamba, and Linear Attention.

RetNet [127], Mega [128], H3 [129]. Specifically, Receptance Weighted Key Value (short for RWKV) [125] is a kind of RNN architecture and is developed based on attention-free Transformer [130] for natural language processing. It simultaneously features in the efficient parallelizable training of transformers and the efficient inference of RNNs. Duan et al. further adapt this framework to the computer vision tasks and propose the Vision-RWKV (VRWKV) [126] model. Their results demonstrate that it beats the ViT in the image classification task and also has significant advantages in speed, and memory usage (when processing the high-resolution inputs). The RWKV architecture is also widely used in many other tasks, such as time series related task [131], online action detection [132], diffusion model [133]. RetNet [127] is short for Retentive Network, which also targets building a large language model that achieves training parallelism, low-cost inference, and high performance, simultaneously. It supports parallel, recurrent, and chunkwise recurrent computation paradigms.

Based on the origin and variations of SSM mentioned above, many SSM-based works are constantly emerging, including but not limited to natural language processing, computer vision, and so on. The following summaries will respectively introduce the expansion and application of various fields.

3.2 Natural Language Processing

In recent years, the development of large language models has revolutionized the field of natural language processing, however, the widely used Transformer architecture is limited by high computational and memory requirements.

To address these issues, many researchers devoted themselves to simplifying the Transformers to achieve efficient computation and limited memory requirements. Among them, State Space Model is one of the most effective solutions we reviewed in this paper.

With the emergence of the Mamba [12], the SSM model is increasingly attracting attention and favor from current researchers. The following works are currently explored in language modeling task [41] [45] [46] [47] [48], deep noise suppression task [42], and clinical note understanding task [49]. To be specific, for the language modeling task, [41] mainly studies the application of gated state spaces in the direction of long-range language modeling and introduces a novel method called GSS (Gated State Space). It can be used on long sequence modeling and effectively reduce the number of participants. Their experiments demonstrate that it achieves 2-3 times faster than the DSS [38]. Grazzi et al. [45] exploit the Mamba on simple function estimation and natural language processing in context learning tasks and validate that the overall performance is indeed better than the S4 version and comparable to other Transformer networks. S4++ [46] finds two issues of S4 architecture, i.e., the non-stationary state (NSS) and dependency bias, and proposes the State Memory Reply (SMR) mechanism to integrate multi-state information into the current state. They also integrate complex dependency bias via an interactive cross-attention mechanism and extensive experimental results show that S4++ outperforms S4 on multiple sequence modeling tasks, demonstrating significant performance gains. [47] synthesizes State Space Model and local attention mechanism to reduce memory consumption and

speed up training efficiency while ensuring performance. The authors use local attention to extract local information, and then use the state-space model to extract the global information missing from local attention. [48] argues that existing State Space Models, while efficient, lack in performance. The authors believe the reason for this is that too many state transitions make the model lose shallow information. So the authors propose a design that integrates the hidden states in the previous layers into the subsequent layers to retain more shallow information. Eventually, after pre-training on Pile, the experimental results of Zero-shot and four-shot on other datasets are significantly improved. For voice tasks, Du et al. [42] combine the high efficiency of impulse neural networks and the ability to model long distances with the state-space model S4 to obtain an spiking neural network, which has a low number of parameters but comparable performance to that of some artificial neural network (ANN) in deep noise suppression task. In addition, for speech separation task, DPMamba [43] proposed by Jiang et al. uses the selective State Space Model Mamba to replace the traditional transformer architecture. DPMamba simultaneously models the short-term and long-term forward and backward dependencies of speech signals through selective state space, achieving comparable results to the dual-path Transformer model Sepformer [134]. SP-Mamba [44] proposed by Li et al. uses TF-GridNet [135] as the basic framework and replaces the Transformer module with a bidirectional Mamba module to capture a wider range of language information. Experimental results show that Mamba-based models play an important role in performance.

In the clinical notes Understanding task, Yang et al. [49] exploits the linear computational complexity of Mamba to model very long sequences of clinical notes, with sequence lengths of up to 16k. The authors use the MIMIC-III dataset to pre-train the Mamba model, which is then tested on a cohort selection task and an ICD coding task, and demonstrates superior performance in modeling clinical language, especially at longer text lengths, when compared to both the Mamba and the clinical Llama models. Compared to Mamba and clinical Llama models, it shows superior performance in modeling clinical language, especially at longer text lengths. In the translation task, [50] formulates the problem of generating dance choreography as a translation task and proposes the MDLT which utilizes existing datasets to learn how to translate audio sequences into corresponding dance poses.

3.3 Computer Vision

Recently, the linear time series modeling of the State Space Model has attracted widespread attention, demonstrating strong performance in the field of natural language processing. Inspired by these progress, many SSM-based vision models have been proposed, including classification task [30], [57], [60], [61], [68], [76], [83], [92]–[96], [101], [112], [137], [138], detection task [80], [109], [117], segmentation task [70], [71], [82], [85], [89], [91], [106], [108], [111], medical tasks [63], [64], [69], [72], [87], [97]–[100], restoration task [77], [110], generation task [31]–[33], video understanding [56], [58], [90], track task [88], and others task [32], [59], [62], [73]–[75], [103]–[105], [107], [116], [118], [120], [121].
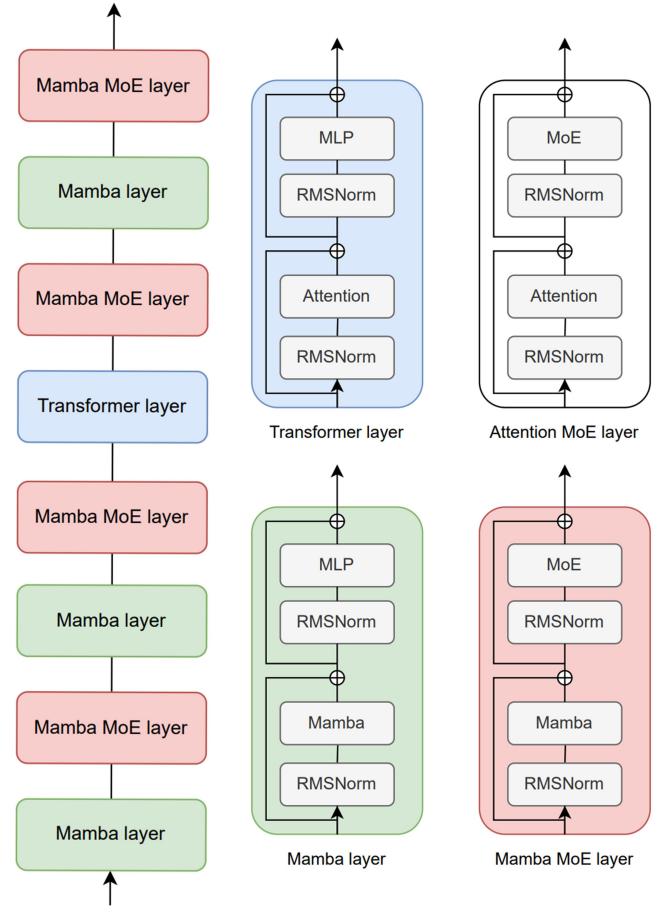

Fig. 6. Illustration of Jamba block [136] and used different types of layers.

In the classification task, S4nd [30] proposes a multi-dimensional and multi-polar graphics component to expand the modeling capability of multi-dimensional data continuous signals, which can model large-scale visual data into dynamic multi-dimensional linear signals. VMamba [60] uses linear complexity to capture the full range of sensory fields, introduces traversal of spatial information across scan blocks, and converts non-causal visual images into ordered patch sequences. Vim [61] uses a bidirectional state-space model to compress visual representation information and understand the global context through location embedding and visual information. Li et al. present Mamba-ND [68], an extension of Mamba designed to handle arbitrary multi-dimensional data by processing input data across dimensions in a row-major order. The authors of [57] design S5 based on S4 to establish the relationship between S5 and S4, utilize multi-input multi-output SSM, and use the state space layer of parallel scanning for long-distance sequence modeling. Baron et al. [76] design a new 2-dimensional State Space Layer for Spatial Inductive Bias. The core goals of this layer are to achieve perception of 2-D position, dynamic spatial localization, and translation and alignment invariance. Chen et al. [79] are the first to integrate residuals into the original VMamba, and maintain the inherent global and local state characteristics of the original VMamba for food classification. Yang et al. [101] propose the PlainMamba, which further adapts Mamba's selective scanning process

(a). VMamba model (VMamba-T)

(b). VSS Block

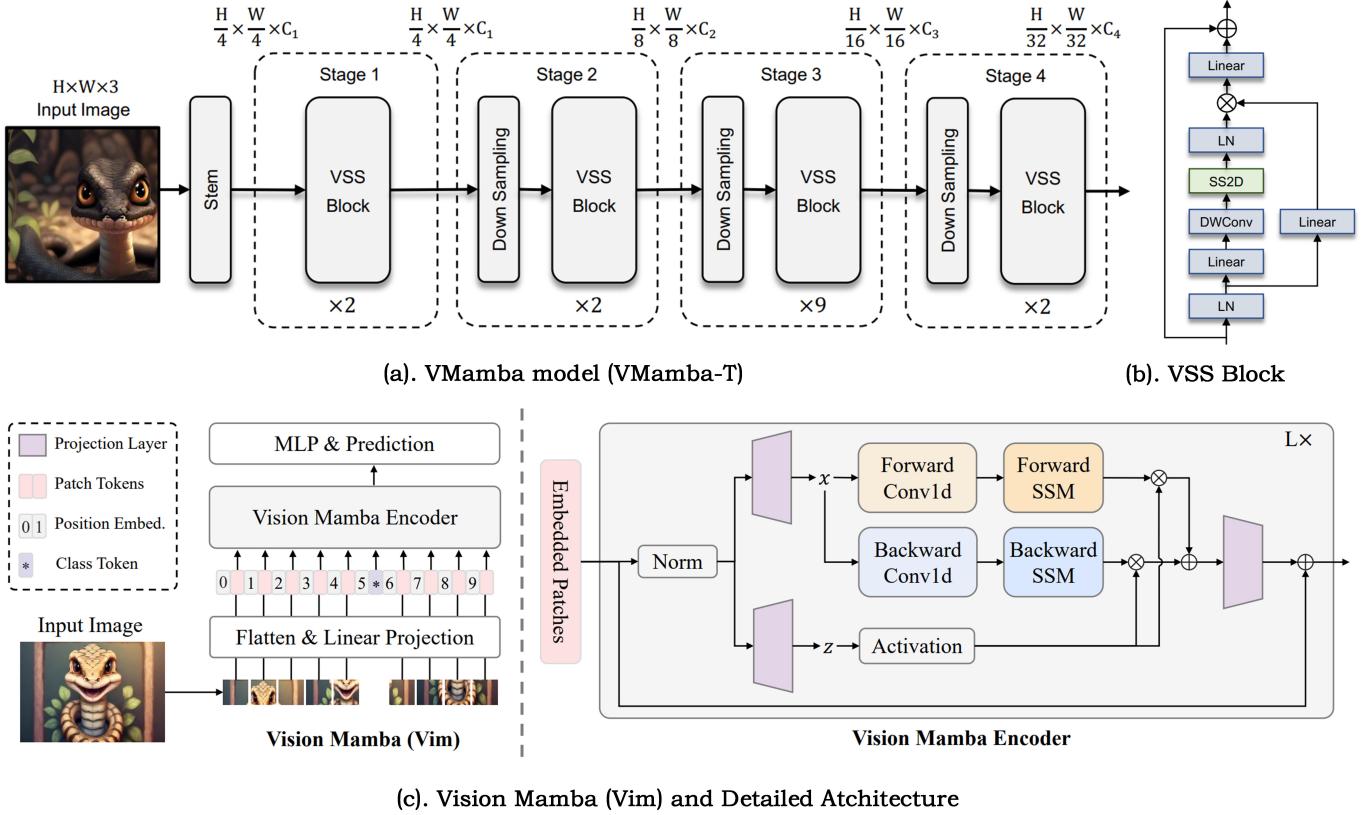(c). Vision Mamba (Vim) and Detailed Atchitecture

Fig. 7. An overview of the VMamba model (VMamba-T) [61] and Vision Mamba (Vim) [60].

to the visual field. By improving spatial continuity through the continuous 2D scanning process and updating direction perception, the model can distinguish spatial relationships of labels by encoding direction information, thereby enhancing its ability to learn features from 2D images. Wang et al. propose InsectMamba [112] that can be used in the insect classification task and improve the classification ability of the model by integrating a State Space Model, a convolutional neural network (CNN), a multi-head self-attention mechanism (MSA), and multi-layer perceptrons (MLPs) in a hybrid state space module (Mix-SSM).

Huang et al. introduce LocalMamba [92], which proposes a new local scanning strategy to preserve the two-dimensional dependencies of spatial tokens. They conduct extensive experiments on various tasks and demonstrate that LocalMamba improves over Vim-T by +3.1% on the ImageNet classification. Xu et al. [93] introduce an SSM model termed MambaTalk which focuses on gesture synthesis and supports long and various sequences. Pei et al. [94] proposes the EfficientVMamba by incorporating additional convolutional branches and further improves the baseline significantly on the ImageNet-1K and COCO detection datasets. Du et al. [95] explore the robustness of VMamba from various aspects, for example, they investigate the resilience to adversarial attacks using both whole-image and patch-specific methods, revealing superior robustness compared to Transformer architectures but with scalability weaknesses. They also assess VMamba's general robustness across diverse scenarios. Shi et al. [96] propose a new image restoration method, VmambaIR, which overcomes some of

the shortcomings of traditional methods by introducing the linear complexity of state-space modeling to a comprehensive image restoration task. Fang et al. [83] present the MamMIL framework to address the classifying of whole slide images which is the first work to combine the selective structured State Space Model (Mamba) and a multi-instance learning (MIL) approach. MamMIL outperforms existing state-of-the-art MIL frameworks based on Transformer in terms of classification performance and memory usage. Li et al. introduce a novel approach to wearable sensor human activity recognition (HAR) called HARMamba [137], which utilizes a lightweight selective State Space Model (SSM) designed to address computational resource constraints typical of real-time mobile applications. Yang et al. introduce a novel hyperspectral image classification framework called HSIMamba [138], which aims to address the complexity and high-dimensional nature of hyperspectral imaging data in remote sensing. The proposed framework incorporates a bidirectional reversed CNN to efficiently extract spectral features, alongside a specialized block for spatial analysis.

For the detection task, Chen et al. [80] propose a Mamba-in-Mamba (MiM-ISTD) structure to detect the infrared small targets. In this structure, the images are evenly divided into "visual sentences" (patches) and further subdivided into "visual words" (sub-patches), and a pure Mamba-based MiM pyramid encoder is designed to extract global and local features. Chen et al. [109] explore the potential of the Mamba architecture for remote sensing image change detection tasks by employing visual Mamba as an encoder which is capable of fully learning the global contextual

information of the input image. Three methods for the modeling of spatio-temporal relationships are proposed for the decoder, taking full advantage of the properties and benefits of the Mamba architecture. He et al. [117] capture long-range and local information effectively through parallel cascaded hybrid state space and multi-kernel convolution operations.

For the segmentation task, a semi-supervised medical image segmentation method termed Semi-Mamba-UNet [70] is proposed which combines a visual mamba-based UNet architecture with the conventional UNet. It utilizes dual networks to generate pseudo labels and mutually cross-supervise each other. Additionally, it employs a self-supervised pixel-level contrastive learning strategy to bolster feature learning capabilities. P-Mamba [71] is designed for Efficient Pediatric Echocardiographic Left Ventricular Segmentation, which tackles the challenges associated with accurately segmenting the left ventricle in pediatric echocardiograms. Liao [89] introduces the LightM-UNet, a streamlined framework that merges Mamba and UNet to tackle computational constraints in medical image segmentation. It extracts profound semantic features and captures extensive spatial dependencies with linear computational complexity. Empirical evaluations on real-world datasets underscore LightM-UNet's supremacy over current leading methods, showcasing substantial reductions in both parameter count and computational overhead. Zhang et al. [91] propose an SSM-based U-Net variant medical image segmentation model, VM-UNetV2, which fully utilizes the capabilities of SSM models. By initializing the encoder using VMamba pretrained weights and employing a deep supervision mechanism, VM-UNetV2 demonstrates competitive segmentation performance on multiple datasets. U-mamba [63], as a general-purpose CNN-SSM network, enhances biomedical image segmentation by integrating local CNN features with long-range dependencies of SSMs. Leveraging ImageNet-based pretraining, Swin-umamba [64], a novel Mamba-based model, outperforms CNNs, ViTs, and existing Mamba models. It demonstrates superior performance with lower memory and computational burden and reveals the essential role of ImageNet-based pretraining in promoting the performance of Mammba family models.

VM-UNet [65] establishes a baseline as the first pure SSM-based model for medical image segmentation. It competes effectively on ISIC17, ISIC18, and Synapse datasets, offering insights for future SSM-based segmentation systems. Gong et al. [66] propose the nnMamba which combines CNNs' detailed feature extraction with SSMs' broad dependency modeling, excelling in 3D medical image tasks. It proposes the Mamba-In-Convolution with Channel-Spatial Siamese learning (MICCSS) block to model the long-range relationship of the voxels. The superior performance is gained in 3D segmentation, classification, and landmark detection across 6 datasets. LMa-UNet [85] is a novel Large Window-based Mamba U-shape Network, leveraging large windows for improved spatial modeling compared to CNNs and Transformers, maintaining efficiency with linear complexity. It introduces a hierarchical and bidirectional Mamba block to enhance global and local spatial modeling. Tang et al. [82] use triple state space to fuse features in spatial and channel dimensions, and residual blocks to extract dense context features. Kazi et al. [102] take advantage of

Mamba-UNet and the lighter version of the Hierarchical Upsampling Network (HUNet), the local feature extraction ability of the convolutional neural network is combined with the remote dependency modeling ability of the State Space Model. RS3Mamba [108] propose a novel two-branch network called RS3Mamba, which introduces a novel visual state space (VSS) model, Mamba, to the task of semantic segmentation of remotely sensed imagery. RS3Mamba constructs an auxiliary branch using the VSS blocks to provide additional global information for the main branch and introduces a co-completion module (CCM) to augment and fuse features from the dual encoder. Hao et al. [106] introduce a 3D CBCT segmentation method for teeth, termed T-Mamba, which enhances spatial position preservation and feature enhancement in the frequency domain by fusing shared position coding and frequency-based features. T-Mamba is the first work that introduces frequency features into the visual mamba architecture. Zhu et al. [113] propose a new semantic segmentation framework Samba based on the Mamba architecture and design specifically for high-resolution remote sensing images. Samba demonstrates the effectiveness and potential of the Mamba architecture in semantic segmentation of remote sensing images, surpassing current state-of-the-art CNN and ViT-based methods. Ma et al. [108] propose a novel dual branch network called RS3Mamba,which utilizes VSS blocks to construct auxiliary branches, providing additional global information for convolutional based main branches. In addition, considering the feature differences between the two branches, a Collaborative Completion Module (CCM) is introduced to enhance and fuse features from the dual encoder. Archit et al. [119] propose a new medical image segmentation network architecture, ViM-UNet. It is based on the latest Vision Mamba architecture and compared with traditional UNet and Transformer-based UNETR.

For the medical image based analysis, Guo et al. [97] introduce a medical MR-CT deformable registration method based on the Mamba framework, named MambaMorph. The key to this method lies in achieving voxel-level spatial correspondence capture across different imaging modalities, which is crucial for medical image analysis. Xie et al. introduce a new polyp segmentation model ProMamba [99] based on the Vision Mamba architecture and prompts technology. It is the first time to introduce the Vision Mamba and prompts into polyp segmentation. Wu et al. [100] introduce a novel neural network for medical image segmentation based on SSM and SS2D, called High-order Vision Mamba UNet (H-vmunet), which gradually reduces the introduction of redundant information through advanced interaction and enhances the ability of SS2D to learn local features at each interaction stage. Vivim is proposed by Yang et al. [98], which targets effectively compressing long-term spatio-temporal representations into sequences of different scales through the designed time Mamba blocks for medical video object segmentation. Due to the scarcity of large labeled medical datasets, Wang et al. [72] propose the Weak-Mamba-Unet architecture, which attempts to address this challenge by training a Mamba-based UNet in a weakly-supervised manner. It leverages convolutional neural networks (CNNs), Vision Transformers (ViTs), and Vmamba to predict the data labels, then, generate dense pseudo labels.
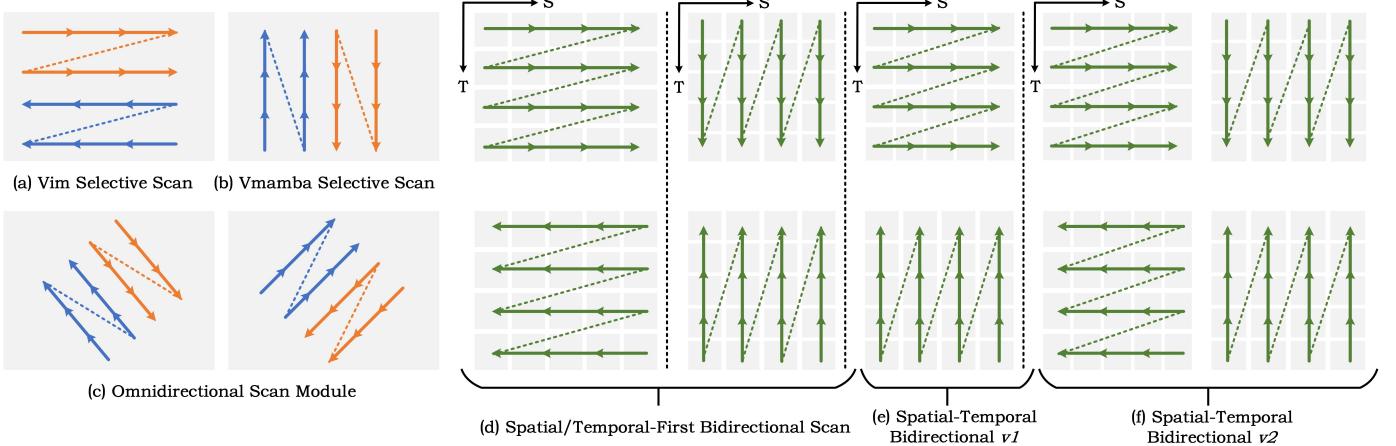
Fig. 8. Different selective scan methods used in SSMs proposed for image and video processing. (a) VMamba [61], (b) Vision Mamba [60], (c) RSMamba [139], (d-f) Video Mamba [84].

Zheng et al. [69] describe a novel network architecture called FD-Vision Mamba (FDVM-Net) designed to correct exposure abnormalities in endoscopic images. This is crucial for maintaining image quality to assist healthcare professionals in their decision-making process. FDVM-Net operates in the frequency domain and reconstructs the endoscopic image's frequency representation to improve exposure. Xing et al. [62] propose the SegmamBA module to enhance 3D feature modeling, which uses gated spatial convolution internally to enhance feature representation in spatial dimension to deal with long-distance dependency. Yue et al. [81] propose the MedMamba based on the State Space Model and convolutional layers for medical image classification. It can effectively capture long-range dependencies while maintaining the ability to extract local features, which is suitable for medical images of different modalities. Huang et al. [78] inherit the advantages of the original Mamba linear complexity and global receptive field, and propose an arbitrary mask mechanism to adapt the Mamba to the image reconstruction task, termed MambaMIR-GAN. Schiff et al. [87] extend the Mamba block into a component supporting bi-directional BiMamba and a MambaDNA supporting RC equivariant. Then, they use the MambaDNA as a basis for Caduceus and incorporate pre-training and fine-tuning strategies for DNA Sequence Modeling.

For the restoration tasks, Guo et al. [77] propose a new image restoration model, termed MambaIR, which aims to explore the potential of Mamba in low-level vision, the model leverages the long-range dependent modeling capabilities of the Mamba state-space model while combining prior knowledge unique to image restoration tasks, such as local block repetition and channel interaction. Serpent [110] uses the State Space Model to maintain a global receptive field with linear scaling of input sizes which significantly reduces the cost of computing resources and GPU memory.

For the generation task, ZigMa [32] introduces a new diffusion model based on the Mamba structure, called ZigMa, which targets addressing the scalability and quadratic complexity issues of existing diffusion models, especially in Transformer structures. DiffuSSM [31] is a scalable state-space model that handles higher resolutions and can retain a detailed image representation throughout the diffusion process, as it does not use global compression. DiS [33] is a new category of diffusion models that are based on a state space architecture. It aims to train diffusion models for image data, replacing the traditional U-Net-like backbone with a state space backbone that operates on raw patches or latent space.

For video understanding, ViS4mer [56] utilizes a multi-scale temporal structured state-space sequence decoder for long-term inference. The resolution of spatiotemporal features and channel dimension of each decoder layer are gradually reduced, enabling the learning of complex long-range spatiotemporal dependencies. Wang et al. propose the LSMCL [58] which is a learning method of short and long mask contrast and can predict long-range spatiotemporal information. Chen et al. [90] evaluate the Mamba's potential as an alternative to Transformers in video understanding, explore different roles that the Mamba can play in video modeling, and assess its performance across diverse video understanding tasks. Li et al. [84] propose a video understanding model based on the State Space Model, Video-Mamba, which can efficiently process long videos.

To maintain the consistency of dual-camera tracking and address the large variation in the endoscope tip appearance, Zhang et al. [88] propose a cross-camera mutual template strategy (CMT) and introduce a dynamic transient mutual template during tracking. A Mamba-based motion-guided predictive head (MMH) is introduced to minimize the interference caused by large area occlusion and the distortion caused by the endoscope tip light source.

In the other tasks, as more researchers recognize the advantages of Mamba, this model has gained traction across various fields. Pan-Mamba [73] represents the first foray into the pan-sharpening domain. It comprises two main modules: the channel swapping Mamba and the cross-modal Mamba. The channel swapping Mamba aims to fuse and enhance the diversity of features from PAN channels and LRMS channels in a lightweight and efficient manner. The latter module, the cross-modal Mamba, is deployed after the channel swapping Mamba to filter redundant modal characteristics through gating mechanisms. DreamerV3 [59]

is a universal and extensible method based on the world model, which overcomes the limitations of fixed parameter range in various fields in terms of the input, dimension, and reward of data. For long-range prediction, Naman et al. [74] introduce a novel approach to sequence modeling, called Spectral State SSM, which is based on learning linear dynamical systems (LDS) using the spectral filtering algorithm. This architecture guarantees stable and efficient learning even for marginally stable symmetric LDS. For reinforcement learning tasks, HIEROS [75], a hierarchical policy aims at improving sample efficiency. HIEROS utilizes a hierarchical world model, specifically an S5 layer-based world model (S5WM), and an efficient time-balanced sampling method. It outperforms existing approaches in terms of mean and median normalized human scores on the Atari 100k benchmark and demonstrates superior exploration capabilities. Cheng et al. [86] explore how modern State Space Models, Vim, can enhance the performance of convolutional neural networks (CNN) and visual Transformers (ViT) in the field of single image super-resolution (SISR) through a wider range of activation regions. VMRNN [103] is a new recurrent unit that combines Vision Mamba blocks with LSTM for precise and efficient spatiotemporal forecasting. Shen et al. [104] introduce Gamba, an end-to-end, amortized 3D reconstruction model from single-view images. Their main discovery involves utilizing a substantial number of 3D Gaussians to enhance the efficiency of the 3D Gaussian splatting process. Additionally, they introduce a Mamba-based sequential network, enabling context-dependent reasoning and linear scalability with sequence (token) length, aiming to tackle high memory demands and resource-intensive rendering processes. Wang et al. [105] introduce a novel visual Mamba-based framework called VMambaMorph, which has cross-scanning modules for deformable 3D image registration. Li et al. [107] propose a novel approach called SpikeMba for dealing with temporal video localization tasks. SpikeMba integrates Impulse Neural Networks and State Space Models (SSMs) to efficiently capture the fine-grained relationships between multimodal features. Zou et al. [116] proposes a new remote photoplethysmography (rPPG) signal detection method based on Mamba, called RhythmMamba. RhythmMamba is an end-to-end method that employs multi-temporal constraints to capture both periodic patterns and short-term trends in rPPG. Additionally, it utilizes frequency domain feedforward to enhance Mamba's ability to robustly interpret the quasi-periodic rPPG patterns.

3.4 Graph

In addition to the standard grid data (e.g., image), structured graph data is also widely studied in artificial intelligence, such as the social network and protein structure data. Because its input type is sequential data, thus, we can apply the SSMs to process the graph-structured data. Specifically, GraphS4mer [52] leverages the Structured State Space (S4) architecture to capture long-range temporal dependencies and introduces a graph structure learning layer to dynamically evolve graph structures, adapting to the data's spatial correlations over time. GMNs [53] is a new class of Graph Neural Networks (GNNs) based on

selective State Space Models, tackling the limitations of traditional GNNs in capturing long-range dependencies and computational efficiency. The framework introduces a graph tokenization process that bridges node-level and subgraph-level tokenization, facilitating efficient learning of graph structures. Another concurrent work Graph-Mamba [51] is also developed based on the Mamba architecture. Graph-Mamba includes a node prioritization technique to prioritize important nodes for more access to context and employs a permutation-based training recipe to minimize sequence-related biases. Ali Behrouz et al. propose the GRED [53] which is a new graph representation learning architecture that aggregates other nodes based on their shortest distance to the target for a given target node. They adopt the linear RNN to encode the skip representation sequence. Gregor et al. [140] discuss the issues of teachers being unable to accurately learn the next token predictor through mandatory training, and demonstrate the failure of Transformer and Mamba architectures in multi-token prediction training through the simplest planning task. Li et al. [55] introduce STG Mamba which is the first attempt to process STG learning using a powerful selective State Space Model.

3.5 Multi-modal and Multi-media

The State Space Model can also be adapted for multi-modal/multi-media tasks. Specifically, S4ND [30] extends State Space Models (SSMs) to multidimensional signals, enabling the modeling of large-scale visual data as continuous multidimensional signals. This method has been demonstrated to be effective across different dimensions (1D, 2D, and 3D), encompassing applications in image and video classification. Grazzi et al. [45] evaluate Mamba with in-context learning (ICL) capabilities similar to Transformer. The analysis shows that, like Transformer, Mamba appears to solve the ICL problem by gradually improving its internal representation like an iterative optimization strategy. For ICL tasks involving longer input sequences, Mamba can be an effective alternative to Transformer. Park et al. [141] also evaluate Mamba's performance and their results show that Mamba's performance in standard regression ICL tasks is comparable to Transformer's. Its performance in sparse parity learning tasks is better. However, it performed poorly on tasks involving non-standard retrieval functions. The MambaFormer [141], consisting of Mamba together with attention blocks, was used to solve the above challenges, outperforming any single model in each task. Zucchet et al. [142] reveal a closer conceptual relationship between RNN and Transformer. The experimental results prove that RNN and Transformer are not completely exclusive models. It is also shown that linear self-attention can be achieved in theory and practice by learning gated RNNs with multiplicative interactions, bridging the gap between these two architectures. Ali et al. [143] explore the learning mechanisms of Mamba models, in particular how dependencies are captured and their similarity to other established layers, such as RNN, CNN, or attention mechanisms. An important relationship between the Mamba and the self-attention layer is established. The basic properties of the Mamba model are clarified by showing that they depend on implicit attention to be realized by a unique data-controlled
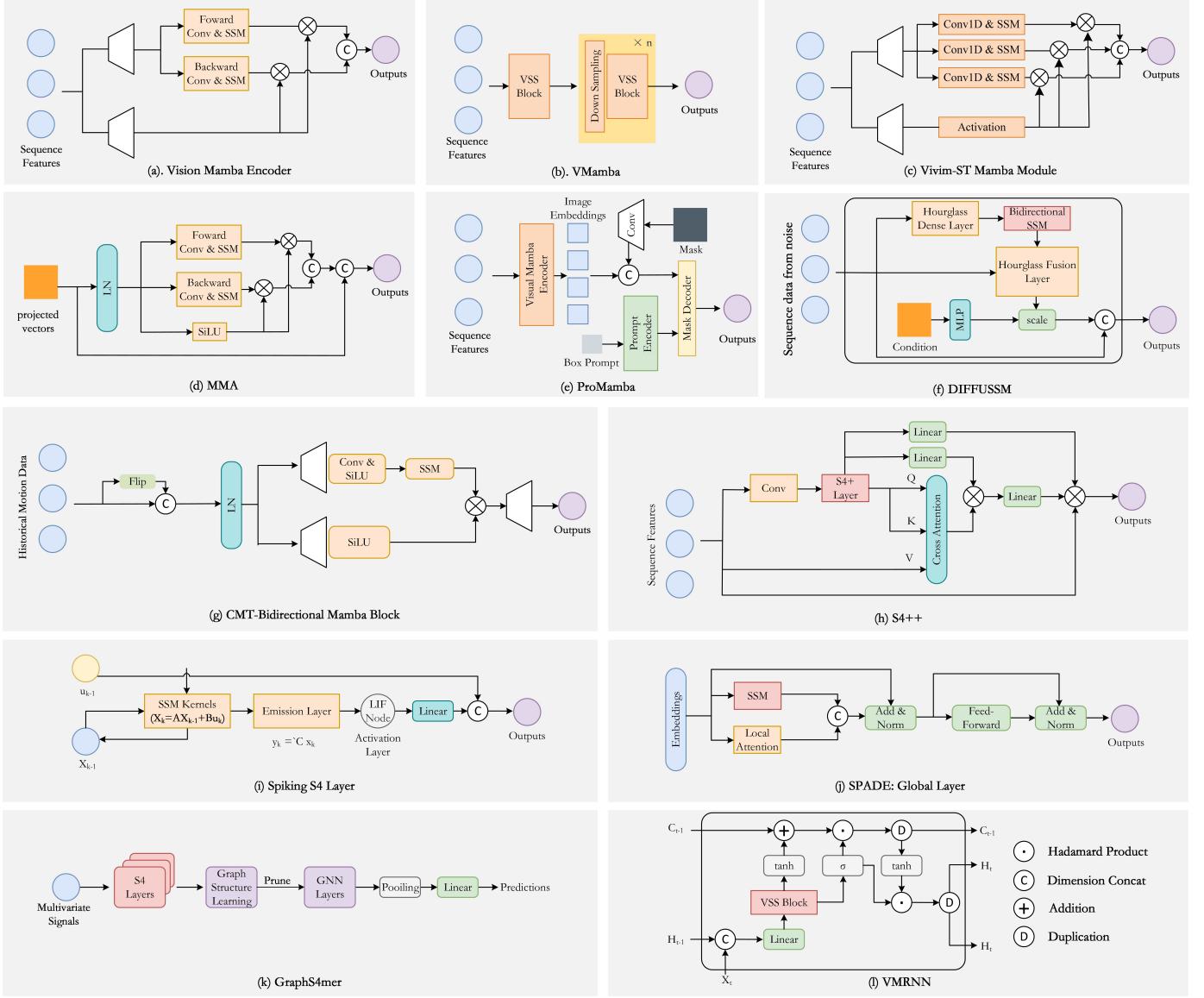
Fig. 9. Representative blocks designed based on State Space Model (a [61], b [60], c [98], d [86], e [99], f [31], g [88], h [46], i [42], j [47], k [52], l [103]).

linear operator, indicating that the selective state-space layer is an attention model. By utilizing the obtained attention matrices, a set of interpretability techniques based on these hidden attention matrices are provided. MambaMIL [144] integrates the Mamba framework into MIL, with SR-Mamba as the core component, which is good at capturing remote dependencies between dispersed positive instances. MambaMIL can efficiently capture more discriminant features and mitigate the challenges associated with overfitting and high computational overhead, marking the first application of the Mamba framework in computational pathology.

Motion Mamba [88], composed of Hierarchical Temporal Mamba (HTM) and Bidirectional Spatial Mamba (BSM), represents the first integration of Mamba models in the field of motion generation. HTM and BSM are designed for temporal and spatial modeling, respectively, while integrating selective scanning mechanisms into motion generation tasks. Compared with the previous diffusion-based motion generation method, which mainly uses a Transformer, motion Mamba achieves state-of-the-art (SOTA) performance. Note that the inference speed is also sped up by four times. VL-Mamba [145] is the first effort to explore the state-space model Mamba to solve the expensive computational overhead in the Transformer architecture in multimodal learning tasks. CMViM [146] focuses on the application of multimodal representation learning to 3D high-resolution medical images, especially Alzheimer's disease (AD). It is developed based on MAE [150] framework and replaces ViT [151] module with Vim [61] module, therefore, reducing complexity from quadratic to linear level. Moreover, the intra-modality and inter-modality contrastive learning methods are introduced to enhance the ability of the multimodal Vim encoder to model discriminative features in the same modality and mitigate the misaligned representation between modalities. Cobra [147] explores the combination of language models with linear computational complexity and

TABLE 6
Summary of existing SSM-based Multi-modal and Multi-media algorithms.

#ID	Algorithm	Publish	Domain	Parameters	Architecture	Downstream Tasks	Accuracy	Code
96	**S5** [57]	ICLR23	Multi-modal Multi-media	280K	SSM	Classification	Speech Commands classification: (16kHz):96.52 (8kHz):94.53	URL
97	**Grazzi et al.** [45]	arXiv24	Multi-modal Multi-media	-	-	-	-	-
98	**MambaFormer** [141]	arXiv24	Multi-modal Multi-media	-	Mamba+Former	-	-	-
99	**Zucchet et al.** [142]	arXiv24	Multi-modal Multi-media	-	-	-	-	-
100	**Mamba** [12]	arXiv24	Multi-modal Multi-media	Mamba-130M Mamba-370M Mamba-790M Mamba-1.4B	Mamba	Synthetic Zero-shot	Synthetic tasks:99.8 Zero-shot(Average ACC) 44.7(130M) 50.0(370M) 57.1(790M) 59.7(1.4B)	URL
101	**Ali et al.** [143]	arXiv24	Multi-modal Multi-media	ViM-S,ViT-S	Mamba Transformer	Segmentation	ViM-S:(mAP) (mIoU) Raw-Attention 74.88, 45.09 Attn-Rollout 80.78, 51.51 Mamba-Attr 81.70, 54.24 ViT-S:(mAP) (mIoU) Raw-Attention 77.25, 36.94 Attn-Rollout 80.34, 47.85 Mamba-Attr 84.85, 60.63	URL
102	**MambaMIL** [144]	arXiv24	Multi-modal Multi-media	-	Mamba	Survival Prediction Cancer Subtyping	Survival Prediction 0.680(ResNet-50) 0.693(PLIP) Cancer Subtyping:(AUC) (ACC) ResNet-50 0.845, 0.619 PLIP 0.822, 0.582	URL
103	**Motion Mamba** [88]	arXiv24	Multi-modal Multi-media	-	Mamba	Motion Synthesis Text-to-Motion	Motion Synthesis 0.502(R Precision top 1) Text-to-Motion 0.419(R Precision top 1)	URL
104	**VL-Mamba** [145]	arXiv24	Multi-modal Multi-media	Mamba LLM-2.8B	Mamba	Multimodal Learning	VQA-v2:76.6 GQA:56.2 SQA-IMG:65.4 TextVQA:48.9 POPE:84.4 MME:1369.6 MMB :57.0 MM-Vet:32.6	URL
105	**CMViM** [146]	arXiv24	Multi-modal Multi-media	50M	Mamba	AD Classification	ACC:69.3 AUC:84.1	-
106	**Cobra** [147]	arXiv24	Multi-modal Multi-media	Mamba-2.8B	Mamba	visual question-answering closed-set prediction	VQA-v2:75.9 GQA:58.5 VizWiz:52.0 TextVQA:46.0 POPE:88.0 VSR:63.6	URL
107	**DMamba** [148]	arXiv24	Multi-modal Multi-media	-	Mamba	RL	HalfCheetah-m:42.8±0.08 Hopper-m:83.5±12.5 Walker-m:78.2±0.6	URL
108	**Sigma** [149]	arXiv24	Multi-modal Multi-media	VMamba-T VMamba-S	Mamba	Multi-modal semantic segmentation	RGB-D: NYU Depth V2: 53.9(VMamba-T)57.0(VMamba-S) SUN RGB-D: 50.0(VMamba-T)52.4(VMamba-S)	URL

multimodal inputs. It replaces the Transformer networks commonly used in current models with a more efficient Mamba architecture.

In terms of visual and linguistic information fusion, Zhao et al. [147] optimizes the internal information integration of the Mamba language model to achieve a more effective expression. Decision Mamba(DMamba) [148] integrates the Mamba framework into the Decision Transformer (DT) [152]. A series of experiments comparing Decision Mamba and DT show that Mamba is effective in reinforcement learning (RL) tasks. But simply applying Mamba blocks to DT does not improve efficiency, because the RL tasks considered by the authors have a large number of CPU and GPU interactions. Another deficiency is the absence of a hyper-parameter search and an analysis of how to use the Mamba block more effectively to reflect the data structure of RL tasks. Sigma [149] is the first State Space Model successfully applied in multi-modal semantic seg-

mentation. It is composed of VMamba, an attention-based Mamba fusion mechanism and a channel-aware Mamba decoder, and has shown excellent performance in various experiments. However, Sigma is underutilized in handling longer sequences, and the memory consumption of Mamba encoders is still relatively large, making it difficult to deploy on lightweight edge devices.

3.6 Event Stream/Point Cloud Data

Inspired by the success of the State Space Model (SSM) in natural language processing, PointMamba [153] leverages the strengths of SSM to introduce a framework boasting global modeling capabilities while maintaining linear complexity. This innovative model operates by taking embedded point patches as inputs, employing a reordering strategy, and subsequently feeding these point patches into a series of Mamba blocks to bolster the global modeling capability of SSM. PCM [154] proposes a consistent traverse serialization

TABLE 7
Summary of existing SSM-based Point cloud and Event stream algorithms.

#ID	Algorithm	Publish	Domain	Parameters	Architecture	Downstream Tasks	Accuracy	Efficiency	Code
109	**PointMamba** [153]	arXiv24	point	Classification:12.3M Segmentation:17.4M	SSM	Classification Segmentation	Classification(ScanObjectNN) OBJ-BG:88.3 OBJ-ONLY:87.78 PB-T50-RS:82.48 Segmentation(ShapeNetPart) Cls. mIoU:83.94 Inst. mIoU :85.8	Classification FLOPs:3.6G Segmentation FLOPs:14.3G	URL
110	**PCM** [154]	arXiv24	point	Classification PCM-Tiny:6.9M PCM:34.2M Segmentation PCM-Tiny:8.8M PCM:40.6M	SSM	Classification Segmentation	Classification(ScanObjectNN) (PCM-Tiny)OA:86.9±0.4 (PCM-Tiny)mAcc:85.0±0.3 (PCM)OA:88.1±0.3 PCM)mAcc:86.6±0.2 Segmentation(ShapeNetPart) (PCM-Tiny)Cls. mIoU:85.0 (PCM-Tiny)Inst. mIoU:86.9 (PCM)Cls. mIoU:85.3±0.1 (PCM)Inst. mIoU:87.0±0.2	-	URL
111	**Point Mamba** [155]	arXiv24	point	Classification:3.08M Segmentation:31.99M	SSM	Classification Segmentation	Classification(ModelNet40) (Point Mamba-O)Accuracy:92.7 (Point Mamba-C)Accuracy:93.4 Segmentation(ScanNet) (Point Mamba)mIoU:74.6 (Point Mamba voting)mIoU:75.7	Classification FLOPs:1.31G Segmentation FLOPs:55.07G	URL
112	**3DMambaIPF** [156]	arXiv24	point	-	Mamba	Filtering	Filtering(PU-Net 10K points) CD(2.5% noise):32.62 P2M(2.5% noise):9.92 Filtering(PU-Net 50K points) CD(2.5% noise):9.28 P2M(2.5% noise):5.31	-	-
113	**3DMambaComplete** [157]	arXiv24	point	34.06 M	Former+Mamba	Point cloud completion	Point cloud completion(KITTI) MMD:0.491 FD+MMD:0.501	FLOPs:7.12G	-
114	**Zubi'c et al** [158]	arXiv24	event	S4D-ViT-B:16.5M S5-ViT-B:17.5M	Former+SSM	Detection	Object detection(Gen 1) (S4D-ViT-B)mAP:46.2 (S5-ViT-B)mAP:47.4	-	-

strategy that converts a point cloud to a 1-D sequence of points and ensures that adjacent points in the sequence are also adjacent in space. Consistent traverse serialization strategy produces six variants by arranging the order of x, y, and z coordinates, and the author introduces order prompt to inform Mamba of the arrangement rules of the sequence. In addition, a positional embedding method based on spatial coordinate mapping is proposed to add point cloud position information. Point Mamba [155] designs an octree-based ordering mechanism for irregular points,ensuring the preservation of their spatial proximity and causal dependence. The points undergo a sequence of Point Mamba blocks and downsampling layers to extract layered point characteristics. Zhou et al. propose 3DMambaIPF [156], which integrates Mamba into the point cloud filtering task and introduces a fast differentiable rendering loss. This approach has demonstrated strong performance in handling large-scale point clouds. Li et al. propose 3DMambaComplete [157], which incorporates the HyperPoint Generation module, HyperPoint Spread module, and deformation method for point cloud reconstruction. The HyperPoint Generation module introduces Mamba's selection mechanism to encode point cloud features. Zubi'c et al. [158] introduce a state-space models (SSMs) with learnable time-scale parameters to the event-based vision, enabling adaptation to different frequency time inputs without having to retrain the network at different frequencies.

3.7 Time Series Data

As the SSM is a sequence model, it is very intuitive and effective to adapt the SSMs to handle multivariate time series data [180], [184], [185]. Specifically, the primary challenges in the task of long-term time-series forecasting (LTSF) lie in the difficulty of capturing long-term dependency relationships and the poor linear scalability. TimeMachine [180] addresses these issues by introducing a method that leverages Mamba to capture long-term dependencies in multivariate time series data. By utilizing an integrated architecture with multiple Mamba modules, TimeMachine effectively resolves the challenges associated with channel mixing and channel independence. This approach enables selective prediction of global and local contextual information across different scales. Experimental validation demonstrates that TimeMachine significantly improves accuracy while maintaining excellent scalability.

3.8 Others

In addition to the aforementioned domains, the SSM can also be adopted in many other applications. Real-world sensors are mostly nonlinear and subject to interference from external variables, which renders traditional local linear prediction algorithms ineffective in practical scenarios. Bhirangi [179] et al. established a benchmark for the task of continuous sequence prediction (CSP) and concurrently proposed the Hierarchical State Space Model (HiSS). This model constructs a temporal hierarchy by stacking multiple layers of structured spatial state models with varying resolutions. Experimental results demonstrate that HiSS outper-

TABLE 8
Summary of existing SSM-based other algorithms.

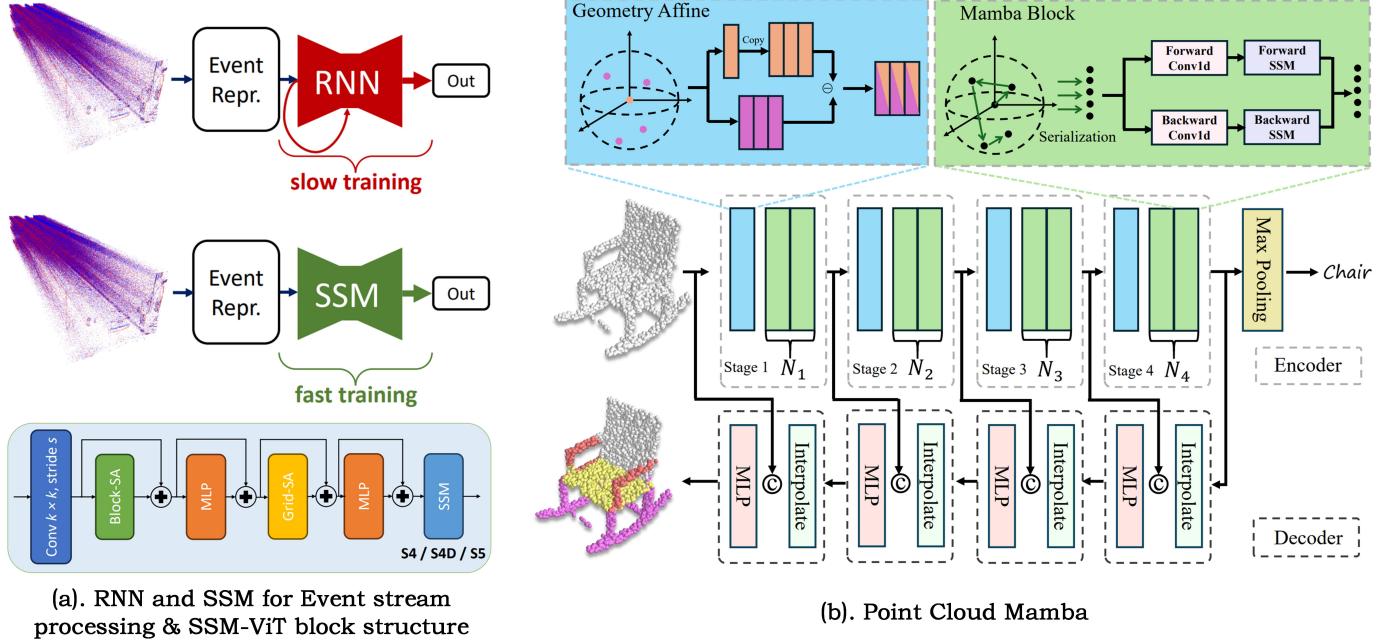| #ID	Algorithm	Publish	Domain	Parameters	Architecture	Downstream Tasks	Accuracy	Efficiency	Code
115	**SaShiMi** [159]	ICML22	Audio	23.0M	S4	Generation	YouTubeMix TestNLL:1.294 MOS(fidelity): 2.84±0.09 MOS(musicality): 3.11±0.09	-	URL
116	**BiGS** [160]	arXiv22	NLP	119M	SSM	Modeling	-	length 128: 8.1e+10 length 512: 3.2e+11 length 1024:	URL
117	**Massaroli et al.** [161]	NeurIPS23	NLP	154M	SSM+CNN	LM-Eval-Harness	(LAMBADA) Acc 43.2 (Winogrande) Acc 52.7 (PIQA) Acc 64.6	-	-
118	**ConvSSM** [162]	arXiv23	NLP	2D 20M 3D 100M	SSM+CNN	Sequence modeling	FVD(71 ± 9) PSNR(16.4 ± 0.1) SSIM(0.788 ± 0.002) LPIPS(0.134 ± 0.003)	3× faster than ConvLSTM, generates samples 400× faster than Transformers	URL
119	**Lu et al.** [163]	NeurIPS23	TSP	-	SSM	BML	-	-	URL
120	**Wang et al.** [164]	arXiv23	NLP	-	SSM	associative recalls image classifications	MNIST:99.3	-	URL
121	**MoE-Mamba** [165]	arXiv24	NLP	25M 542M 100M 2439M	SSM+MoE	Sequence modeling	-	2.35× fewer training steps	URL
122	**MambaByte** [166]	arXiv24	NLP	353M 972M 1.6B	SSM	Context modeling	BPB 0.930(PG19) 0.908(Stories) 0.966(Books) 0.663(ArXiv) 0.396 (Code)	-	URL
123	**BlackMamba** [167]	arXiv24	NLP	2.8B 1.5B	SSM	QA	0.397(HellaSwag) 0.712(PIQA) 0.521(WinoGrande) 0.542(Lambada) 0.603(ARC-e) 0.245(ARC-c) 0.242(OpenBookQA)	1.2e+21 Training FLOPs 6.4e+20 Training FLOPs	URL
124	**LOCOST** [168]	EACL24	NLP	234M	SSM	Summarization	R-1=43.8 R-2=17.0 R-L=39.7	-	-
125	**Samsami et al.** [169]	ICLR24	CV	-	SSM	RL	-	-	-
126	**GateLoop** [170]	arXiv23	NLP	125M	SSM	Autoregressive Modeling	(WikiText-103) Acc 0.43 (WikiText-103) Perplexity 13.4	-	-
127	**Liu et al.** [171]	arXiv24	NLP	-	SSM	Multi tasking	PathX:90.21	PathX running time 14min 40s	-
128	**PTD** [172]	ICLR24	NLP	-	SSM	Classification	Speech Commands:96.04	-	-
129	**David et al.** [173]	arXiv24	others	-	SSM+HMM	Prediction	Fashion dataset MASE:0.692	-	-
130	**FlashFFTConv** [174]	arXiv24	others	-	Conv+SSM	Modeling	Classification Path-X: accuracy: 96.9	FLOPS: 56.5M	URL
131	**Mamba4Rec** [175]	arXiv24	NLP	-	SSM	Recommendation performance	HR@10 (MovieLen-1k) 0.3121 (Amazon-Beauty) 0.0812 (Amazon-Video-Game) 0.1152	-	URL
132	**Silva et al.** [176]	arXiv24	NLP	-	Mamba	Prediction	(Coma) AUROC 0.99 (Delirium) AUROC 0.90 (Deceased) AUROC 0.97	-	-
133	**oSpatial-Mamba** [177]	arXiv24	speech denoising	1.4M	SSM	Enhancement	SI-SDR SDR (static-speaker cases) 13.7 15.2 (moving-speaker cases) 10.7 12.2	-	URL
134	**Caduceus** [87]	arXiv24	Medicine	-	SSM	Classification	acc top-1 Mouse Enhancers 0.793 Human Enhancer Ensembl 0.900 Human Regulatory 0.873 Human NonTATA Promoters 0.945	-	URL
135	**CMT MMH** [88]	arXiv24	CV	-	SSM	Object track ´	AVG-err 4.97	-	-
136	**MambaStock** [178]	arXiv24	TSP	-	Mamba	Prediction	MSE=1.1514	-	URL
137	**Bhirangi et al.** [179]	arXiv24	TSP	-	SSM	CSP	-	-	URL
138	**TimeMachine** [180]	arXiv24	TSP	-	Mamba	LTSF	Traffic dataset MSE=0.467 when T=720	-	URL
139	**CLDSSMs** [181]	arXiv24	other	-	DSSM	Prediction	WEATHER dataset MSE: 11.31±0.67	-	-
140	**Poli et al.** [182]	arXiv24	MAD	70M to 7B	Mechanistic Architecture Design	-	-	-	-
141	**LaRocque et al.** [183]	arXiv24	others	-	Mamba	Classification	Vulpi dataset AVG=86.76 BorealTC dataset AVG=93.68	-	URL

Fig. 10. (a). Comparison between RNN/SSM for Event stream processing and their SSM-ViT block structure [158]; (b). Point Cloud Mamba [154]

TABLE 9
Summary of existing SSM-based other algorithms.

#ID	Algorithm	Publish	Domain	Parameters	Architecture	Downstream Tasks	Accuracy	Efficiency	Code
142	**S/D-Mamba** [184]	arXiv24	TSF	-	Mamba	LTSF	MSE 0.066(D-Mamba) 0.066(S-Mamba) 0.171(D-Mamba) 0.171(S-Mamba)	-	URL
143	**SiMBA** [185]	arXiv24	others	Small: Monarch: 18.5M Base: Monarch: 26.9M Large: Monarch: 42M	SSM+CNN EinFFT	Classification Multi-Variate TSF OD Learning Segmentation	ImageNet-1K(acc/top1) SiMBA-S:84.0 SiMBA-B:84.7 SiMBA-L:83.9	FLOPs: (Monarch) SiMBA-S: 3.6G SiMBA-B: 5.5G SiMBA-L: 8.7G	URL
144	**Xu et al.** [186]	arXiv24	NLP	-	Mamba	Language modeling	-	-	URL
145	**Sharma et al.** [187]	arXiv24	others	-	Mamba	Factual Recall	-	-	-
146	**Yin et al.** [188]	arXiv24	Audio	-	SSM	Audio Production	-	-	-
147	**Marco et al.** [189]	arXiv24	others	-	SSM	Prediction	fit index: 86.5	-	
148	**Yang et al.** [190]	arXiv24	others	-	Mamba	prediction	KuaiRand(2k) dataset NDCG@5:55.84 LFM-1b(2k) dataset NDCG@5:74.87 KuaiRand(5k) dataset NDCG@5:57.13 LFM-1b(5k) dataset NDCG@5:78.23	KuaiRand(2k) dataset GPU memory(GB):8.36G LFM-1b(2k) dataset NDCG@5:7.6G KuaiRand(5k) dataset NDCG@5:14.68G LFM-1b(5k) dataset NDCG@5:14.46G	URL

forms other sequence models by at least 23% in terms of mean squared error (MSE) across multiple real-world sensor datasets. LOCOST [168] introduced an encoder-decoder architecture based on state-space models for conditional text generation tasks with long-context inputs. This approach effectively reduced computational complexity and memory usage, significantly enhancing the speed of both training and inference stages. MambaStock [178] utilizes the structured state space (S4) architecture to capture the nonlinearity in stock data, enabling accurate predictions of future stock prices. Lu et al. [163] proposed an improvement to the simplified structured state-space sequence model (S5), enabling the reset of hidden states within trajectories during the model training phase. Specifically, to enable the model to handle variable-length sequences, this paper modifies the association operator and introduces a reset annotation

that preserves association properties in S5. Additionally, to test the generalization ability of the model, a challenging Meta-RL setup is also introduced. [188] introduces a new method for developing a realistic digital dynamic range compressor model for digital audio production by analyzing its simulation prototype. The learned representations are often affected by the high order of the model, which makes them unsuitable for control design. [189] proposes a system theory based model order reduction technique specifically for linear dynamic blocks in SSM to address this challenge.

Wang et al. [191] demonstrate that the approximation of any continuous sequence-to-sequence relationship can be achieved by stacking state-space models with inter-layer nonlinear activation. Furthermore, experimental results indicate that this approach enhances the model's capacity to learn complex sequence patterns. Finally, through theo-

retical analysis and numerical verification, it is concluded that state-space models do not fundamentally address the issue of exponential decaying memory. Samsami et al. [169] propose a method named R2I to enhance long-term memory and long-term credit, which integrates a set of state-space models into the world model of model-based reinforcement learning (MBRL) agents, thereby solving the issue that existing MBRL agents were unable to deal with the long-term intervals between actions and outcomes. Experimental results demonstrated that R2I achieved state-of-the-art performance in memory and credit assignment RL tasks, while also exhibiting faster convergence speed. Black-Mamba [167] merging SSMs with mixture-of-experts (MoE) significantly reduces inference costs, paving the way for efficient and scalable text generation tasks. MambaByte [166] is a token-free selective State Space Model designed for learning directly from raw bytes and its recurrent nature enables fast text generation, highlighting its practicality for large-scale models and paving the way for future developments in token-free language modeling. Self pretraining (SPT) [192] challenges the conventional approach of comparing long-sequence models from scratch, revealing that pre-training with data-driven priors significantly alters performance evaluations. By leveraging pre-training, the research achieves substantial improvements across various architectures, closing the performance gap between Transformers and SSMs and even surpassing previous SSM results on tasks. Laughing Hyena Distillery [161] proposes Laughing Hyena, a new distillation method that extracts compact state-space models from pre-trained long convolutional sequence models without loss of quality, utilizes rational function approximation and model downscaling techniques to extract low-dimensional state-space models in the convolutional layers, and achieves automated regression generation with constant memory and constant time complexity. Improved Hyena improves pre-training quality and reduces the number of filters to be distilled by binding filter weights to heads across channels.

GateLoop [170] introduces GateLoop, a fully data-controlled linear RNN using data-controlled gated inputs and outputs for efficient auto-regressive language modeling. A memory horizon dataset for synthetic language modeling is also presented to highlight the superiority of GateLoop by comparing the advantages and disadvantages of data-controlled and non-data-controlled state transitions. A parallel scanning training strategy and an equivalent attention substitution model are also demonstrated. A multi-cohort study on the prediction of acute brain dysfunction states using selective State Space Models [176] develop a data-driven, automated data-driven approach for the prediction of ABD in critically ill patients in the ICU by utilizing rich electronic health record (EHR) data. Their study demonstrated high performance by dynamically predicting delirium, coma, and death during ICU stays and validated on two public datasets. S/D-Mamba [184] introduces two simple Mamba-based models: S-Mamba and D-Mamba, both of which use Mamba Block to extract variable correlations (VC). S-Mamba uses a Mamba Block to handle correlations between variables. D-Mamba is more sensitive to VC by adjusting the parameters compared to S-Mamba. D-Mamba adds an extra Mamba block to the Mamba layer

to handle VCs compared to S-Mamba, and the extra Mamba block is more sensitive to correlations between variables by adjusting the parameters. Experimental results show that both models outperform the traditional methods in terms of performance while saving GPU memory and training time. Liu et al. propose a novel method, Mamba4Rec [175], which is proposed to model dependencies between sequences. To demonstrate the performance of Mamba4Rec, this paper experiments on MovieLen-1M, Amazon-Beauty, and Amazon-Video-Games, which reached state-of-the-art performance. Quan et al. [177], propose a novel model to handle multi-channel speech enhancement based on original SpatialNet. They propose oSpatialNet-Mamba which reaches top performance, whose core advantage is the State Space Model. Note that, various tasks have been tested on the model, which all performed well. Schiff et al. introduce a novel bioinformatics model called Caduceus [87], which can bi-directionally and equivalently model the DNA sequence. Based on MambaDNA, the Caduceus is the first family of RC-equivalent and bi-directional long-range DNA language models, which introduces pre-training and fine-tuning strategies. Also, it outperforms previous long-range models on the Genomic benchmarks. Zhang et al. introduce a novel motion-guided tracker and a motion-guided prediction head [88] based on Mamba. Karan et al. [159] proposes SaShiMi, a multi-level structure based on S4 model long sequence modeling. It provides a simple improvement to its parameterization by drawing connections to Hurwitz matrices. In addition, SaShiMi improves non-recursive generation performance in non-recursive states. A new prediction model that combines discrete state space hidden Markov models has been proposed by David et al. [173]. It introduces a variable separated posterior distribution and a two-stage training program to alternately train the parameters of the latent state and the emission distribution. By learning a set of emission laws and dynamically activating them based on hidden processes. FlashFFTConv [174] proposes a convolutional optimization method called FlashFFTConv, which uses matrix factorization to calculate the fast Fourier transform and utilizes matrix multiplication units for kernel fusion of long sequences, and reduce I/O costs effectively.

Several related works have explored different aspects of state-space models (SSMs) and their applications in various domains. [181] propose a deep state-space model (DSSM) called Continuous Learning DSSM (CLDSSM). CLDSSM integrates regularization-based continual learning (CL) methods to efficiently update multiple dynamic systems without catastrophic forgetting. [172] focuses on enhancing the robustness of SSMs for long sequence tasks through approximate diagonalization. The authors propose a method that approximates diagonalization to improve the robustness of SSMs. By simplifying the problem and considering pure diagonal structures, the proposed approach achieves computational efficiency and allows channel communication. In [171], the *curse of memory* in SSMs is addressed through stable re-parameterization. The authors introduce a parameterization technique for SSMs that effectively enhances their memory limits. [164] provide a data-dependent generalization bound for SSMs, highlighting the interplay between the SSM parameters and the temporal dependencies of training sequences. Building upon this generalization bound, they

propose a scaling rule for model initialization to improve the robustness of SSMs in accommodating different temporal patterns in the sequence data. Wang et al. [160] propose a sequence routing method based on State Space Model and attempt to pre-train a big model without attention. Bidirectional Gated SSM (BiGS) proposed in the paper combines an SSM layer and a multiplicative gating architecture to effectively simplify the sequence modelling task. It reduces computational resources and time for model training by omitting the computationally intensive attention matrix. This approach successfully reduces resource consumption by about 30% while maintaining comparable performance to traditional pre-trained models. Although the BiGS model does not consider pairwise interactions, it is able to match BERT's pre-training accuracy on the GLUE benchmark test and can be scaled up to 4096 tokens of long-form pre-training without approximation. This approach provides an effective pre-training solution for NLP tasks in resource-limited environments and has the potential to be applied to a wider range of NLP scenarios.

Poli et al. [182] propose a new framework named MAD (Mechanistic Architecture Design),which aims at evaluating and predicting the design and scalability of hybrid architectures through synthetic tasks. The purpose of this research is to simplify the process by employing an end-to-end pipeline, including small-scale capability unit tests that can predict scaling laws, thereby identifying and testing new hybrid architectures. The study not only focuses on the design and scalability issues of hybrid architectures but also validates the effectiveness of its theories and methods through large-scale data analysis.

Smith [162] is a novel spatiotemporal modeling approach focused on improving the efficiency and performance of modeling long sequence data. It combines the advantages of Convolutional Neural Networks (CNNs) and state space methods to effectively overcome the limitations of traditional models in dealing with complex spatial correlations and long time dependencies. ConvSSM significantly improves the speed of model training and prediction through parallel scanning and fast auto-regressive generation techniques. Meanwhile, it draws on state-space methods such as S4 and S5 to provide effective parameterization and initialization strategies for long-distance dependency modeling. This approach not only reduces the consumption of computational resources but also maintains a performance level comparable to that of complex models. Compared to other models, such as Transformer, whose computational cost grows significantly with sequence length, and ConvLSTM, which has a slower training speed, ConvSSM demonstrates its potential in long sequence spatiotemporal modeling. In addition, researchers are also exploring ways to further improve model performance by optimizing convolutional kernel design and combining the advantages of different models. [165] proposes an approach that fuses a hybrid Mixture of Expert (MoE) mechanism and a selective State Space Model (SSM) with the aim of optimising the efficiency and performance of sequence modeling. This approach introduces MoE on top of the Mamba model, achieving similar performance in fewer training steps and maintaining the inference performance advantage over the Transformer model. The MoE model utilizes dynamic gating, expert caching, and load balancing techniques to address the communication and memory issues faced by large models during the inference phase, while conditionally computing to extend the model without significantly increasing the computational cost while expanding the model capacity. It is shown that MoE models with instruction fine-tuning and task-specific fine-tuning are able to achieve better performance than denser models with the same computational complexity. The success of MoE-Mamba demonstrates that the performance and efficiency of sequence modeling tasks can be effectively improved by a well-designed MoE architecture, which opens up new possibilities for processing large-scale sequence data. Xu et al. [186] demonstrate the potential of Mamba models for classical information retrieval tasks by evaluating the performance of models based on the Mamba architecture in a document ranking task. Compared to Transformer-based language models, Mamba models achieve competitive performance in the same training configuration. However, the Mamba model falls short in terms of training throughput compared to efficient attention implementations, limiting its potential for efficient training and deployment. Although the study focuses on models with parameters less than 1B, they find that this may change when scaling to larger models and employing different training configurations. Thus, the effectiveness and performance of Mamba models in other classical information retrieval tasks remain to be further investigated. Amo et al. [193] introduce the SSM system and summarize the research progress in the field of control-theoretic. Sharma et al. [187] are inspired by the research found in the autoregressive transformer language model that knowledge recall can be specific to specific modules and marker positions, and aims to locate factual recall in Mamba. Olucha et al. proposed an overview of the state-of-the-art and comparative study of linear parameter-varying state-space (LPV-SS) model downscaling [194]. These comparisons can help to select the best downscaling method for a given LPV-SS model. Yang et al. propose the Rec-Mamba [190] model for sequence recommendation tasks. This model better models users' preference information that changes over time through the Mamba module, improving personalized recommendation performance and reducing computational complexity. Compared to SASRec, the training time is reduced by approximately 70%. LaRocque et al. [183] compares the performance of Convolutional Neural Networks (CNNs) and the novel State Space Model (SSM)-based Mamba architecture, revealing intriguing insights into their respective strengths and the benefits of dataset fusion for improved terrain.

4 EXPERIMENTS

In this section, we give an experimental comparison of five downstream tasks, including single-/multi-label classification, visual object tracking, pixel-level segmentation, image-to-text generation, and person/vehicle re-identification. More details will be introduced in the following subsections, respectively.
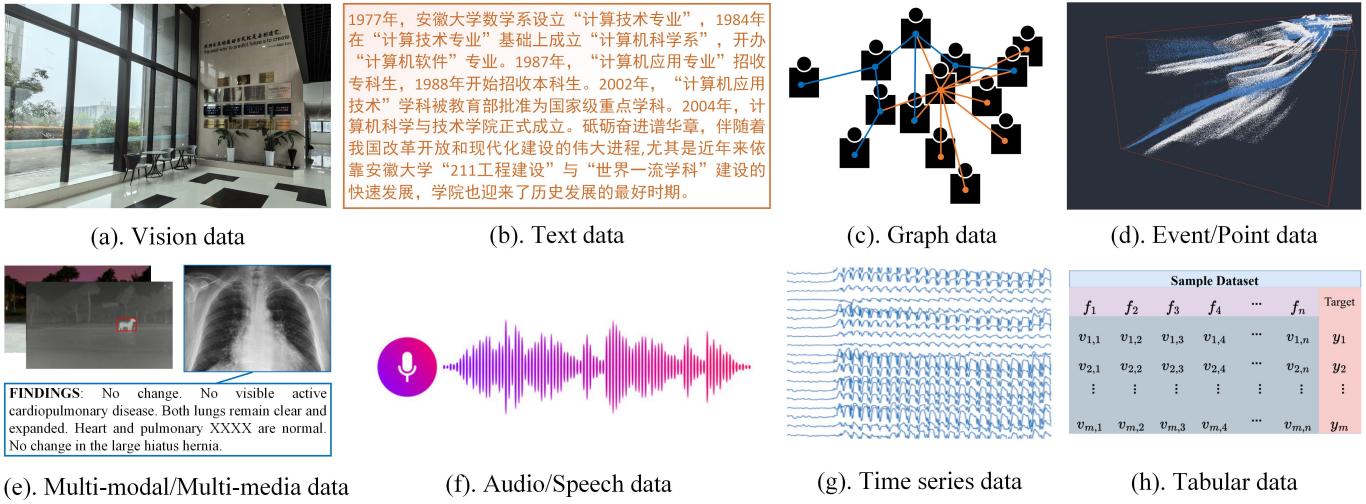
(a). Vision data

(b). Text data

(c). Graph data

(d). Event/Point data

(e). Multi-modal/Multi-media data

(f). Audio/Speech data

(g). Time series data

(h). Tabular data

Fig. 11. Representative input data that can be processed using State Space Model.

(a). Results on the Kinetics-400 dataset

(b). Results on the HMDB-51 and UCF-101 dataset

(c). Results on the LVU dataset

(d). Results on the ImageNet-1K dataset

(e). Results on the Abdomen, Endoscopy and Microscopycell dataset

(f). Results on MRI Cardiac Test Set

(g). Results on ISIC17 dataset

Fig. 12. Experimental results on (a, b, c) Video-based recognition, (d) Image-based recognition, (e, f, g) Medical image-based segmentation.

4.1 Single-/Multi-label Classification

For the single-label classification problem, we calculate the accuracy of existing works on the widely used ImageNet-1K [2] dataset. As shown in Fig. 12 (d), we can find that the base version of VMamba [60] and Mamba-2D [68] achieves better results on the ImageNet1K dataset, i.e., 83.2% and 83% on the top-1 accuracy, respectively. It is also easy to find that current Mamba-based vision models are all tiny, small, or base versions, and seldom pre-train a large or huge version of the Mamaba network. The overall performance is comparable to some Transformer

based models, but still inferior to the state-of-the-art on the ImageNet classification dataset.

For the multi-label classification, we select the Pedestrian Attribute Recognition (PAR) task [6][3] and conduct experiments on the PA100K [208] and PETA [209] datasets. The PA100K dataset contains 100,000 samples collected from 598 scenarios and involves 26 pedestrian attributes. We split the training, validation, and testing subset based on default settings (8:1:1). The PETA dataset involves 61 binary at-

3. https://github.com/wangxiao5791509/
Pedestrian-Attribute-Recognition-Paper-List

TABLE 10
Comparison with state-of-the-art methods on PETA and PA100K datasets. The first and second are shown in red and blue, respectively. "-" means this indicator is not available. VTB* indicates that VTB uses CLIP's feature extractor.

Methods	Backbone	PETA					PA100K				
		mA	Acc	Prec	Recall	F1	mA	Acc	Prec	Recall	F1
JLAC (AAAI 2020) [195]	ResNet50	86.96	80.38	87.81	87.09	87.50	82.31	79.47	87.45	87.77	87.61
SCRL (TCSVT 2020) [196]	ResNet50	87.2	-	89.20	87.5	88.3	80.6	-	88.7	84.9	82.1
SSCsoft (ICCV 2021) [197]	ResNet50	86.52	78.95	86.02	87.12	86.99	81.87	78.89	85.98	89.10	86.87
IAA-Caps (PR 2022) [198]	OSNet	85.27	78.04	86.08	85.80	85.64	81.94	80.31	88.36	88.01	87.80
MCFL (NCA 2022) [199]	ResNet-50	86.83	78.89	84.57	88.84	86.65	81.53	77.80	85.11	88.20	86.62
DRFormer (NC 2022) [200]	ViT-B/16	89.96	81.30	85.68	91.08	88.30	82.47	80.27	87.60	88.49	88.04
VAC-Combine (IJCV 2022) [201]	ResNet50	-	-	-	-	-	82.19	80.66	88.72	88.10	88.41
DAFL (AAAI 2022) [202]	ResNet50	87.07	78.88	85.78	87.03	86.40	83.54	80.13	87.01	89.19	88.09
CGCN (TMM 2022) [203]	ResNet	87.08	79.30	83.97	89.38	86.59	-	-	-	-	-
CAS-SAL-FR (IJCV 2022) [204]	ResNet50	86.40	79.93	87.03	87.33	87.18	82.86	79.64	86.81	87.79	85.18
PromptPAR (arXiv24 [205]	ViT-L/14	88.76	82.84	89.04	89.74	89.18	87.47	83.78	89.27	91.70	90.15
SequencePAR (arXiv24 [206]	ViT-L/14	-	84.92	90.44	90.73	90.46	-	83.94	90.38	90.23	90.10
VTB (TCSVT 2022) [207]	ViT-B/16	85.31	79.60	86.76	87.17	86.71	83.72	80.89	87.88	89.30	88.21
VTB* (TCSVT 2022) [207]	ViT-L/14	86.34	79.59	86.66	87.82	86.97	85.30	81.76	87.87	90.67	88.86
VTB (TCSVT 2022) [207]	ViT-S	82.51	77.23	85.75	84.95	85.01	78.76	77.61	87.41	85.35	85.94
Vim-PAR	Vim-S	81.08	73.75	80.91	84.96	82.52	80.41	78.03	85.39	88.37	86.39

tributes and 19,000 person images. The training, validation, and testing subset contains 9500, 1900, and 7600 images, respectively. By following its default settings, 35 pedestrian attributes are selected for the experiment.

The ViT-S [19] and Mamba-based network Vim-S [61] are adopted as the backbone for this experiment. We follow the vision-language fusion based PAR framework VTB [207] which takes the pedestrian image and attribute set as the input and predicts the logistic scores of each attribute. From the experimental results reported in Table 10, we can find that the Vim-S based PAR model achieves 81.08/73.75/80.91/84.96/82.52 on the PETA dataset, and 80.41/78.03/85.39/88.37/86.39 on the PA100K dataset. These results are significantly better than the ViT-S based model, but still significantly inferior to the compared PAR algorithms developed based on the Transformer network. For example, the ViT-B based VTB achieves 85.31/79.60/86.76/87.17/86.71, 83.72/80.89/87.88/89.30/88.21 on the PETA and PA100K datasets.

4.2 Visual Object Tracking

In this subsection, we compare the Mamba with Transformer, and CNN based backbone for the tracking task[4] based on OSTrack [210]. Specifically, the CNN based trackers are TrDiMP [211], ToMP50 [212], DiMP50 [213], PrDiMP [214], KYS [215], and ATOM [216]; the Transformer based trackers are HDETrack [217], AiATrack [218], STARK [219], TransT [220], MixFormer [221], and SimTrack [222]. To achieve a fair comparison, we train and test these trackers on a large-scale event-based tracking dataset, EventVOT [217], which contains 841, 18, and 282 videos, respectively. The detailed experimental results are reported in Table 11 and Fig. 13. Note that, three widely used evaluation metrics are used for the comparison, including Success Rate (SR), Precision Rate (PR), and Normalized Precision Rate (NPR).

---

4. https://github.com/wangxiao5791509/Single_Object_Tracking_Paper_List

---

TABLE 11
Comparison between different trackers on the EventVOT dataset.

Trackers	Source	Backbone	SR	PR	NPR	Params(M)	FPS
TrDiMP	CVPR21		39.9	34.8	48.7	26.3	26
ToMP50	CVPR22		37.6	32.8	47.4	26.1	25
DiMP50	ICCV19	ResNet50	52.6	51.1	67.2	26.1	43
PrDiMP	CVPR20		55.5	57.2	70.4	26.1	30
KYS	ECCV20		38.7	37.3	49.8	–	20
ATOM	CVPR19		44.4	44.0	57.5	8.4	30
HDETrack	CVPR24		57.8	62.2	73.5	92.1	105
AiATrack	ECCV22		57.4	59.7	72.8	15.8	38
STARK	ICCV21	ViT	44.5	39.6	55.7	28.1	42
TransT	CVPR21		54.3	56.5	68.8	18.5	50
MixFormer	CVPR22		49.9	49.6	63.0	35.6	25
SimTrack	ECCV22		55.4	57.5	69.9	57.8	40
OSTrack	ECCV22	ViT-B	55.4	60.4	71.1	92.1	105
		ViT-S	52.0	53.2	66.8	54.3	109
		Vim-S	55.6	59.1	70.4	4.1	41

According to Table 11, we can find that the performance is slightly decreased when replacing the ViT using the Mamba backbone network, meanwhile, it brings about a huge reduction in the number of parameters (4.1M only). Therefore, we can draw the conclusion that the Mamba network will be a promising choice for the event-based tracking.

4.3 Pixel-level Segmentation

Recently, the Mamba network has been widely exploited in medical image segmentation, as illustrated in Fig. 12 (e, f, g). For example, the Swin-Transformer based model Swin-UNet [223] attains 89.33/99.57/88.46 (Dice, IoU, Accuracy) on the MRI Cardiac dataset. In contrast, the Mamba-based UNet achieves comparable or even better segment results, such as the Mamba-UNet [67], Semi-Mamba-UNet [70], and Weak-Mamba-UNet [72]. These results fully demonstrate the effectiveness of Mamba architecture for medical image segmentation.

4.4 Image-to-Text Generation

For the image-to-text generation, we select the X-ray report generation task which takes the X-ray medical
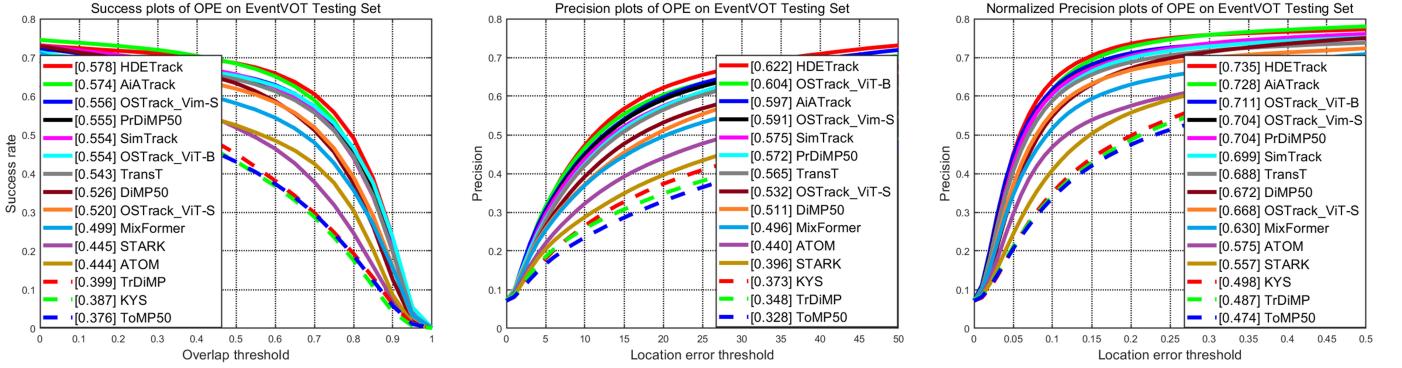
Fig. 13. Visualization of the tracking results on EventVOT dataset.

image as the input and generates the medical report[5]. For the experiment, we select the R2GenGPT[6] as our baseline and evaluated its performance on the IU-Xray dataset [224]. R2GenGPT consists of a visual encoder (Swin Transformer [20]), a linear layer, and a large language model (llama-2-7B-chat [225]). The training approach involves freezing the language model initially and subsequently fine-tuning the visual encoder and the linear layer. We replaced the Swin Transformer with Vim model [61] and compared the results with other methods in Table 12. As both models utilize pre-trained components, Vision Mamba demonstrates superior performance over the Swin Transformer model in terms of BLEU-4 and ROUGE-L scores.

TABLE 12
Comparison between the performance of R2Gen-GPT-Vim-Small and with other methods on IU-Xray dataset. R2Gen-GPT-Vim-S* and R2GenGPT-Vim-S denote the Vim-S are initialized with and without pre-trained parameters, respectively.

Methods	Backbone	CIDEr	BLEU-4	ROUGE-L
R2Gen [226]	CNN	0.398	0.165	0.371
KERP [227]	CNN	0.280	0.162	0.339
HRGP [228]	CNN	0.343	0.151	0.322
MKG [229]	CNN	0.304	0.147	0.367
PPKED [230]	CNN	0.351	0.168	0.376
MGSK [231]	CNN	0.382	0.178	0.381
CA [232]	ResNet-50	-	0.169	0.381
CMCL [233]	CNN	-	0.162	0.378
DCL [234]	CNN	0.586	0.163	0.383
R2GenGPT	Swin-B	0.524	0.152	0.352
R2GenGPT	Vim-S	0.388	0.152	0.355
R2GenGPT	Vim-S*	0.382	0.171	0.371

4.5 Person/Vehicle Re-Identification

As shown in Table 13, we conduct experiments on two re-identification (re-ID) tasks, i.e., the person re-identification [257] and vehicle re-identification [256]. For the person re-ID, four widely used datasets are used, including MSMT17 [258], Market1501 [259], DukeMTMC [260], and Occluded-Duke [261] dataset. These datasets are captured from different scenes, and the samples are collected

5. https://github.com/Event-AHU/Medical_Image_Analysis
6. https://github.com/wang-zhanyu/R2GenGPT

from surveillance systems with overlapping coverage of cameras, which has challenges such as cross-time span, occlusion, and background interference. For the vehicle re-ID, VeRi-776 [262] and VehicleID [263] datasets are utilized for the experimental validation. Different from pedestrian samples, the change of observation viewpoints also brings significant appearance differences for vehicles, for thus the vehicle datasets are additionally provided with viewpoint labels to mark the different viewpoints of the vehicle samples. For the above datasets, we use the Cumulative Matching Characteristic (CMC) curve and mean Average Precision (mAP) as evaluation metrics.

Referring to mainstream frameworks such as TransReID [255] and Strong Baseline [264], we retained ID Loss, Triplet Loss, and BN Layer, and replaced the CNN and Transformer backbones using Vim [61] and VMamba [60] to explore the potential of Mamba for re-identification tasks, and the compared results are shown in Table 13. The selective scanning mechanism (SSM) proposed by the Mamba model allows for sequence modeling with low complexity, and Vim and VMamba further build on it by proposing an SSM modeling approach for 2D image data. Compared to CNN-based models that require complex module design, the simple Mamba network already has effectiveness. Even compared with the models with high complexity such as DeiT [265] and ViT [19], the bidirectional scanning mechanism proposed by Vim has fewer training parameters, and it shows effectiveness on the VehicleID dataset. In contrast, VMamba's cross-scanning mechanism, which does not rely on Transformer's structure (*e.g.*, position embedding and class token), has achieved comparable results on the Market1501, DukeMTMC, and VeRi-776 datasets. For this reason, we expect more Mamba-based studies applicable to the re-identification task in the future.

5 CHALLENGE AND OPPORTUNITY

State Space Model has been widely studied and applied in many applications, however, the research in this direction is still in its early stages. To help the readers quickly grasp the frontiers, this paper puts forward several research points worthy of attention.

● **Current SSMs model still performs inferior to the mainstream of Transformer networks.** From the experimental results reported in Section 4, we can find that there is

TABLE 13
Comparison with methods based on CNN and Transformer on Person Re-identification and Vehicle Re-identification datasets.

Backbone	Method	MSMT17		Market1501		DukeMTMC		Occluded-Duke		Method	VeRi-776		VehicleID	
		mAP	R1	mAP	R1	mAP	R1	mAP	R1		mAP	R1	R1	R5
CNN	CBN [235]	42.9	72.8	77.3	91.3	67.3	82.5	-	-	PRReID [236]	72.5	93.3	72.6	88.6
	OSNet [237]	52.9	78.7	84.9	94.8	73.5	88.6	-	-	SAN [238]	72.5	93.3	79.7	94.3
	MGN [239]	52.1	76.9	86.9	95.7	78.4	88.7	-	-	UMTS [240]	75.9	95.8	80.9	87.0
	RGA-SC [241]	57.5	80.3	88.4	96.1	-	-	-	-	VANet [242]	66.3	89.8	83.3	96.0
	SAN [243]	55.7	79.2	88.0	96.1	75.7	87.9	-	-	SPAN [244]	68.9	94.0	-	-
	SCSN [245]	58.5	83.8	88.5	95.7	79.0	91.0	-	-	PGAN [246]	79.3	96.5	78.0	93.2
	ABDNet [247]	60.8	82.3	88.3	95.6	78.6	89.0	-	-	PVEN [248]	79.5	95.6	84.7	97.0
	PGFA [249]	-	-	76.8	91.2	65.5	82.6	37.3	51.4	SAVER [250]	79.6	96.4	79.9	95.2
	HOReID [251]	-	-	84.9	94.2	75.6	86.9	43.8	55.1	CFVMNet [252]	77.1	95.3	81.4	94.1
	ISP [253]	-	-	88.6	95.3	80.0	89.6	52.3	62.8	GLAMOR [254]	80.3	96.5	78.6	93.6
Transformer	DeiT-B/16 [255]	61.4	81.9	86.6	94.4	78.9	89.3	53.1	60.6	DeiT-B/16 [255]	78.4	95.9	83.1	96.8
	ViT-B/16 [255]	61.0	81.8	86.8	94.7	79.3	88.8	53.1	60.5	ViT-B/16 [255]	78.2	96.5	82.3	96.1
	VehicleMAE [256]	-	-	-	-	-	-	-	-	VehicleMAE [256]	85.6	97.9	-	-
Mamba	Vim-T/16	40.1	62.6	75.7	89.4	66.5	81.8	35.4	45.1	Vim-T/16	62.9	89.2	67.0	88.2
	Vim-S/16	42.2	66.2	77.5	89.7	67.4	83.0	40.8	51.3	Vim-S/16	61.6	89.6	78.2	94.8
	VMamba-T/16	51.0	75.6	83.3	92.8	74.9	87.3	49.4	58.3	VMamba-T/16	77.3	95.9	78.5	93.5
	VMamba-B/16	51.1	75.3	84.3	93.2	77.4	88.0	48.1	57.4	VMamba-B/16	77.5	95.6	82.5	96.1

still room for performance improvement based on SSM. The SSMs pre-trained on the large-scale dataset, such as ImageNet [2], play a critical role in many downstream tasks, however, the base, large, and huge versions of SSMs are rarely released. We believe this may be an obstacle to the high performance on the CV tasks.

• **The advantages of the SSMs in GPU usage are worth further exploration and research.** According to our experiments, the memory consumption is lower or comparable to the Transformer networks on some downstream tasks. A significant improvement in this aspect can be observed, but some tasks are not. The study on mining the lower GPU memory consumption is worth further exploration and research.

• **To further explore its advantages in high-resolution or long-term vision data is a direction worthy of attention and research.** Since the SSMs architecture significantly reduces the complexity of the model theoretically, its modeling capability on high-resolution data (remote sensing data, X-ray medical images) or long-term sequence data (long-term video frames) is of great value. However, these aspects are not addressed well using other strong models like the Transformer network.

• **Pre-trained big models using SSMs architecture.** In the pre-trained big model era, the scaling of deep neural networks is an important step for general artificial intelligence. Current big models are built based on CNN or Transformer networks, and seldom of them adopt the SSMs architecture. Recently, Jamba [136] released by AI21Labs is a novel large language model built by fusing the Transformer, Mamba, and MoE (Mixture-of-Experts). It supports the input of context length up to 256K tokens and also achieves comparable performance with Mixtral-8x7B [266] and Llama-2 70B [225]. The study on building pure Mamba or hybrid architectures will be a promising direction for pre-trained big models.

• **Multi-modal learning using SSMs architecture.** Early multi-modal related works focused on how to learn modality-specific and modality-shared representations. Influenced by the Transformer network, current multi-modal algorithms usually directly encode and fuse the multiple cues in a unified Transformer network [267], [268]. Thus, the cost of the inference phase may be twice compared with a single modality only. How to design new SSMs-based backbones for cost-sensitive multi-modal learning is an important research topic.

• **Developing novel scan operators for the SSMs.** The scan is a key operator for the SSMs architecture and the 1D and 2D data are usually processed with different scan mechanisms. For example, VMamba [60] scans an image using *CSM* (scan expand) and merges the four output features as the final 2D feature map. To deal with more special remote sensing data, some researchers have proposed additional scanning mechanisms to capture skewed feature representations to obtain more comprehensive features [139]. A comparison of different scan schemes can be found in Fig. 8. Therefore, it is natural to design novel scan schemes to enhance the feature learning of SSMs. For example, it is possible to develop new track-changing scan methods to better encode the point cloud and event streams.

• **The generalization performance of SSMs still deserves attention and further research and improvement.** Compared with the limited receptive field and greater complexity of CNN and the Transformer, SSMs have linear complexity and global receptive fields, which may have greater advantages and potential in the field of domain generalization. However, current SSM based networks illustrate limited domain generalization ability, as noted in DGMamba [120]. Long et al. [120] attempt to address this issue from the perspective of hidden states and inappropriate scan mechanisms by proposing the Hidden State Suppressing (HSS) and Semantic-aware Patch Refining (SPR) strategies. We believe more insights and improvements can be conducted to further improve the overall performance of domain generalization.

• **Use the latest SSM model to empower the existing deep neural network model.** In the early stage of the third wave of deep learning, many clever neural network modules or designs are proposed, for example, knowledge distillation, pyramid structure, network in network [269], diffusion model, GAN, etc. Enhancing the SSM based on these successful modules or introducing SSM into these modules may bring us better performance.

6 CONCLUSION

In this paper, we revisit and summarize the existing works on the State Space Model to help the readers quickly capture the cutting-edge research. We first give an introduction to the origin of the State Space Model, then, we dive into the main streams of SSMs and review these works from the perspective of origin algorithm, natural language processing, computer vision, graph, multi-modal/multi-media, event/point data, time series, and other domains. Due to the applications of SSMs in each domain still in the early stages, in this paper, we conduct/summarize experiments on multiple research problems, such as single-/multi-label classification, visual object tracking, pixel-level segmentation, image-to-text generation, person/vehicle re-identification, etc. From the experimental results, we can find that current SSMs achieve similar performance with some Transformer networks. However, the overall results are still inferior to the state-of-the-art models. Also, the decrease in memory usage can be observed in the downstream tasks. After that, we summarize the challenges still existing in the SSMs and propose several research opportunities to help the related researchers better understand this direction.

Given the limited time and expertise, this review may still have noticeable shortcomings, such as insufficiently objective and fair comments, omissions in the reviewed articles, and suggestions that may lack depth and detail. We hope readers can understand this and sincerely hope this review can better promote the development of the State Space Model and even artificial intelligence.

ACKNOWLEDGMENT

REFERENCES

[1] A. Krizhevsky, I. Sutskever, and G. E. Hinton, "Imagenet classification with deep convolutional neural networks," in *Proceedings of Advances in Neural Information Processing Systems*, 2012.

[2] J. Deng, W. Dong, R. Socher, L.-J. Li, K. Li, and L. Fei-Fei, "Imagenet: A large-scale hierarchical image database," in *Proceedings of the IEEE/CVF Conference on Computer Vision and Pattern Recognition*, 2009, pp. 248–255.

[3] C. Szegedy, W. Liu, Y. Jia, P. Sermanet, S. Reed, D. Anguelov, D. Erhan, V. Vanhoucke, and A. Rabinovich, "Going deeper with convolutions," in *Proceedings of the IEEE/CVF Conference on Computer Vision and Pattern Recognition*, 2015, pp. 1–9.

[4] K. He, X. Zhang, S. Ren, and J. Sun, "Deep residual learning for image recognition," in *Proceedings of the IEEE/CVF Conference on Computer Vision and Pattern Recognition*, 2016, pp. 770–778.

[5] C. Szegedy, W. Liu, Y. Jia, P. Sermanet, S. Reed, D. Anguelov, D. Erhan, V. Vanhoucke, and A. Rabinovich, "Going deeper with convolutions," in *Proceedings of the IEEE/CVF Conference on Computer Vision and Pattern Recognition*, 2015, pp. 1–9.

[6] X. Wang, S. Zheng, R. Yang, A. Zheng, Z. Chen, J. Tang, and B. Luo, "Pedestrian attribute recognition: A survey," *Pattern Recognition*, vol. 121, p. 108220, 2022.

[7] D. Silver, A. Huang, C. J. Maddison, A. Guez, L. Sifre, G. Van Den Driessche, J. Schrittwieser, I. Antonoglou, V. Panneershelvam, M. Lanctot *et al.*, "Mastering the game of go with deep neural networks and tree search," *Nature*, vol. 529, no. 7587, pp. 484–489, 2016.

[8] S. Hochreiter and J. Schmidhuber, "Long short-term memory," *Neural Computation*, vol. 9, no. 8, pp. 1735–1780, 1997.

[9] K. Cho, B. van Merriënboer, Ç. Gulçehre, D. Bahdanau, F. Bougares, H. Schwenk, and Y. Bengio, "Learning phrase representations using rnn encoder–decoder for statistical machine translation," in *Proceedings of the Conference on Empirical Methods in Natural Language Processing*, 2014, pp. 1724–1734.

[10] P. Velickovic, G. Cucurull, A. Casanova, A. Romero, P. Lio', and Y. Bengio, "Graph attention networks," *arXiv preprint arXiv:1710.10903*, 2017.

[11] Z. Wu, S. Pan, F. Chen, G. Long, C. Zhang, and S. Y. Philip, "A comprehensive survey on graph neural networks," *IEEE Transactions on Neural Networks and Learning Systems*, vol. 32, no. 1, pp. 4–24, 2020.

[12] A. Gu and T. Dao, "Mamba: Linear-time sequence modeling with selective state spaces," *arXiv preprint arXiv:2312.00752*, 2023.

[13] A. Vaswani, N. Shazeer, N. Parmar, J. Uszkoreit, L. Jones, A. N. Gomez, Ł. Kaiser, and I. Polosukhin, "Attention is all you need," in *Proceedings of Advances in Neural Information Processing Systems*, 2017.

[14] B. Min, H. Ross, E. Sulem, A. P. B. Veyseh, T. H. Nguyen, O. Sainz, E. Agirre, I. Heintz, and D. Roth, "Recent advances in natural language processing via large pre-trained language models: A survey," *ACM Computing Surveys*, vol. 56, no. 2, pp. 1–40, 2023.

[15] J. D. M.-W. C. Kenton and L. K. Toutanova, "Bert: Pre-training of deep bidirectional transformers for language understanding," in *Proceedings of Annual Conference of the North American Chapter of the Association for Computational Linguistics*, 2019, pp. 4171–4186.

[16] Y. Sun, S. Wang, S. Feng, S. Ding, C. Pang, J. Shang, J. Liu, X. Chen, Y. Zhao, Y. Lu, W. Liu, Z. Wu, W. Gong, J. Liang, Z. Shang, P. Sun, W. Liu, O. Xuan, D. Yu, H. Tian, H. Wu, and H. Wang, "Ernie 3.0: Large-scale knowledge enhanced pre-training for language understanding and generation," *arXiv preprint arXiv:2107.02137*, 2021.

[17] M. Lewis, Y. Liu, N. Goyal, M. Ghazvininejad, A. Mohamed, O. Levy, V. Stoyanov, and L. Zettlemoyer, "Bart: Denoising sequence-to-sequence pre-training for natural language generation, translation, and comprehension," in *Proceedings of the Annual Meeting of the Association for Computational Linguistics*, 2020, pp. 7871–7880.

[18] J. Achiam, S. Adler, S. Agarwal, L. Ahmad, I. Akkaya, F. L. Aleman, D. Almeida, J. Altenschmidt, S. Altman, S. Anadkat *et al.*, "Gpt-4 technical report," *arXiv preprint arXiv:2303.08774*, 2023.

[19] A. Dosovitskiy, L. Beyer, A. Kolesnikov, D. Weissenborn, X. Zhai, T. Unterthiner, M. Dehghani, M. Minderer, G. Heigold, S. Gelly, J. Uszkoreit, and N. Houlsby, "An image is worth 16x16 words: Transformers for image recognition at scale," *arXiv preprint arXiv:2010.11929*, 2020.

[20] Z. Liu, Y. Lin, Y. Cao, H. Hu, Y. Wei, Z. Zhang, S. Lin, and B. Guo, "Swin transformer: Hierarchical vision transformer using shifted windows," in *Proceedings of the IEEE/CVF International Conference on Computer Vision*, 2021, pp. 10 012–10 022.

[21] X. Wang, G. Chen, G. Qian, P. Gao, X.-Y. Wei, Y. Wang, Y. Tian, and W. Gao, "Large-scale multi-modal pre-trained models: A comprehensive survey," *Machine Intelligence Research*, vol. 20, no. 4, pp. 447–482, 2023.

[22] A. Radford, J. W. Kim, C. Hallacy, A. Ramesh, G. Goh, S. Agarwal, G. Sastry, A. Askell, P. Mishkin, J. Clark *et al.*, "Learning transferable visual models from natural language supervision," in *Proceedings of the International Conference on Machine Learning*, 2021, pp. 8748–8763.

[23] Y. Xin, S. Luo, H. Zhou, J. Du, X. Liu, Y. Fan, Q. Li, and Y. Du, "Parameter-efficient fine-tuning for pre-trained vision models: A survey," *arXiv preprint arXiv:2402.02242*, 2024.

[24] H. Ren, H. Dai, Z. Dai, M. Yang, J. Leskovec, D. Schuurmans, and B. Dai, "Combiner: Full attention transformer with sparse computation cost," in *Proceedings of Advances in Neural Information Processing Systems*, 2021, pp. 22 470–22 482.

[25] D. Han, X. Pan, Y. Han, S. Song, and G. Huang, "Flatten transformer: Vision transformer using focused linear attention," in *Proceedings of the IEEE/CVF International Conference on Computer Vision*, 2023, pp. 5961–5971.

[26] A. Katharopoulos, A. Vyas, N. Pappas, and F. Fleuret, "Transformers are rnns: Fast autoregressive transformers with linear attention," in *Proceedings of the International Conference on Machine Learning*, 2020, pp. 5156–5165.

[27] K. Choromanski, V. Likhosherstov, D. Dohan, X. Song, A. Gane, T. Sarlós, P. Hawkins, J. Davis, A. Mohiuddin, L. Kaiser, D. Be-

langer, L. J. Colwell, and A. Weller, "Rethinking attention with performers," *arXiv preprint arXiv:2009.14794*, 2020.

[28] S. Yang, B. Wang, Y. Shen, R. Panda, and Y. Kim, "Gated linear attention transformers with hardware-efficient training," *arXiv preprint arXiv:2312.06635*, 2023.

[29] A. Gu, K. Goel, and C. R'e, "Efficiently modeling long sequences with structured state spaces," *arXiv preprint arXiv:2111.00396*, 2021.

[30] E. Nguyen, K. Goel, A. Gu, G. Downs, P. Shah, T. Dao, S. Baccus, and C. Ré, "S4nd: Modeling images and videos as multidimensional signals with state spaces," in *Proceedings of Advances in Neural Information Processing Systems*, 2022, pp. 2846–2861.

[31] J. N. Yan, J. Gu, and A. M. Rush, "Diffusion models without attention," *arXiv preprint arXiv:2311.18257*, 2023.

[32] V. T. Hu, S. A. Baumann, M.-S. Gui, O. Grebenkova, P. Ma, J. S. Fischer, and B. Ommer, "Zigma: A dit-style zigzag mamba diffusion model," *arXiv preprint arXiv:2403.13802*, 2024.

[33] Z. Fei, M. Fan, C. Yu, and J. Huang, "Scalable diffusion models with state space backbone," *arXiv preprint arXiv:2402.05608*, 2024.

[34] A. Gu, I. Johnson, K. Goel, K. Saab, T. Dao, A. Rudra, and C. Ré, "Combining recurrent, convolutional, and continuous-time models with linear state space layers," in *Proceedings of Advances in Neural Information Processing Systems*, 2021, pp. 572–585.

[35] R. E. Kalman, "A new approach to linear filtering and prediction problems," *Journal of Basic Engineering*, vol. 82, no. 1, pp. 35–45, 1960.

[36] A. Gu, T. Dao, S. Ermon, A. Rudra, and C. Ré, "Hippo: Recurrent memory with optimal polynomial projections," *arXiv preprint arXiv:2008.07669*, 2020.

[37] A. Gu, K. Goel, A. Gupta, and C. Ré, "On the parameterization and initialization of diagonal state space models," in *Proceedings of Advances in Neural Information Processing Systems*, 2022, pp. 35 971–35 983.

[38] A. Gupta, A. Gu, and J. Berant, "Diagonal state spaces are as effective as structured state spaces," *Proceedings of Advances in Neural Information Processing Systems*, pp. 22 982–22 994, 2022.

[39] A. Orvieto, S. L. Smith, A. Gu, A. Fernando, C. Gulcehre, R. Pascanu, and S. De, "Resurrecting recurrent neural networks for long sequences," in *Proceedings of the International Conference on Machine Learning*, 2023, pp. 26 670–26 698.

[40] A. Gu, I. Johnson, A. Timalsina, A. Rudra, and C. Ré, "How to train your hippo: State space models with generalized orthogonal basis projections," *arXiv preprint arXiv:2206.120370*, 2022.

[41] H. Mehta, A. Gupta, A. Cutkosky, and B. Neyshabur, "Long range language modeling via gated state spaces," *arXiv preprint arXiv:2206.13947*, 2022.

[42] Y. Du, X. Liu, and Y. Chua, "Spiking structured state space model for monaural speech enhancement," *arXiv preprint arXiv:2309.03641*, 2023.

[43] X. Jiang, C. Han, and N. Mesgarani, "Dual-path mamba: Short and long-term bidirectional selective structured state space models for speech separation," *arXiv preprint arXiv:2403.18257*, 2024.

[44] K. Li and G. Chen, "Spmamba: State-space model is all you need in speech separation," *arXiv preprint arXiv:2403.02063*, 2024.

[45] R. Grazzi, J. Siems, S. Schrodi, T. Brox, and F. Hutter, "Is mamba capable of in-context learning?" *arXiv preprint arXiv:2402.03170*, 2024.

[46] B. Qi, J. Gao, D. Li, K. Zhang, J. Liu, L. Wu, and B. Zhou, "S4++: Elevating long sequence modeling with state memory reply," 2024. [Online]. Available: https://openreview.net/forum?id=bdnw4qjfH9

[47] S. Zuo, X. Liu, J. Jiao, D. X. Charles, E. Manavoglu, T. Zhao, and J. Gao, "Efficient long sequence modeling via state space augmented transformer," *arXiv preprint arXiv:2212.08136*, 2022.

[48] W. He, K. Han, Y. Tang, C. Wang, Y. Yang, T. Guo, and Y. Wang, "Densemamba: State space models with dense hidden connection for efficient large language models," *arXiv preprint arXiv:2403.00818*, 2024.

[49] Z. Yang, A. Mitra, S. Kwon, and H. Yu, "Clinicalmamba: A generative clinical language model on longitudinal clinical notes," *arXiv preprint arXiv:2403.05795*, 2024.

[50] A. R. de Sousa Porfírio Correia and L. A. Alexandre, "Music to dance as language translation using sequence models," *arXiv preprint arXiv:2403.15569*, 2024.

[51] C. Wang, O. Tsepa, J. Ma, and B. Wang, "Graph-mamba: Towards long-range graph sequence modeling with selective state spaces," *arXiv preprint arXiv:2402.00789*, 2024.

[52] S. Tang, J. A. Dunnmon, Q. Liangqiong, K. K. Saab, T. Baykaner, C. Lee-Messer, and D. L. Rubin, "Modeling multivariate biosignals with graph neural networks and structured state space models," in *Proceedings of the International Conference on Learning Representations Workshops*, 2023.

[53] A. Behrouz and F. Hashemi, "Graph mamba: Towards learning on graphs with state space models," *arXiv preprint arXiv:2402.08678*, 2024.

[54] G. Bachmann and V. Nagarajan, "The pitfalls of next-token prediction," *arXiv preprint arXiv:2403.06963*, 2024.

[55] L. Li, H. Wang, W. Zhang, and A. Coster, "Stg-mamba: Spatial-temporal graph learning via selective state space model," *arXiv preprint arXiv:2403.12418*, 2024.

[56] M. M. Islam and G. Bertasius, "Long movie clip classification with state-space video models," in *Proceedings of European Conference on Computer Vision*, 2022, pp. 87–104.

[57] J. T. Smith, A. Warrington, and S. Linderman, "Simplified state space layers for sequence modeling," in *Proceedings of the International Conference on Learning Representations*, 2022.

[58] J. Wang, W. Zhu, P. Wang, X. Yu, L. Liu, M. Omar, and R. Hamid, "Selective structured state-spaces for long-form video understanding," in *Proceedings of the IEEE/CVF Conference on Computer Vision and Pattern Recognition*, 2023, pp. 6387–6397.

[59] D. Hafner, J. Pasukonis, J. Ba, and T. Lillicrap, "Mastering diverse domains through world models," *arXiv preprint arXiv:2301.04104*, 2023.

[60] Y. Liu, Y. Tian, Y. Zhao, H. Yu, L. Xie, Y. Wang, Q. Ye, and Y. Liu, "Vmamba: Visual state space model," *arXiv preprint arXiv:2401.10166*, 2024.

[61] L. Zhu, B. Liao, Q. Zhang, X. Wang, W. Liu, and X. Wang, "Vision mamba: Efficient visual representation learning with bidirectional state space model," *arXiv preprint arXiv:2401.09417*, 2024.

[62] Z. Xing, T. Ye, Y. Yang, G. Liu, and L. Zhu, "Segmamba: Long-range sequential modeling mamba for 3d medical image segmentation," *arXiv preprint arXiv:2401.13560*, 2024.

[63] J. Ma, F. Li, and B. Wang, "U-mamba: Enhancing long-range dependency for biomedical image segmentation," *arXiv preprint arXiv:2401.04722*, 2024.

[64] J. Liu, H. Yang, H.-Y. Zhou, Y. Xi, L. Yu, Y. Yu, Y. Liang, G. Shi, S. Zhang, H. Zheng *et al.*, "Swin-umamba: Mamba-based unet with imagenet-based pretraining," *arXiv preprint arXiv:2402.03302*, 2024.

[65] J. Ruan and S. Xiang, "Vm-unet: Vision mamba unet for medical image segmentation," *arXiv preprint arXiv:2402.02491*, 2024.

[66] H. Gong, L. Kang, Y. Wang, X. Wan, and H. Li, "nnmamba: 3d biomedical image segmentation, classification and landmark detection with state space model," *arXiv preprint arXiv:2402.03526*, 2024.

[67] Z. Wang, J.-Q. Zheng, Y. Zhang, G. Cui, and L. Li, "Mamba-unet: Unet-like pure visual mamba for medical image segmentation," *arXiv preprint arXiv:2402.05079*, 2024.

[68] S. Li, H. Singh, and A. Grover, "Mamba-nd: Selective state space modeling for multi-dimensional data," *arXiv preprint arXiv:2402.05892*, 2024.

[69] Z. Zheng and J. Zhang, "Fd-vision mamba for endoscopic exposure correction," *arXiv preprint arXiv:2402.06378*, 2024.

[70] Z. Wang and C. Ma, "Semi-mamba-unet: Pixel-level contrastive cross-supervised visual mamba-based unet for semi-supervised medical image segmentation," *arXiv preprint arXiv:2402.07245*, 2024.

[71] Z. Ye and T. Chen, "P-mamba: Marrying perona malik diffusion with mamba for efficient pediatric echocardiographic left ventricular segmentation," *arXiv preprint arXiv:2402.08506*, 2024.

[72] Z. Wang and C. Ma, "Weak-mamba-unet: Visual mamba makes cnn and vit work better for scribble-based medical image segmentation," *arXiv preprint arXiv:2402.10887*, 2024.

[73] X. He, K. Cao, K. Yan, R. Li, C. Xie, J. Zhang, and M. Zhou, "Pan-mamba: Effective pan-sharpening with state space model," *arXiv preprint arXiv:2402.12192*, 2024.

[74] N. Agarwal, D. Suo, X. Chen, and E. Hazan, "Spectral state space models," *arXiv preprint arXiv:2312.06837*, 2023.

[75] P. Mattes, R. Schlosser, and R. Herbrich, "Hieros: Hierarchical imagination on structured state space sequence world models," *arXiv preprint arXiv:2310.05167*, 2023.

[76] E. Baron, I. Zimerman, and L. Wolf, "A 2-dimensional state space layer for spatial inductive bias," in *Proceedings of the International Conference on Learning Representations*, 2023.

[77] H. Guo, J. Li, T. Dai, Z. Ouyang, X. Ren, and S.-T. Xia, "Mambair: A simple baseline for image restoration with state-space model," *arXiv preprint arXiv:2402.15648*, 2024.

[78] J. Huang, L. Yang, F. Wang, Y. Wu, Y. Nan, A. I. Aviles-Rivero, C.-B. Schönlieb, D. Zhang, and G. Yang, "Mambamir: An arbitrary-masked mamba for joint medical image reconstruction and uncertainty estimation," *arXiv preprint arXiv:2402.18451*, 2024.

[79] C.-S. Chen, G.-Y. Chen, D. Zhou, D. Jiang, and D.-S. Chen, "Resvmamba: Fine-grained food category visual classification using selective state space models with deep residual learning," *arXiv preprint arXiv:2402.15761*, 2024.

[80] T. Chen, Z. Tan, T. Gong, Q. Chu, Y. Wu, B. Liu, J. Ye, and N. Yu, "Mim-istd: Mamba-in-mamba for efficient infrared small target detection," *arXiv preprint arXiv:2403.02148*, 2024.

[81] Y. Yue and Z. Li, "Medmamba: Vision mamba for medical image classification," *arXiv preprint arXiv:2403.03849*, 2024.

[82] H. Tang, L. Cheng, G. Huang, Z. Tan, J. Lu, and K. Wu, "Rotate to scan: Unet-like mamba with triplet ssm module for medical image segmentation," *arXiv preprint arXiv:2403.17701*, 2024.

[83] Z. Fang, Y. Wang, Z. Wang, J. Zhang, X. Ji, and Y. Zhang, "Mammil: Multiple instance learning for whole slide images with state space models," *arXiv preprint arXiv:2403.05160*, 2024.

[84] K. Li, X. Li, Y. Wang, Y. He, Y. Wang, L. Wang, and Y. Qiao, "Videomamba: State space model for efficient video understanding," *arXiv preprint arXiv:2403.06977*, 2024.

[85] J. Wang, J. Chen, D. Chen, and J. Wu, "Large window-based mamba unet for medical image segmentation: Beyond convolution and self-attention," *arXiv preprint arXiv:2403.07332*, 2024.

[86] C. Cheng, H. Wang, and H. Sun, "Activating wider areas in image super-resolution," *arXiv preprint arXiv:2403.08330*, 2024.

[87] Y. Schiff, C.-H. Kao, A. Gokaslan, T. Dao, A. Gu, and V. Kuleshov, "Caduceus: Bi-directional equivariant long-range dna sequence modeling," *arXiv preprint arXiv:2403.03234*, 2024.

[88] Y. Zhang, W. Yan, K. Yan, C. P. Lam, Y. Qiu, P. Zheng, R. S.-Y. Tang, and S. S. Cheng, "Motion-guided dual-camera tracker for low-cost skill evaluation of gastric endoscopy," *arXiv preprint arXiv:2403.05146*, 2024.

[89] W. Liao, Y. Zhu, X. Wang, C. Pan, Y. Wang, and L. Ma, "Lightmunet: Mamba assists in lightweight unet for medical image segmentation," *arXiv preprint arXiv:2403.05246*, 2024.

[90] G. Chen, Y. Huang, J. Xu, B. Pei, Z. Chen, Z. Li, J. Wang, K. Li, T. Lu, and L. Wang, "Video mamba suite: State space model as a versatile alternative for video understanding," *arXiv preprint arXiv:2403.09626*, 2024.

[91] M. Zhang, Y. Yu, L. Gu, T. Lin, and X. Tao, "Vm-unet-v2 rethinking vision mamba unet for medical image segmentation," *arXiv preprint arXiv:2403.09157*, 2024.

[92] T. Huang, X. Pei, S. You, F. Wang, C. Qian, and C. Xu, "Localmamba: Visual state space model with windowed selective scan," *arXiv preprint arXiv:2403.09338*, 2024.

[93] Z. Xu, Y. Lin, H. Han, S. Yang, R. Li, Y. Zhang, and X. Li, "Mambatalk: Efficient holistic gesture synthesis with selective state space models," *arXiv preprint arXiv:2403.09471*, 2024.

[94] X. Pei, T. Huang, and C. Xu, "Efficientvmamba: Atrous selective scan for light weight visual mamba," *arXiv preprint arXiv:2403.09977*, 2024.

[95] C. Du, Y. Li, and C. Xu, "Understanding robustness of visual state space models for image classification," *arXiv preprint arXiv:2403.10935*, 2024.

[96] Y. Shi, B. Xia, X. Jin, X. Wang, T. Zhao, X. Xia, X. Xiao, and W. Yang, "Vmambair: Visual state space model for image restoration," *arXiv preprint arXiv:2403.11423*, 2024.

[97] T. Guo, Y. Wang, and C. Meng, "Mambamorph: a mamba-based backbone with contrastive feature learning for deformable mr-ct registration," *arXiv preprint arXiv:2401.13934*, 2024.

[98] Y. Yang, Z. Xing, and L. Zhu, "Vivim: a video vision mamba for medical video object segmentation," *arXiv preprint arXiv:2401.14168*, 2024.

[99] J. Xie, R. Liao, Z. Zhang, S. Yi, Y. Zhu, and G. Luo, "Promamba: Prompt-mamba for polyp segmentation," *arXiv preprint arXiv:2403.13660*, 2024.

[100] R. Wu, Y. Liu, P. Liang, and Q. Chang, "H-vmunet: High-order vision mamba unet for medical image segmentation," *arXiv preprint arXiv:2403.13642*, 2024.

[101] C. Yang, Z. Chen, M. Espinosa, L. Ericsson, Z. Wang, J. Liu, and E. J. Crowley, "Plainmamba: Improving non-hierarchical mamba in visual recognition," *arXiv preprint arXiv:2403.17695*, 2024.

[102] K. S. Sanjid, M. T. Hossain, M. S. S. Junayed, and D. M. M. Uddin, "Integrating mamba sequence model and hierarchical upsampling network for accurate semantic segmentation of multiple sclerosis legion," *arXiv preprint arXiv:2403.17432*, 2024.

[103] Y. Tang, P. Dong, Z. Tang, X. Chu, and J. Liang, "Vmrnn: Integrating vision mamba and lstm for efficient and accurate spatiotemporal forecasting," *arXiv preprint arXiv:2403.16536*, 2024.

[104] Q. Shen, X. Yi, Z. Wu, P. Zhou, H. Zhang, S. Yan, and X. Wang, "Gamba: Marry gaussian splatting with mamba for single view 3d reconstruction," *arXiv preprint arXiv:2403.18795*, 2024.

[105] Z. Wang, J.-Q. Zheng, C. Ma, and T. Guo, "Vmambamorph: a visual mamba-based framework with cross-scan module for deformable 3d image registration," *arXiv preprint arXiv:2404.05105*, 2024.

[106] J. Hao, L. He, and K. F. Hung, "T-mamba: Frequency-enhanced gated long-range dependency for tooth 3d cbct segmentation," *arXiv preprint arXiv:2404.01065*, 2024.

[107] W. Li, X. Hong, and X. Fan, "Spikemba: Multi-modal spiking saliency mamba for temporal video grounding," *arXiv preprint arXiv:2404.01174*, 2024.

[108] X. Ma, X. Zhang, and M.-O. Pun, "Rs3mamba: Visual state space model for remote sensing images semantic segmentation," *arXiv preprint arXiv:2404.02457*, 2024.

[109] H. Chen, J. Song, C. Han, J. Xia, and N. Yokoya, "Changemamba: Remote sensing change detection with spatio-temporal state space model," *arXiv preprint arXiv:2404.03425*, 2024.

[110] M. Shahab Sepehri, Z. Fabian, and M. Soltanolkotabi, "Serpent: Scalable and efficient image restoration via multi-scale structured state space models," *arXiv preprint arXiv:2403.17902*, 2024.

[111] Y. Yang, C. Ma, J. Yao, Z. Zhong, Y. Zhang, and Y. Wang, "Remamber: Referring image segmentation with mamba twister," *arXiv preprint arXiv:2403.17839*, 2024.

[112] Q. Wang, C. Wang, Z. Lai, and Y. Zhou, "Insectmamba: Insect pest classification with state space model," *arXiv preprint arXiv:2404.03611*, 2024.

[113] Q. Zhu, Y. Cai, Y. Fang, Y. Yang, C. Chen, L. Fan, and A. Nguyen, "Samba: Semantic segmentation of remotely sensed images with state space model," *arXiv preprint arXiv:2404.01705*, 2024.

[114] A. Behrouz, M. Santacatterina, and R. Zabih, "Mambamixer: Efficient selective state space models with dual token and channel selection," *arXiv preprint arXiv:2403.19888*, 2024.

[115] R. Wu, Y. Liu, P. Liang, and Q. Chang, "Ultralight vm-unet: Parallel vision mamba significantly reduces parameters for skin lesion segmentation," *arXiv preprint arXiv:2403.20035*, 2024.

[116] B. Zou, Z. Guo, X. Hu, and H. Ma, "Rhythmmamba: Fast remote physiological measurement with arbitrary length videos," *arXiv preprint arXiv:2404.06483*, 2024.

[117] H. He, Y. Bai, J. Zhang, Q. He, H. Chen, Z. Gan, C. Wang, X. Li, G. Tian, and L. Xie, "Mambaad: Exploring state space models for multi-class unsupervised anomaly detection," *arXiv preprint arXiv:2404.06564*, 2024.

[118] S. Chaudhuri and S. Bhattacharya, "Simba: Mamba augmented u-shiftgcn for skeletal action recognition in videos," *arXiv preprint arXiv:2404.07645*, 2024.

[119] A. Archit and C. Pape, "Vim-unet: Vision mamba for biomedical segmentation," *arXiv preprint arXiv:2404.07705*, 2024.

[120] S. Long, Q. Zhou, X. Li, X. Lu, C. Ying, Y. Luo, L. Ma, and S. Yan, "Dgmamba: Domain generalization via generalized state space model," *arXiv preprint arXiv:2404.07794*, 2024.

[121] S. Peng, X. Zhu, H. Deng, Z. Lei, and L.-J. Deng, "Fusionmamba: Efficient image fusion with state space model," *arXiv preprint arXiv:2404.07932*, 2024.

[122] A. Gu, A. Gupta, K. Goel, and C. Ré, "On the parameterization and initialization of diagonal state space models," *arXiv preprint arXiv:2206.11893*, 2022.

[123] F. Bonassi, C. Andersson, P. Mattsson, and T. B. Schön, "Structured state-space models are deep wiener models," *arXiv preprint arXiv:2312.06211*, 2023.

[124] N. M. Cirone, A. Orvieto, B. Walker, C. Salvi, and T. Lyons, "Theoretical foundations of deep selective state-space models," *arXiv preprint arXiv:2402.19047*, 2024.

[125] B. Peng, E. Alcaide, Q. Anthony, A. Albalak, S. Arcadinho, S. Biderman, H. Cao, X. Cheng, M. Chung, L. Derczynski *et al.*, "Rwkv: Reinventing rnns for the transformer era," in *Findings of*

the Association for Computational Linguistics: EMNLP 2023, 2023, pp. 14 048–14 077.

[126] Y. Duan, W. Wang, Z. Chen, X. Zhu, L. Lu, T. Lu, Y. Qiao, H. Li, J. Dai, and W. Wang, "Vision-rwkv: Efficient and scalable visual perception with rwkv-like architectures," *arXiv preprint arXiv:2403.02308*, 2024.

[127] Y. Sun, L. Dong, S. Huang, S. Ma, Y. Xia, J. Xue, J. Wang, and F. Wei, "Retentive network: A successor to transformer for large language models," *arXiv preprint arXiv:2307.08621*, 2023.

[128] X. Ma, C. Zhou, X. Kong, J. He, L. Gui, G. Neubig, J. May, and L. Zettlemoyer, "Mega: Moving average equipped gated attention," in *The Eleventh International Conference on Learning Representations*, 2022.

[129] D. Y. Fu, T. Dao, K. K. Saab, A. W. Thomas, A. Rudra, and C. Re, "Hungry hungry hippos: Towards language modeling with state space models," in *The Eleventh International Conference on Learning Representations*, 2022.

[130] S. Zhai, W. Talbott, N. Srivastava, C. Huang, H. Goh, R. Zhang, and J. Susskind, "An attention free transformer," *arXiv preprint arXiv:2105.14103*, 2021.

[131] H. Hou and F. R. Yu, "Rwkv-ts: Beyond traditional recurrent neural network for time series tasks," *arXiv preprint arXiv:2401.09093*, 2024.

[132] Z. Zhu, W. Shao, and D. Jiao, "Tls-rwkv: Real-time online action detection with temporal label smoothing," *Neural Processing Letters*, vol. 56, no. 2, pp. 1–13, 2024.

[133] Z. Fei, M. Fan, C. Yu, D. Li, and J. Huang, "Diffusion-rwkv: Scaling rwkv-like architectures for diffusion models," *arXiv preprint arXiv:2404.04478*, 2024.

[134] C. Subakan, M. Ravanelli, S. Cornell, M. Bronzi, and J. Zhong, "Attention is all you need in speech separation," in *Proceedings of International Conference on Acoustics, Speech and Signal Processing*, 2020, pp. 21–25.

[135] Z.-Q. Wang, S. Cornell, S. Choi, Y. Lee, B. Kim, and S. Watanabe, "Tf-gridnet: Making time-frequency domain models great again for monaural speaker separation," in *Proceedings of International Conference on Acoustics, Speech and Signal Processing*, 2022, pp. 1–5.

[136] O. Lieber, B. Lenz, H. Bata, G. Cohen, J. Osin, I. Dalmedigos, E. Safahi, S. Meirom, Y. Belinkov, S. Shalev-Shwartz *et al.*, "Jamba: A hybrid transformer-mamba language model," *arXiv preprint arXiv:2403.19887*, 2024.

[137] S. Li, T. Zhu, F. Duan, L. Chen, H. Ning, and Y. Wan, "Harmamba: Efficient wearable sensor human activity recognition based on bidirectional selective ssm," *arXiv preprint arXiv:2403.20183*, 2024.

[138] J. X. Yang, J. Zhou, J. Wang, H. Tian, and A. W. C. Liew, "Hsimamba: Hyperspectral imaging efficient feature learning with bidirectional state space for classification," *arXiv preprint arXiv:2404.00272*, 2024.

[139] S. Zhao, H. Chen, X. Zhang, P. Xiao, L. Bai, and W. Ouyang, "Rs-mamba for large remote sensing image dense prediction," *arXiv preprint arXiv:2404.02668*, 2024.

[140] Y. Ding, A. Orvieto, B. He, and T. Hofmann, "Recurrent distance filtering for graph representation learning," *arXiv preprint arXiv:2312.01538*, 2024.

[141] J. Park, J. Park, Z. Xiong, N. Lee, J. Cho, S. Oymak, K. Lee, and D. Papailiopoulos, "Can mamba learn how to learn? a comparative study on in-context learning tasks," *arXiv preprint arXiv:2402.04248*, 2024.

[142] N. Zucchet, S. Kobayashi, Y. Akram, J. von Oswald, M. Larcher, A. Steger, and J. Sacramento, "Gated recurrent neural networks discover attention," *arXiv preprint arXiv:2309.01775*, 2023.

[143] A. Ali, I. Zimerman, and L. Wolf, "The hidden attention of mamba models," *arXiv preprint arXiv:2403.01590*, 2024.

[144] S. Yang, Y. Wang, and H. Chen, "Mambamil: Enhancing long sequence modeling with sequence reordering in computational pathology," *arXiv preprint arXiv:2403.06800*, 2024.

[145] G. L. C. S. Z. Z. S. M. W. Q. Qiao Yanyuan, Yu Zheng and L. Jing, "Vl-mamba: Exploring state space models for multimodal learning," *arXiv preprint arXiv:2403.13600*, 2024.

[146] G. Yang, K. Du, Z. Yang, Y. Du, Y. Zheng, and S. Wang, "Cmvim: Contrastive masked vim autoencoder for 3d multimodal representation learning for ad classification," *arXiv preprint arXiv:2403.16520*, 2024.

[147] H. Zhao, M. Zhang, W. Zhao, P. Ding, S. Huang, and D. Wang, "Cobra: Extending mamba to multi-modal large language model for efficient inference," *arXiv preprint arXiv:2403.14520*, 2024.

[148] T. Ota, "Decision mamba: Reinforcement learning via sequence modeling with selective state spaces," *arXiv preprint arXiv:2403.19925*, 2024.

[149] Z. Wan, Y. Wang, S. Yong, P. Zhang, S. Stepputtis, K. Sycara, and Y. Xie, "Sigma: Siamese mamba network for multi-modal semantic segmentation," *arXiv preprint arXiv:2404.04256*, 2024.

[150] K. He, X. Chen, S. Xie, Y. Li, P. Dollár, and R. Girshick, "Masked autoencoders are scalable vision learners," *arXiv preprint arXiv:2111.06377*, 2021.

[151] A. Dosovitskiy, L. Beyer, A. Kolesnikov, D. Weissenborn, X. Zhai, T. Unterthiner, M. Dehghani, M. Minderer, G. Heigold, S. Gelly, J. Uszkoreit, and N. Houlsby, "An image is worth 16x16 words: Transformers for image recognition at scale," *arXiv preprint arXiv:2010.11929*, 2021.

[152] L. Chen, K. Lu, A. Rajeswaran, K. Lee, A. Grover, M. Laskin, P. Abbeel, A. Srinivas, and I. Mordatch, "Decision transformer: Reinforcement learning via sequence modeling," in *Proceedings of Advances in Neural Information Processing Systems*, 2021, pp. 15 084–15 097.

[153] D. Liang, X. Zhou, X. Wang, X. Zhu, W. Xu, Z. Zou, X. Ye, and X. Bai, "Pointmamba: A simple state space model for point cloud analysis," *arXiv preprint arXiv:2402.10739*, 2024.

[154] T. Zhang, X. Li, H. Yuan, S. Ji, and S. Yan, "Point cloud mamba: Point cloud learning via state space model," *arXiv preprint arXiv:2403.00762*, 2024.

[155] J. Liu, R. Yu, Y. Wang, Y. Zheng, T. Deng, W. Ye, and H. Wang, "Point mamba: A novel point cloud backbone based on state space model with octree-based ordering strategy," *arXiv preprint arXiv:2403.06467*, 2024.

[156] Q. Zhou, W. Yang, B. Fei, J. Xu, R. Zhang, K. Liu, Y. Luo, and Y. He, "3dmambaipf: A state space model for iterative point cloud filtering via differentiable rendering," *arXiv preprint arXiv:2404.05522*, 2024.

[157] Y. Li, W. Yang, and B. Fei, "3dmambacomplete: Exploring structured state space model for point cloud completion," *arXiv preprint arXiv:2404.07106*, 2024.

[158] N. Zubi'c, M. Gehrig, and D. Scaramuzza, "State space models for event cameras," *arXiv preprint arXiv:2402.15584*, 2024.

[159] K. Goel, A. Gu, C. Donahue, and C. Ré, "It's raw! audio generation with state-space models," in *Proceedings of the International Conference on Machine Learning*, 2022, pp. 7616–7633.

[160] J. Wang, J. N. Yan, A. Gu, and A. M. Rush, "Pretraining without attention," *arXiv preprint arXiv:2212.10544*, 2022.

[161] S. Massaroli, M. Poli, D. Fu, H. Kumbong, R. Parnichkun, D. Romero, A. Timalsina, Q. McIntyre, B. Chen, A. Rudra *et al.*, "Laughing hyena distillery: Extracting compact recurrences from convolutions," in *Proceedings of Advances in Neural Information Processing Systems*, 2023.

[162] J. Smith, S. De Mello, J. Kautz, S. Linderman, and W. Byeon, "Convolutional state space models for long-range spatiotemporal modeling," in *Proceedings of Advances in Neural Information Processing Systems*, 2023.

[163] C. Lu, Y. Schroecker, A. Gu, E. Parisotto, J. Foerster, S. Singh, and F. Behbahani, "Structured state space models for in-context reinforcement learning," in *Proceedings of Advances in Neural Information Processing Systems*, 2023.

[164] S. Wang and Q. Li, "Stablessm: Alleviating the curse of memory in state-space models through stable reparameterization," *arXiv preprint arXiv:2311.14495*, 2023.

[165] M. Pióro, K. Ciebiera, K. Król, J. Ludziejewski, and S. Jaszczur, "Moe-mamba: Efficient selective state space models with mixture of experts," *arXiv preprint arXiv:2401.04081*, 2024.

[166] J. Wang, T. Gangavarapu, J. N. Yan, and A. M. Rush, "Mambabyte: Token-free selective state space model," *arXiv preprint arXiv:2403.13660*, 2024.

[167] Q. Anthony, Y. Tokpanov, P. Glorioso, and B. Millidge, "Blackmamba: Mixture of experts for state-space models," *arXiv preprint arXiv:2402.01771*, 2024.

[168] F. L. Bronnec, S. Duong, M. Ravaut, A. Allauzen, N. F. Chen, V. Guigue, A. Lumbreras, L. Soulier, and P. Gallinari, "Locost: State-space models for long document abstractive summarization," *arXiv preprint arXiv:2401.17919*, 2024.

[169] M. R. Samsami, A. Zholus, J. Rajendran, and S. Chandar, "Mastering memory tasks with world models," *arXiv preprint arXiv:2403.04253*, 2024.

[170] T. Katsch, "Gateloop: Fully data-controlled linear recurrence for sequence modeling," *arXiv preprint arXiv:2311.01927*, 2023.

[171] F. Liu and Q. Li, "From generalization analysis to optimization designs for state space models," 2024. [Online]. Available: https://openreview.net/forum?id=EGjvMcKrrl

[172] A. Yu, A. Nigmetov, D. Morozov, M. W. Mahoney, and N. B. Erichson, "Robustifying state-space models for long sequences via approximate diagonalization," in *Proceedings of the International Conference on Learning Representations*, 2024.

[173] E. David, J. Bellot, and S. L. Corff, "Variational quantization for state space models," 2024. [Online]. Available: https://openreview.net/forum?id=EAkjVCtRO2

[174] D. Y. Fu, H. Kumbong, E. Nguyen, and C. Ré, "Flashfftconv: Efficient convolutions for long sequences with tensor cores," *arXiv preprint arXiv:2311.05908*, 2023.

[175] C. Liu, J. Lin, J. Wang, H. Liu, and J. Caverlee, "Mamba4rec: Towards efficient sequential recommendation with selective state space models," *arXiv preprint arXiv:2403.03900*, 2024.

[176] B. Silva, M. Contreras, S. Bandyopadhyay, Y. Ren, Z. Guan, J. Balch, K. Khezeli, T. O. Baslanti, B. Shickel, A. Bihorac *et al.*, "A multi-cohort study on prediction of acute brain dysfunction states using selective state space models," *arXiv preprint arXiv:2403.07201*, 2024.

[177] C. Quan and X. Li, "Multichannel long-term streaming neural speech enhancement for static and moving speakers," *arXiv preprint arXiv:2403.07675*, 2024.

[178] Z. Shi, "Mambastock: Selective state space model for stock prediction," *arXiv preprint arXiv:2402.18959*, 2024.

[179] R. Bhirangi, C. Wang, V. Pattabiraman, C. Majidi, A. Gupta, T. Hellebrekers, and L. Pinto, "Hierarchical state space models for continuous sequence-to-sequence modeling," *arXiv preprint arXiv:2402.10211*, 2024.

[180] M. A. Ahamed and Q. Cheng, "Timemachine: A time series is worth 4 mambas for long-term forecasting," *arXiv preprint arXiv:2403.09898*, 2024.

[181] Y. Zhang, Z. Lin, Y. Sun, F. Yin, and C. Fritsche, "Regularization-based efficient continual learning in deep state-space models," *arXiv preprint arXiv:2403.10123*, 2024.

[182] M. Poli, A. W. Thomas, E. Nguyen, P. Ponnusamy, B. Deiseroth, K. Kersting, T. Suzuki, B. Hie, S. Ermon, C. R'e, C. Zhang, and S. Massaroli, "Mechanistic design and scaling of hybrid architectures," *arXiv preprint arXiv:2403.17844*, 2024.

[183] D. LaRocque, W. Guimont-Martin, D.-A. Duclos, P. Giguère, and F. Pomerleau, "Proprioception is all you need: Terrain classification for boreal forests," *arXiv preprint arXiv:2403.16877*, 2024.

[184] Z. Wang, F. Kong, S. Feng, M. Wang, H. Zhao, D. Wang, and Y. Zhang, "Is mamba effective for time series forecasting?" *arXiv preprint arXiv:2403.11144*, 2024.

[185] B. N. Patro and V. S. Agneeswaran, "Simba: Simplified mamba-based architecture for vision and multivariate time series," *arXiv preprint arXiv:2403.15360*, 2024.

[186] Z. Xu, "Rankmamba, benchmarking mamba's document ranking performance in the era of transformers," *arXiv preprint arXiv:2403.18276*, 2024.

[187] A. S. Sharma, D. Atkinson, and D. Bau, "Locating and editing factual associations in mamba," 2024.

[188] H. Yin, G. Cheng, C. J. Steinmetz, R. Yuan, R. M. Stern, and R. Dannenberg, "Modeling analog dynamic range compressors using deep learning and state-space models," *arXiv preprint arXiv:2403.16331*, 2024.

[189] M. Forgione, M. Mejari, and D. Piga, "Model order reduction of deep structured state-space models: A system-theoretic approach," *arXiv preprint arXiv:2403.14833*, 2024.

[190] J. Yang, Y. Li, J. Zhao, H. Wang, M. Ma, J. Ma, Z. Ren, M. Zhang, X. Xin, Z. Chen *et al.*, "Uncovering selective state space model's capabilities in lifelong sequential recommendation," *arXiv preprint arXiv:2403.16371*, 2024.

[191] S. Wang and B. Xue, "State-space models with layer-wise nonlinearity are universal approximators with exponential decaying memory," in *Proceedings of Advances in Neural Information Processing Systems*, 2023.

[192] I. Amos, J. Berant, and A. Gupta, "Never train from scratch: Fair comparison of long-sequence models requires data-driven priors," *arXiv preprint arXiv:2310.02980*, 2023.

[193] C. A. Alonso, J. Sieber, and M. N. Zeilinger, "State space models as foundation models: A control theoretic overview," *arXiv preprint arXiv:2403.16899*, 2024.

[194] E. J. Olucha, B. Terzin, A. Das, and R. Tóth, "On the reduction of linear parameter-varying state-space models," *arXiv preprint arXiv:2404.01871*, 2024.

[195] Z. Tan, Y. Yang, J. Wan, G. Guo, and S. Z. Li, "Relation-aware pedestrian attribute recognition with graph convolutional networks," *Proceedings of the AAAI Conference on Artificial Intelligence*, vol. 34, no. 7, pp. 12 055–12 062, 2020.

[196] J. Wu, H. Liu, J. Jiang, M. Qi, B. Ren, X. Li, and Y. Wang, "Person attribute recognition by sequence contextual relation learning," *IEEE Transactions on Circuits and Systems for Video Technology*, vol. 30, no. 10, pp. 3398–3412, 2020.

[197] J. Jia, X. Chen, and K. Huang, "Spatial and semantic consistency regularizations for pedestrian attribute recognition," *Proceedings of the IEEE/CVF International Conference on Computer Vision*, pp. 942–951, 2021.

[198] "Inter-attribute awareness for pedestrian attribute recognition," *Pattern Recognition*, vol. 131, p. 108865, 2022.

[199] L. Chen, J. Song, X. Zhang, and M. Shang, "Mcfl: multi-label contrastive focal loss for deep imbalanced pedestrian attribute recognition," *Neural Computing and Applications*, vol. 34, no. 19, pp. 16 701–16 715, 2022.

[200] Z. Tang and J. Huang, "Drformer: Learning dual relations using transformer for pedestrian attribute recognition," *Neurocomputing*, vol. 497, pp. 159–169, 2022.

[201] H. Guo, X. Fan, and S. Wang, "Visual attention consistency for human attribute recognition," *International Journal of Computer Vision*, vol. 130, no. 4, pp. 1088–1106, 2022.

[202] J. Jia, N. Gao, F. He, X. Chen, and K. Huang, "Learning disentangled attribute representations for robust pedestrian attribute recognition," in *Proceedings of the AAAI Conference on Artificial Intelligence*, 2022, pp. 1069–1077.

[203] H. Fan, H.-M. Hu, S. Liu, W. Lu, and S. Pu, "Correlation graph convolutional network for pedestrian attribute recognition," *IEEE Transactions on Multimedia*, vol. 24, pp. 49–60, 2020.

[204] Y. Yang, Z. Tan, P. Tiwari, H. M. Pandey, J. Wan, Z. Lei, G. Guo, and S. Z. Li, "Cascaded split-and-aggregate learning with feature recombination for pedestrian attribute recognition," *International Journal of Computer Vision*, vol. 129, no. 10, pp. 2731–2744, 2021.

[205] X. Wang, J. Jin, C. Li, J. Tang, C. Zhang, and W. Wang, "Pedestrian attribute recognition via clip based prompt vision-language fusion," *arXiv preprint arXiv:2312.10692*, 2023.

[206] J. Jin, X. Wang, C. Li, L. Huang, and J. Tang, "Sequencepar: Understanding pedestrian attributes via a sequence generation paradigm," *arXiv preprint arXiv:2312.01640*, 2023.

[207] X. Cheng, M. Jia, Q. Wang, and J. Zhang, "A simple visual-textual baseline for pedestrian attribute recognition," *IEEE Transactions on Circuits and Systems for Video Technology*, vol. 32, no. 10, pp. 6994–7004, 2022.

[208] X. Liu, H. Zhao, M. Tian, L. Sheng, J. Shao, S. Yi, J. Yan, and X. Wang, "Hydraplus-net: Attentive deep features for pedestrian analysis," in *Proceedings of the IEEE/CVF International Conference on Computer Vision*, 2017, pp. 350–359.

[209] Y. Deng, P. Luo, C. C. Loy, and X. Tang, "Pedestrian attribute recognition at far distance," in *Proceedings of the ACM International Conference on Multimedia*, 2014, pp. 789–792.

[210] B. Ye, H. Chang, B. Ma, S. Shan, and X. Chen, "Joint feature learning and relation modeling for tracking: A one-stream framework," in *Proceedings of European Conference on Computer Vision*, 2022, pp. 341–357.

[211] N. Wang, W. Zhou, J. Wang, and H. Li, "Transformer meets tracker: Exploiting temporal context for robust visual tracking," in *Proceedings of the IEEE/CVF Conference on Computer Vision and Pattern Recognition*, 2021, p. 1571–1580.

[212] C. Mayer, M. Danelljan, G. Bhat, M. Paul, D. P. Paudel, F. Yu, and L. V. Gool, "Transforming model prediction for tracking," in *Proceedings of the IEEE/CVF Conference on Computer Vision and Pattern Recognition*, 2022, p. 8731–8740.

[213] G. Bhat, M. Danelljan, L. V. Gool, and R. Timofte, "Learning discriminative model prediction for tracking," in *Proceedings of the IEEE/CVF International Conference on Computer Vision*, 2019, p. 6182–6191.

[214] M. Danelljan, L. V. Gool, and R. Timofte, "Probabilistic regression for visual tracking," in *Proceedings of the IEEE/CVF Conference on Computer Vision and Pattern Recognition*, 2019, p. 7183–7192.

[215] G. Bhat, M. Danelljan, L. Van Gool, and R. Timofte, "Know your surroundings: Exploiting scene information for object tracking,"

in *Proceedings of European Conference on Computer Vision*, 2020, p. 205–221.

[216] M. Danelljan, G. Bhat, F. Shahbaz Khan, and M. Felsberg, "Atom: Accurate tracking by overlap maximization," in *Proceedings of the IEEE/CVF Conference on Computer Vision and Pattern Recognition*, 2019, p. 4660–4669.

[217] X. Wang, S. Wang, C. Tang, L. Zhu, B. Jiang, Y. Tian, and J. Tang, "Event stream-based visual object tracking: A high-resolution benchmark dataset and a novel baseline," in *Proceedings of the IEEE/CVF Conference on Computer Vision and Pattern Recognition*, 2024.

[218] S. Gao, C. Zhou, C. Ma, X. Wang, and J. Yuan, "Aiatrack: Attention in attention for transformer visual tracking," in *Proceedings of European Conference on Computer Vision*, 2022, p. 146–164.

[219] B. Ye, H. Chang, B. Ma, and S. Shan, "Joint feature learning and relation modeling for tracking: A one-stream framework," *arXiv preprint arXiv:2203.11991*, 2022.

[220] X. Chen, J. Yan, Bin Zhu, D. Wang, X. Yang, and H. Lu, "Transformer tracking," in *Proceedings of the IEEE/CVF Conference on Computer Vision and Pattern Recognition*, 2021, p. 8126–8135.

[221] Y. Cui, C. Jiang, L. Wang, and W. Gangshan, "Mixformer: End-to-end tracking with iterative mixed attention," in *Proceedings of the IEEE/CVF Conference on Computer Vision and Pattern Recognition*, 2022, p. 13608–13618.

[222] B. Chen, P. Li, L. Bai, L. Qiao, Q. Shen, B. Li, W. Gan, W. Wu, and W. Ouyang, "Backbone is all your need: A simplified architecture for visual object tracking," in *Proceedings of European Conference on Computer Vision*, 2021, p. 375–392.

[223] H. Cao, Y. Wang, J. Chen, D. Jiang, X. Zhang, Q. Tian, and M. Wang, "Swin-unet: Unet-like pure transformer for medical image segmentation," in *Proceedings of European Conference on Computer Vision*, 2022, pp. 205–218.

[224] D. Demner-Fushman, M. D. Kohli, M. B. Rosenman, S. E. Shooshan, L. Rodriguez, S. Antani, G. R. Thoma, and C. J. McDonald, "Preparing a collection of radiology examinations for distribution and retrieval," *Journal of the American Medical Informatics Association*, vol. 23, no. 2, pp. 304–310, 2016.

[225] H. Touvron, L. Martin, K. R. Stone, P. Albert, A. Almahairi, Y. Babaei, N. Bashlykov, S. Batra, P. Bhargava, S. Bhosale, D. M. Bikel, L. Blecher, C. C. Ferrer, M. Chen, G. Cucurull, D. Esiobu, J. Fernandes, J. Fu, W. Fu, B. Fuller, C. Gao, V. Goswami, N. Goyal, A. S. Hartshorn, S. Hosseini, R. Hou, H. Inan, M. Kardas, V. Kerkez, M. Khabsa, I. M. Kloumann, A. V. Korenev, P. S. Koura, M.-A. Lachaux, T. Lavril, J. Lee, D. Liskovich, Y. Lu, Y. Mao, X. Martinet, T. Mihaylov, P. Mishra, I. Molybog, Y. Nie, A. Poulton, J. Reizenstein, R. Rungta, K. Saladi, A. Schelten, R. Silva, E. M. Smith, R. Subramanian, X. Tan, B. Tang, R. Taylor, A. Williams, J. X. Kuan, P. Xu, Z. Yan, I. Zarov, Y. Zhang, A. Fan, M. Kambadur, S. Narang, A. Rodriguez, R. Stojnic, S. Edunov, and T. Scialom, "Llama 2: Open foundation and fine-tuned chat models," *arXiv preprint arXiv:2307.09288*, 2023.

[226] Z. Chen, Y. Song, T.-H. Chang, and X. Wan, "Generating radiology reports via memory-driven transformer," in *Proceedings of the Conference on Empirical Methods in Natural Language Processing*, 2020, pp. 1439–1449.

[227] C. Y. Li, X. Liang, Z. Hu, and E. P. Xing, "Knowledge-driven encode, retrieve, paraphrase for medical image report generation," in *Proceedings of the AAAI Conference on Artificial Intelligence*, 2019, pp. 6666–6673.

[228] Y. Li, X. Liang, Z. Hu, and E. P. Xing, "Hybrid retrieval-generation reinforced agent for medical image report generation," in *Proceedings of Advances in Neural Information Processing Systems*, 2018.

[229] Y. Zhang, X. Wang, Z. Xu, Q. Yu, A. Yuille, and D. Xu, "When radiology report generation meets knowledge graph," in *Proceedings of the AAAI Conference on Artificial Intelligence*, 2020, pp. 12910–12917.

[230] F. Liu, X. Wu, S. Ge, W. Fan, and Y. Zou, "Exploring and distilling posterior and prior knowledge for radiology report generation," in *Proceedings of the IEEE/CVF Conference on Computer Vision and Pattern Recognition*, 2021, pp. 13753–13762.

[231] S. Yang, X. Wu, S. Ge, S. K. Zhou, and L. Xiao, "Knowledge matters: Chest radiology report generation with general and specific knowledge," *Medical Image Analysis*, vol. 80, p. 102510, 2022.

[232] F. Liu, C. Yin, X. Wu, S. Ge, P. Zhang, and X. Sun, "Contrastive attention for automatic chest x-ray report generation," in *Proceedings of Findings of the Association for Computational Linguistics*, 2021, pp. 269–280.

[233] F. Liu, S. Ge, and X. Wu, "Competence-based multimodal curriculum learning for medical report generation," in *Proceedings of the Annual Meeting of the Association for Computational Linguistics and the International Joint Conference on Natural Language Processing*, 2021, pp. 3001–3012.

[234] M. Li, B. Lin, Z. Chen, H. Lin, X. Liang, and X. Chang, "Dynamic graph enhanced contrastive learning for chest x-ray report generation," in *Proceedings of the IEEE/CVF Conference on Computer Vision and Pattern Recognition*, 2023, pp. 3334–3343.

[235] Z. Zhuang, L. Wei, L. Xie, T. Zhang, H. Zhang, H. Wu, H. Ai, and Q. Tian, "Rethinking the distribution gap of person re-identification with camera-based batch normalization," in *Proceedings of European Conference on Computer Vision*. Springer, 2020, pp. 140–157.

[236] B. He, J. Li, Y. Zhao, and Y. Tian, "Part-regularized near-duplicate vehicle re-identification," in *Proceedings of the IEEE/CVF Conference on Computer Vision and Pattern Recognition*, 2019, pp. 3997–4005.

[237] K. Zhou, Y. Yang, A. Cavallaro, and T. Xiang, "Omni-scale feature learning for person re-identification," in *Proceedings of the IEEE/CVF International Conference on Computer Vision*, 2019, pp. 3702–3712.

[238] J. Qian, W. Jiang, H. Luo, and H. Yu, "Stripe-based and attribute-aware network: A two-branch deep model for vehicle re-identification," *Measurement Science and Technology*, vol. 31, no. 9, p. 095401, 2020.

[239] G. Wang, Y. Yuan, X. Chen, J. Li, and X. Zhou, "Learning discriminative features with multiple granularities for person re-identification," in *Proceedings of the ACM International Conference on Multimedia*, 2018, pp. 274–282.

[240] X. Jin, C. Lan, W. Zeng, and Z. Chen, "Uncertainty-aware multi-shot knowledge distillation for image-based object re-identification," in *Proceedings of the AAAI Conference on Artificial Intelligence*, 2020, pp. 11165–11172.

[241] Z. Zhang, C. Lan, W. Zeng, X. Jin, and Z. Chen, "Relation-aware global attention for person re-identification," in *Proceedings of the IEEE/CVF Conference on Computer Vision and Pattern Recognition*, 2020, pp. 3186–3195.

[242] R. Chu, Y. Sun, Y. Li, Z. Liu, C. Zhang, and Y. Wei, "Vehicle re-identification with viewpoint-aware metric learning," in *Proceedings of the IEEE/CVF International Conference on Computer Vision*, 2019, pp. 8282–8291.

[243] X. Jin, C. Lan, W. Zeng, G. Wei, and Z. Chen, "Semantics-aligned representation learning for person re-identification," in *Proceedings of the AAAI Conference on Artificial Intelligence*, 2020, pp. 11173–11180.

[244] T.-S. Chen, C.-T. Liu, C.-W. Wu, and S.-Y. Chien, "Orientation-aware vehicle re-identification with semantics-guided part attention network," in *Proceedings of European Conference on Computer Vision*, 2020, pp. 330–346.

[245] X. Chen, C. Fu, Y. Zhao, F. Zheng, J. Song, R. Ji, and Y. Yang, "Salience-guided cascaded suppression network for person re-identification," in *Proceedings of the IEEE/CVF Conference on Computer Vision and Pattern Recognition*, 2020, pp. 3300–3310.

[246] X. Zhang, R. Zhang, J. Cao, D. Gong, M. You, and C. Shen, "Part-guided attention learning for vehicle re-identification," *arXiv preprint arXiv:1909.06023*, 2019.

[247] T. Chen, S. Ding, J. Xie, Y. Yuan, W. Chen, Y. Yang, Z. Ren, and Z. Wang, "Abd-net: Attentive but diverse person re-identification," in *Proceedings of the IEEE/CVF International Conference on Computer Vision*, 2019, pp. 8351–8361.

[248] D. Meng, L. Li, X. Liu, Y. Li, S. Yang, Z.-J. Zha, X. Gao, S. Wang, and Q. Huang, "Parsing-based view-aware embedding network for vehicle re-identification," in *Proceedings of the IEEE/CVF Conference on Computer Vision and Pattern Recognition*, 2020, pp. 7103–7112.

[249] J. Miao, Y. Wu, P. Liu, Y. Ding, and Y. Yang, "Pose-guided feature alignment for occluded person re-identification," in *Proceedings of the IEEE/CVF International Conference on Computer Vision*, 2019, pp. 542–551.

[250] P. Khorramshahi, N. Peri, J.-c. Chen, and R. Chellappa, "The devil is in the details: Self-supervised attention for vehicle re-identification," in *Proceedings of European Conference on Computer Vision*, 2020, pp. 369–386.

[251] G. Wang, S. Yang, H. Liu, Z. Wang, Y. Yang, S. Wang, G. Yu, E. Zhou, and J. Sun, "High-order information matters: Learning relation and topology for occluded person re-identification," in *Proceedings of the IEEE/CVF Conference on Computer Vision and Pattern Recognition*, 2020, pp. 6449–6458.

[252] Z. Sun, X. Nie, X. Xi, and Y. Yin, "Cfvmnet: A multi-branch network for vehicle re-identification based on common field of view," in *Proceedings of the ACM International Conference on Multimedia*, 2020, pp. 3523–3531.

[253] K. Zhu, H. Guo, Z. Liu, M. Tang, and J. Wang, "Identity-guided human semantic parsing for person re-identification," in *Proceedings of European Conference on Computer Vision*, 2020, pp. 346–363.

[254] A. Suprem and C. Pu, "Looking glamorous: Vehicle re-id in heterogeneous cameras networks with global and local attention," *arXiv preprint arXiv:2002.02256*, 2020.

[255] S. He, H. Luo, P. Wang, F. Wang, H. Li, and W. Jiang, "Transreid: Transformer-based object re-identification," in *Proceedings of the IEEE/CVF International Conference on Computer Vision*, 2021, pp. 15 013–15 022.

[256] X. Wang, W. Wu, C. Li, Z. Zhao, Z. Chen, Y. Shi, and J. Tang, "Structural information guided multimodal pre-training for vehicle-centric perception," in *Proceedings of the AAAI Conference on Artificial Intelligence*, 2024, pp. 5624–5632.

[257] X. Shu, X. Wang, X. Zang, S. Zhang, Y. Chen, G. Li, and Q. Tian, "Large-scale spatio-temporal person re-identification: Algorithms and benchmark," *IEEE Transactions on Circuits and Systems for Video Technology*, vol. 32, no. 7, pp. 4390–4403, 2021.

[258] L. Wei, S. Zhang, W. Gao, and Q. Tian, "Person transfer gan to bridge domain gap for person re-identification," in *Proceedings of the IEEE/CVF Conference on Computer Vision and Pattern Recognition*, 2018, pp. 79–88.

[259] L. Zheng, L. Shen, L. Tian, S. Wang, J. Wang, and Q. Tian, "Scalable person re-identification: A benchmark," in *Proceedings of the IEEE/CVF International Conference on Computer Vision*, 2015, pp. 1116–1124.

[260] Z. Zhang, J. Wu, X. Zhang, and C. Zhang, "Multi-target, multi-camera tracking by hierarchical clustering: Recent progress on dukemtmc project," *arXiv preprint arXiv:1712.09531*, 2017.

[261] J. Miao, Y. Wu, P. Liu, Y. Ding, and Y. Yang, "Pose-guided feature alignment for occluded person re-identification," in *Proceedings of the IEEE/CVF International Conference on Computer Vision*, 2019, pp. 542–551.

[262] X. Liu, W. Liu, H. Ma, and H. Fu, "Large-scale vehicle re-identification in urban surveillance videos," in *Proceedings of the IEEE International Conference on Multimedia and Expo*, 2016, pp. 1–6.

[263] H. Liu, Y. Tian, Y. Yang, L. Pang, and T. Huang, "Deep relative distance learning: Tell the difference between similar vehicles," in *Proceedings of the IEEE/CVF Conference on Computer Vision and Pattern Recognition*, 2016, pp. 2167–2175.

[264] H. Luo, Y. Gu, X. Liao, S. Lai, and W. Jiang, "Bag of tricks and a strong baseline for deep person re-identification," in *Proceedings of the IEEE/CVF Conference on Computer Vision and Pattern Recognition Workshops*, 2019, pp. 1487–1495.

[265] H. Touvron, M. Cord, M. Douze, F. Massa, A. Sablayrolles, and H. Jégou, "Training data-efficient image transformers & distillation through attention," in *Proceedings of the International Conference on Machine Learning*, 2021, pp. 10 347–10 357.

[266] A. Q. Jiang, A. Sablayrolles, A. Roux, A. Mensch, B. Savary, C. Bamford, D. S. Chaplot, D. d. l. Casas, E. B. Hanna, F. Bressand *et al.*, "Mixtral of experts," *arXiv preprint arXiv:2401.04088*, 2024.

[267] C. Tang, X. Wang, J. Huang, B. Jiang, L. Zhu, J. Zhang, Y. Wang, and Y. Tian, "Revisiting color-event based tracking: A unified network, dataset, and metric," *arXiv preprint arXiv:2211.11010*, 2022.

[268] X. Wang, J. Huang, S. Wang, C. Tang, B. Jiang, Y. Tian, J. Tang, and B. Luo, "Long-term frame-event visual tracking: Benchmark dataset and baseline," *arXiv preprint arXiv:2403.05839*, 2024.

[269] M. Lin, Q. Chen, and S. Yan, "Network in network," *arXiv preprint arXiv:1312.4400*, 2013.